Modelling the influence of physicochemical material feed properties on ammonium nitrate product quality

S Eisenberg
22125787

Dissertation submitted in fulfilment of the requirements for the degree Masters in Chemical Engineering at the Potchefstroom Campus of the North-West University

Supervisors: Mr AF van der Merwe
Prof KR Uren

November 2016

Declaration

I, Suné Eisenberg, hereby declare that the dissertation entitled: "*Modelling the influence of physicochemical material feed properties on ammonium nitrate product quality*", submitted in fulfilment of the requirements for a Master's degree in Chemical Engineering (M. Eng), is my own work, except where acknowledged in the text and that this dissertation has not been submitted to any other tertiary institution either in or part or as a whole.

Signed at Potchefstroom, on the_____ day of _____, 2016.

_____

Suné Eisenberg

Acknowledgements

I would like to thank my Lord and Saviour Jesus Christ for the ability, opportunity and blessing to work on such a project. I would also like to thank the following people and institutions that contributed to the completion of this research project.

- The Omnia Group (Pty) Ltd. for their financial support and the opportunity to work on this project.
- Mr. Imtiaz Laher for his patience and help.
- Mr. Frikkie van der Merwe for his guidance, support and advice during this project.
- Professors Kenny Uren and George van Schoor for their advice and support.
- My family for their love, support and continuous motivation.
- The Le Roux family for their generosity and support.
- Cornand le Roux for his patience, support, understanding and motivation, anytime anywhere.

Abstract

In this study the effect of the physicochemical material feed properties of ammonium nitrate on the product granule quality in a fluidised bed granulator was investigated.

The effect of atomising air pressure, binder spray concentration, binder spray temperature, binder spray rate and feed particle size on the final particles' abrasion resistance, size, shape, porosity and flowability was investigated on a production plant using a five factor, five level central composite design. The data obtained from the experimental work was then subjected to regression analysis, where multiple linear regression models with and without two-way interaction effects as well as a second order regression model was obtained for each of the quality parameters. The models obtained were evaluated by using the coefficient of determination (R^2), the mean square error (MS_r) and the F-test. The models deemed adequate were then validated using a different data set.

The abrasion resistance and particle shape was adequately described by multiple linear regression equations with two-way interactions. The identified physicochemical material feed properties of ammonium nitrate therefore successfully describes both the particles' resistance to abrasion as well as the particle shape. The particle size was positively evaluated during the model development phase but proved to be inadequate during validation. The physicochemical material feed properties of ammonium nitrate and the experimental design alone were unable to describe the particle size adequately.

All the regression models obtained for both the particle porosity and flowability were deemed inadequate in describing these two quality parameters during both the model development and validation phases. Both quality parameters are associated with high measurement errors which could explain the complete inefficiency of the models obtained.

A further in-depth investigation of the particle size, particle porosity and flowability is needed to quantify the effect of the physicochemical material feed properties of ammonium nitrate on these quality parameters.

Key words:

Fluidised bed granulation, statistical modelling, ammonium nitrate, physicochemical properties

Table of contents

List of abbreviations and acronyms

Abbreviation or acronyms	Description
A	Abrasion resistance
AAT	Atomising air temperature
AN	Ammonium nitrate
ANOVA	Analysis of variance
BD	Bulk density
BP	Boiling point
BPE	Boiling point elevation
C	Circularity
CI	Carr’s Index
DAP	Difference in atomising air pressure
FAF	Fluidising air flow
FAT	Fluidising air temperature
FBMG	Fluidised bed melt granulation
Fd_{50}	Feed particle mean diameter
FFE	Falling film evaporator
HR	Hausner ratio
P	Porosity
Pd_{50}	Product particle mean diameter

PGAN	Porous granular ammonium nitrate
PSD	Particle size distribution
RSM	Response surface methodology
RW	Relative width
SEM	Scanning electron microscope
SLC	Spray liquid concentration
SLF	Spray liquid flow rate
SLT	Spray liquid temperature
TD	Tapped density
TD	True density

List of figures

List of tables

List of symbols

Symbol	Description	Unit
P_c	Capillary tension	N/m
γ_{LV}	Interfacial tension	N/m
Θ	Contact angle	°
φ	Particle shape factor	-
d_{pm}	Particle mean diameter	mm
d_{pi}	Particle initial diameter	mm
d_{10}	Particle diameter at 10% of the cumulative distribution	mm
d_{50}	Particle diameter at 50% of the cumulative distribution	mm
d_{90}	Particle diameter at 90% of the cumulative distribution	mm
χ	Granule porosity	-
X	Growth rate	%
π	PI	-
P	Particle perimeter	mm
A	Projected area	mm
n_f	Number of fractional factorial design points	-
n_0	Number of centre points	-
n_α	Number of axial points	-
N	Number of design points	-
k	Number of factors	-
α	Distance from axial to centre point	-
r_s	Spearman's rho	-
x_i	Rank of X_i	-
y_i	Rank of Y_i	-
$\bar{x}$	Average rank value for X_i	-
$\bar{y}$	Average rank value for Y_i	-

Y	Dependent variable	-
X_i	Independent variable i	-
ε	Error in determining the response variable Y	-
$\hat{Y}$	Predicted response value	-
b_0	Regression coefficient	-
b_i	Regression coefficient for independent variable X_i	-
b_{ij}	Regression coefficient for the interaction between X_i and X_j	-
b_{ii}	Regression coefficient for the second order X_i	-
SS_R	Sum of squares regression	-
SS_r	Sum of squares residual	-
SS_{lof}	Sum of squares lack of fit	-
SS_{pe}	Sum of squares pure error	-
SS_T	Sum of squares total	-
MS_R	Mean square regression	-
MS_r	Mean square error or residual	-
MS_{lof}	Mean square lack of fit	-
MS_{pe}	Mean square pure error	-
S_{b_i}	Variance in regression coefficient calculation	-
$S_y{}^2$	Reproducibility of variance	-
R^2	Coefficient of determination	-
F	Fischer's criterion	-

1. Introduction

1.1 Background and motivation

Ammonium nitrate (AN), a white crystal-like solid, is mainly used as a fertilizer in the agricultural sector and as an explosive substance in mining and comes in the commercial form of granules or prills, either formed by granulation or prilling. The Omnia Group (Pty) Ltd., the beneficiary of this project, uses their own unique granulation process in order to produce porous ammonium nitrate granules. To better understand the behaviour of this unique process, various studies are being done on their porous granular ammonium nitrate (PGAN) plant.

In the granulation process, a fluidised bed granulator (FBG) produces granules by spraying a diluted molten AN solution onto fluidised seed material using spray nozzles (Saleh *et al.*, 2003). This process is portrayed in Figure 1.1.

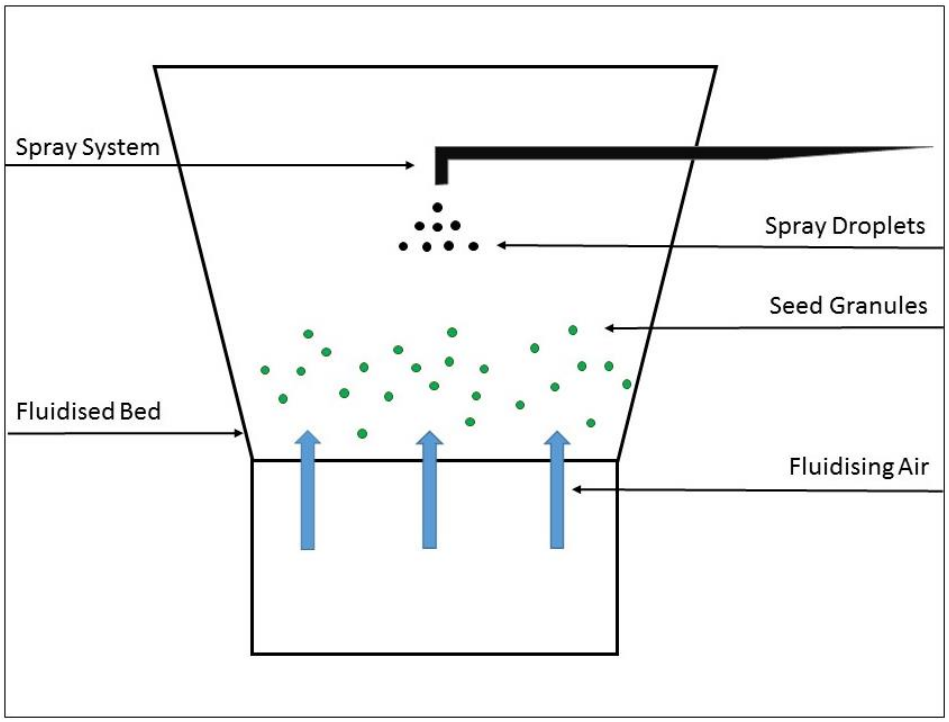

Figure 1.1 Schematic drawing of a fluidised bed granulator – taken from Poncelet & Vétérinaire (2002)

As the spray liquid droplets collide with the fluidising seed particles, new larger particles are formed with improved physical properties. Two growth mechanisms exist for the production of ammonium nitrate in a fluidised bed granulator namely agglomeration and layering. Agglomeration occurs when small particles adhere to one another to form larger particles with liquid bridges while layering occurs when liquid melt forms a dense layer around the

particle (Srinivasakannan & Balasubramaniam, 2003). Scanning electron microscope (SEM) pictures of both an agglomerated and layered particle can be seen in Figure 1.2.

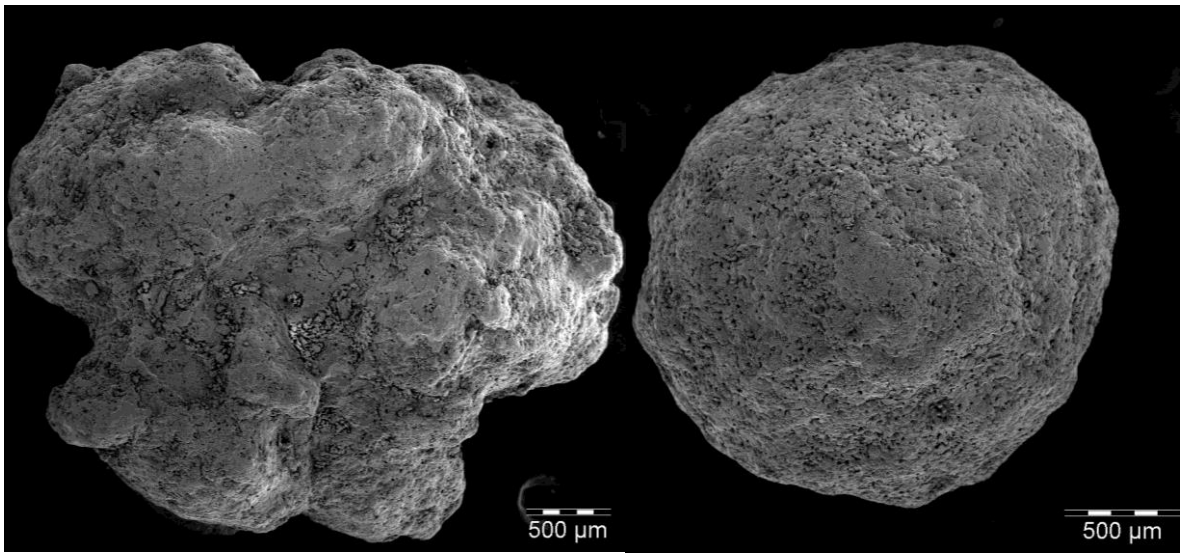

Figure 1.2 SEM images of an agglomerated and layered particle respectively

The liquid bridges form between colliding particles, when agglomerates are formed, as well as the layers that form around individual particles during layering will depend greatly on the physical properties of the liquid feed as well as bed characteristics.

Pont *et al.* (2001) determined that the viscosity and interfacial tension have a huge role in the growth mechanism of particles, both of which are dependent on the liquid sprayed through the nozzle into the bed. A study by Hemati *et al.* (2003) showed there are a significant number of process variables that influence the growth mechanism within the granulator, the most important being the fluidising inlet air temperature, atomising air flow rate, nozzle position and fluidising air velocity. Other important granule characteristics or quality parameters that were identified from literature are the granule size, granule strength, granule shape and flowability (Abberger *et al.*, 2002; Aleksić *et al.*, 2015; Hemati *et al.*, 2003). These granule properties are all dependent on the granulator process variables, and by changing the levels of these process variables, the product quality is altered. Hemati *et al*. (2003) states that all process variables are interdependent and when understood, this interdependency can be used to produce the most desirable product.

More often than not the granule quality is measured offline, having the distinct disadvantage that no real-time process corrections can be made to improve the granule quality (Närvänen *et al.*, 2009). Developing an off-line quality control method could be useful in determining the ideal or close to ideal process conditions to reach optimal product quality or to even just reduce the deviation in the product quality obtained.

Throughout literature the importance of nozzle design and operation, the spray liquid properties and the bed conditions in fluidised bed granulation are highlighted. Investigating these various components of the fluidised bed granulator separately and in a system can give valuable information contributing to the overall understanding of the fluidised bed granulation system.

1.2 Focus of this study

The focus of this study is on modelling the effects of the physicochemical material properties of the AN being fed to the fluidised bed granulator on the quality related properties of the AN product. Physicochemical feed properties refer to both the chemical and physical properties of ammonium nitrate such as concentration, temperature, particle size distribution and flowrate.

Due to the nature of this process it would be inadequate to look at a few identified elements without knowing what kind of contribution they have on the complete system, and therefore the study will be approached in three distinct phases. The first phase will give a picture of where precisely the physicochemical material feed properties of ammonium nitrate fit into the overall process. The second phase will focus solely on the isolated effects of the physicochemical material feed properties on granule quality. In the third and last phase the effect of the physicochemical material feed properties on granule quality will be validated.

1.3 Objectives of this study

The objective of this study is to determine the influence of the physicochemical material feed properties of ammonium nitrate feed, which includes molten ammonium nitrate solution as well as the ammonium nitrate seed material, on the product quality.

The physicochemical material feed properties for ammonium nitrate in this process can be seen in Table 1.1.

Table 1.1 Physicochemical material feed properties of ammonium nitrate

Physicochemical Property	Description
Feed particle size	Feed particle size refers to the average size (d_{50}) of the ammonium nitrate seed particles fed into the granulator.
Spray liquid concentration	The diluted ammonium nitrate solution sprayed into the bed during granulation can vary in concentration. Concentration also has an effect on viscosity and density.
Spray liquid temperature	The temperature of the diluted ammonium nitrate solution sprayed into the granulator during granulation.
Spray liquid flowrate	The diluted ammonium nitrate solution is sprayed into the bed through ten nozzles and the amount of ammonium nitrate injected into the bed is controlled.
Atomizing air pressure	The atomising air pressure is used to atomise the liquid ammonium nitrate into the fluidised bed granulator through the various nozzles. The atomising air pressure has an effect on the ammonium nitrate droplet size entering the bed.

The product quality parameters include the product size distribution, product particle shape, product particle porosity, product flowability and particle degradation.

1.4 Scope of this study

The scope of this investigation can be seen in Figure 1.3. Supplementary information and raw data are presented in the appendices.

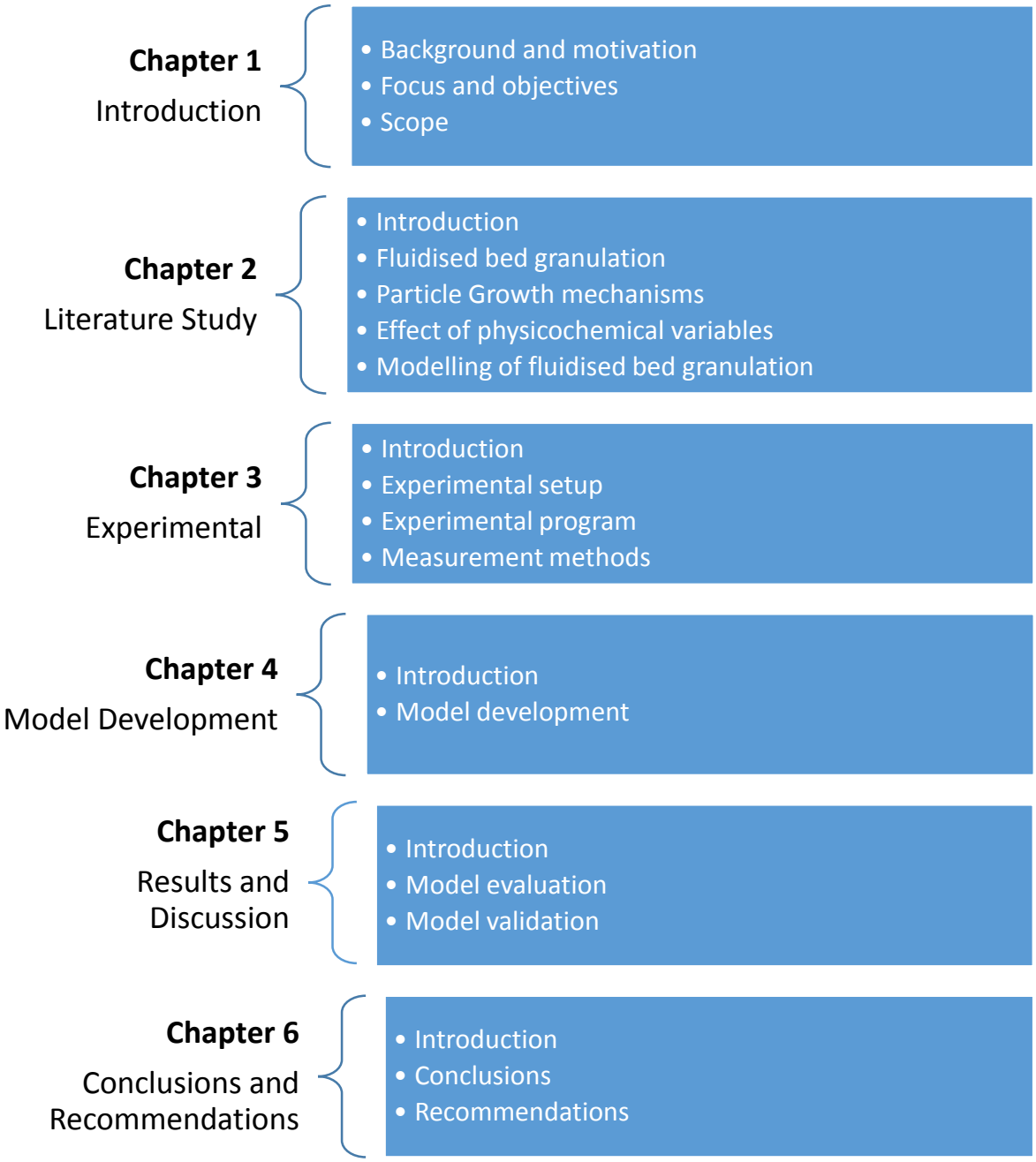

Figure 1.3 Scope of the investigation

2. Literature Study

2.1 Introduction

2.1.1 A brief history of ammonium nitrate

Ammonium nitrate (AN) or NH_4NO_3 was the first nitrogen based solid fertiliser produced on a large scale. In the 1940s, the large-scale production of ammonium nitrate started and it was initially used to produce ammunition during World War II. Shortly after the end of the war AN was made available as a commercial fertiliser (International Plant Nutrition Institute, 2015).

2.1.2 Manufacturing of AN

A neutralisation reaction of ammonia by nitric acid, shown in equation 2.1, is used to produce ammonium nitrate. It can also be produced by the dual decomposition reaction of nitrate- and ammonium salts such as sodium nitrate and ammonium sulphate as seen in equation 2.2.

$$NH_3 + HNO_3 \rightarrow NH_4NO_3 + heat \quad [2.1]$$

$$(NH_4)_2SO_4 + 2NaNO_3 \rightarrow 2NH_4NO_3 + Na_2SO_4 \quad [2.2]$$

The reaction shown in equation 2.1 takes place in liquid form with an excess nitric acid. Ammonium nitrate particles are acquired through crystallising a concentrated ammonium nitrate solution (Patnaik, 2003).

2.1.3 Physical properties of AN

Ammonium nitrate is highly hygroscopic, extremely soluble in water, has a density of 1.725 g/m^3 and a melting point of 169.6°C. Ammonium nitrate occurs in five stable crystallographic forms that can be seen in Table 2.1 (Patnaik, 2003; Vargeese *et al.*, 2009).

Table 2.1 Crystallographic forms of ammonium nitrate (Taken from Patnaik, 2003)

Phase	Structure	Stability Range
i.	Tetragonal	<18°C
ii.	Rhombic	-18 – 32.1°C
iii.	Rhombic	32.1 – 84.2°C
iv.	Tetragonal	84.2 – 125.2°C
v.	Cubic	125.2 – 169.6°C

Other physical properties of granule AN will be discussed later in this chapter.

2.1.4 Applications of AN

Ammonium nitrate is widely used as both a fertiliser and an explosive. The advantage it has over other fertilisers is its ability to maintain pH while adding both ammonia and nitrate to the soil. When added to other compounds such as calcium carbonate or calcium phosphate it can also be used as a mixed fertiliser (Patnaik, 2003).

Ammonium nitrate salt is highly explosive when combined with any carbonaceous material, fuel oil or powdered aluminium. Nitrous oxide, used as an anaesthetic or in freezing mixtures, is also manufactured from ammonium nitrate (Patnaik, 2003).

2.2 Fluidised bed granulation

2.2.1 Process description

A standard wet fluidised bed granulator produces granules by spraying a solution onto seed material in a fluidised bed using a nozzle system (Saleh *et al.*, 2003). A powdered seed material is fed into the granulator and is usually fluidised by a flow of air directed upwards from the foot of the granulator while a solution is sprayed through one or more nozzles usually located in the top of the granulator, opposing the flow of air as seen in Figure 2.1.

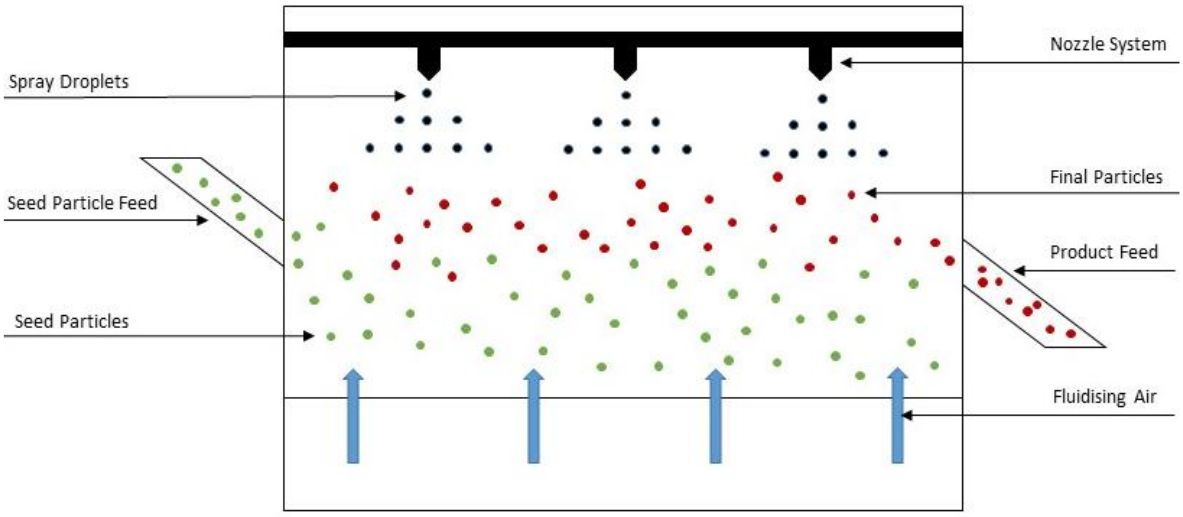

Figure 2.1 Schematic drawing of a fluidised bed granulation – Taken from Poncelet & Vétérinaire (2002)

Small droplets collide with fluidised particles to initiate particle growth. This process is commonly used to increase the physicochemical and mechanical properties of granules as well as their flowability (Liu *et al.*, 2013). After the collision takes place the new particles are

dried by the fluidising air. The collision and drying process repeats itself until the particles reach optimal size and then leave the bed on the opposite end of the granulator.

Various forms of granulation exist namely dry, wet and melt granulation. During dry granulation solid fines are added to the bed that stick to the seed material while in wet granulation a liquid binder is sprayed into the bed and onto the seed material. The melt in melt granulation refers to a molten liquid that is sprayed into the bed instead of a regular binder liquid (Veliz Moraga *et al.*, 2015). For the purpose of this study, fluidised bed melt granulation (FBMG) is being investigated.

2.2.2 Rate processes

Fluidised bed melt granulation consists of various mechanisms or rate processes to make up the granulation process. The basic granulation mechanism can be divided into three distinct sections namely wetting, progressive growth and finally breakage and consolidation (Ennis & Litster, 1997; Goldschmidt *et al.*, 2003; Iveson *et al.*, 2001).

Tan *et al.* (2006) continued to sequentially describe these rate processes that occur simultaneously during granulation, starting off with particle and droplet collision, solidification of the binder, particle to particle collision, liquid bridge formation and finally the breakage of the solid bridge. These proposed rate processes by Tan *et al.* (2006), seen in Figure 2.2, are helpful in describing fluidised bed granulation especially in situations where the droplet sizes are smaller than that of the particles.

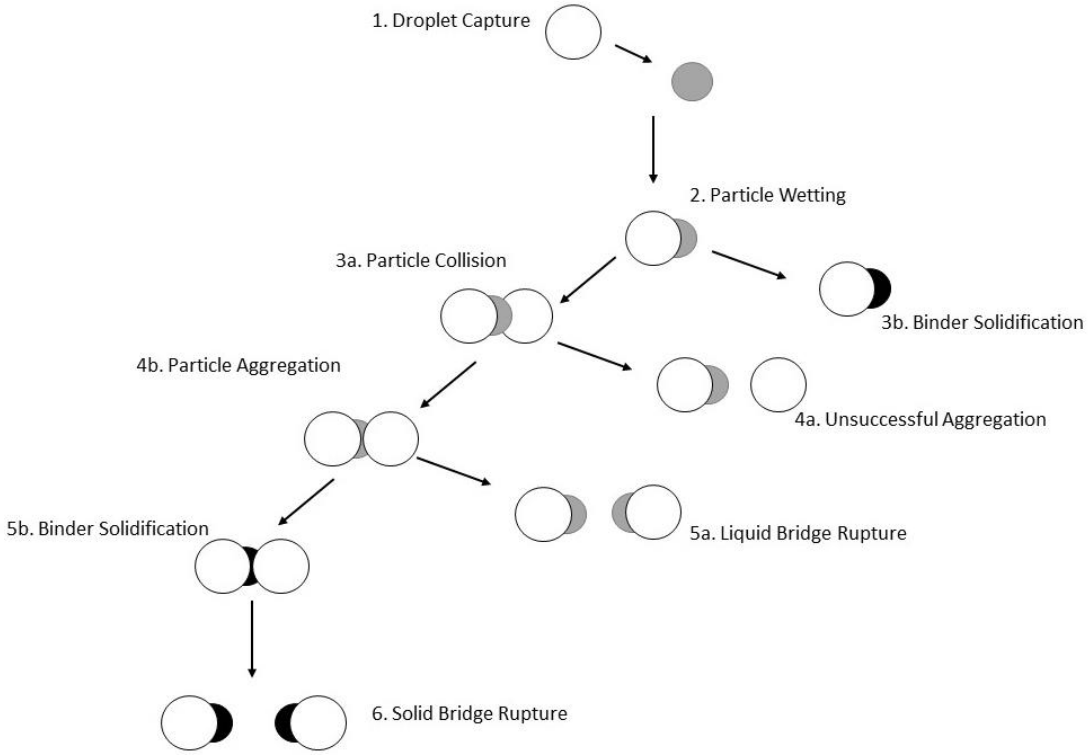

Figure 2.2 Rate Processes in a Fluidised Bed Granulation – Adapted from Tan *et al.* (2006)

The sequence of events starts off with (1) the collision of particles and droplets in the fluidised bed spray zone which (2) produces wet particles. Thereafter two possibilities exist, either the binder will solidify (3a) on the particle or collisions will occur between the wet particle and other particles (3b) of which the second possibility being more likely due to the fast particle collision rate. After particle collisions (3b) aggregates are formed (4b) or aggregation can be unsuccessful (4a) in the event of insufficient binder viscosity to dampen kinetic energy forces. If successful particle aggregation occurs, the liquid bridges connecting particles will either solidify (5b) or split (5a), which depends on the binder solidification rate. Solid bridges can also break (6) due to process conditions if these solid bridges aren't strong enough (Tan *et al.*, 2006). Due to the nature of fluidised bed granulation these sequences cannot be expected to occur sequentially.

2.2.3 Granulation product

The quality of product granules are usually characterised by a number of attributes, such as granule size, shape, strength, porosity and flowability, and can be considerably influenced by the characteristics of materials used during granulation as well as factors related to the process. From literature some of these factors were identified and are summarised in Table 2.2. A positive effect indicates an increase in the factor will result in an increase of the characteristic while a negative effect indicates an increase in the factor will result in a decrease of the characteristic and vice versa.

Table 2.2 Factors that affect granulation product quality (Adapted from various sources)

Characteristic	Affected By	Sources	Effect
Mean Granule Size	Spray liquid flowrate	(Liu *et al.*, 2013) (Hemati *et al.*, 2003) (Tan *et al.*, 2006)	Positive
	Droplet size	(Tan *et al.*, 2006)	Positive
	Nozzle spray pulse	(Liu *et al.*, 2013)	Positive
	Atomising air pressure	(Liu *et al.*, 2013) (Hemati *et al.*, 2003)	Negative
	Fluidising air velocity	(Smith & Nienow, 1983) (Tan *et al.*, 2006)	Negative
	Initial seed particle size	(Smith & Nienow, 1983)	Negative
	Binder concentration	(Pont *et al.*, 2001)	Negative
	Surface tension	(Pont *et al.*, 2001)	Positive
Porosity	Binder concentration	(Rajniak *et al.*, 2007)	Positive
	Feed size distribution	(Walker *et al.*, 2005)	Positive
Particle shape	Feed size distribution	(Walker *et al.*, 2005)	Negative
	Atomising air pressure	(Aleksić *et al.*, 2015)	Negative
	Amount of binder	(Wong *et al.*, 2013)	Positive
	Binder viscosity	(Schæfer, 2001)	Negative

Particle Strength	Binder viscosity	(Schæfer, 2001)	Positive
	Initial seed particle shape	(Schæfer, 2001)	Negative
	Binder concentration	(Walker *et al.*, 2005)	Positive
	Surface tension	(Braumann *et al.*, 2010)	Positive
Flowability	Atomising air pressure	(Aleksić *et al.*, 2015) (Poncelet & Vétérinaire, 2002)	Negative
	Binder concentration	(Mehta *et al.*, 2005)	Positive
	Amount of binder	(Wong *et al.*, 2013)	Positive

2.3 Particle growth mechanisms

Two particle growth mechanisms exist for the production of ammonium nitrate in a fluidised bed granulator namely agglomeration and layering. Agglomeration occurs when small particles adhere to one another to form larger particles while layering occurs when liquid melt forms a dense layer around the particle (Srinivasakannan & Balasubramaniam, 2003).

2.3.1 Agglomeration

As previously stated agglomerates form when wet particles adhere to one another during the granulation process. During the collision of particles, one of the particles still has to be wet enough for a liquid bridge to be formed between the various particles. A schematic description of agglomeration can be seen in Figure 2.3.

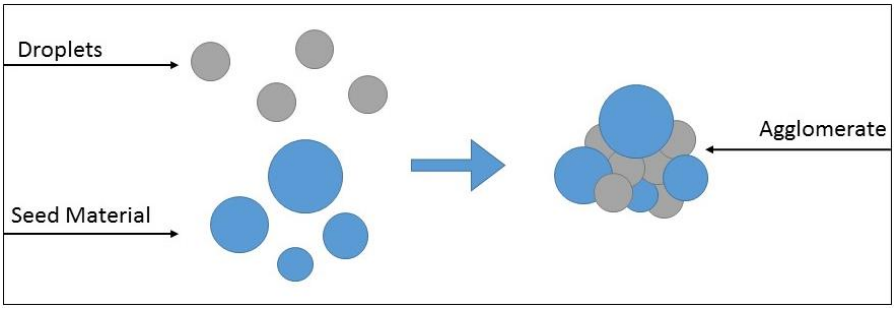

Figure 2.3 Formation of Agglomerate Granules

Becher & Schlunder (1998) identified two constraints for agglomeration: 1) collision probability, which depends on the design of the granulator, the conditions of fluidisation and the properties of the particles and 2) the liquid coverage of one of the colliding particles which depends on the spraying (wetting) and drying procedure. The purpose of producing agglomerates is to improve the flow properties of seed particles as well as to reduce process dust and risk of explosion associated with the process (Pont *et al.*, 2001).

2.3.2 Layering

Layering takes place when the binder liquid covers the entire surface of the particle and forms a layer around it. The particle then either dries before a particle to particle collision can occur, or the breakup forces inside the bed are larger than the cohesive bond strength between particles. The purpose of producing layered particles is to control particle release time and to change their surface properties (Pont *et al.*, 2001). A schematic drawing of layering can be seen in Figure 2.4.

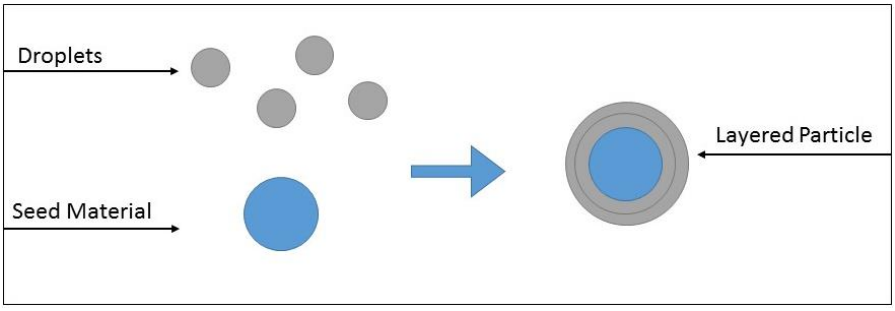

Figure 2.4 Formation of Layered Granules

SEM images of both a layered and agglomerate particle was presented in Figure 1.2.

2.3.3 Liquid bridges

The particle growth mechanism hinges on the formation (or lack of formation) of liquid bridges. The resistance of liquid bridges to breakup forces hinges on capillary tension which induces capillary forces. Capillary tension (P_c) is affected by various factors such as particle

shape and size, viscosity, contact angle and interfacial tension (Pont *et al.*, 2001). Schubert *et al.* (1975) presented equation 2.3 to characterise the effects of γ_{LV}, the interfacial tension between air and liquid, θ, the contact angle of the liquid, air and solid particle, ϕ, the particle shape factor, d_p, solid particle mean diameter and χ, the granule porosity, on the capillary tension.

$$P_c = \gamma_{LV} \cos\theta \frac{6}{\phi d_{pm}} \frac{1-\chi}{\chi} \quad [2.3]$$

During the study by Pont *et al.* (2001), the influence of contact angle and the particle shape factor was examined. It was determined that agglomerate formation is favoured by an increase in $\gamma_{LV} \cos\theta$, the adhesion strength of liquid on the particle surface. The effect of other variables on adhesion strength can be seen in Table 2.3.

Table 2.3 Variable effect on surface tension and contact angle (taken from Pont *et al.*, 2001)

Variable	**Effect**	
Concentration Increase	$\gamma_{LV} \cos\theta$	Decreases
Surface Tension Decrease	$\gamma_{LV} \cos\theta$	Decreases

Pont *et al.* (2001) however stated that this equation assumes static adhesion between particles when in fact the dynamic forces from liquid bridges well exceeds the static forces from liquid bridges, which is a result of surface tension, particle wettability and viscous force.

2.3.4 Effect of process variables on particle growth mechanism

Table 2.4 provides a list of all the process variables found in literature that have an influence on the particle growth mechanism. When utilised correctly these variables can determine whether agglomerate or layered particles are produced (Hemati *et al.*, 2003).

Table 2.4 Variables that have a distinct influence on the particle growth mechanism (Taken from various sources)

Variable	Source
Nozzle position	(Hemati *et al.*, 2003)
Fluidising Air Velocity	(Hemati *et al.*, 2003) (Smith & Nienow, 1983)
Fluidising Air Temperature	(Hemati *et al.*, 2003)
Liquid spray rate	(Hemati *et al.*, 2003)
Atomisation air flow rate	(Hemati *et al.*, 2003)
Bed temperature	(Hemati *et al.*, 2003)
Initial Particle size	(Smith & Nienow, 1983)
Binder Concentration	(Hemati *et al.*, 2003)
Contact Angle	(Pont *et al.*, 2001)
Binder Viscosity	(Ramachandran *et al.*, 2008) (Iveson *et al.*, 2001)

2.3.5 Effects of particle growth mechanism on bed operation

If the spray liquid is not distributed evenly, or in excess, large lumps of wet agglomerates may form that can lead to the defluidisation of the bed, known as wet quenching. However if the particle growth takes place at a too high rate, big agglomerates can be formed and the operating fluidisation velocity will be exceeded by the minimum fluidisation velocity. This can also lead to defluidisation and the loss of fluidisation in a well fluidised bed. This is termed dry quenching (Becher & Schlünder, 1998; Srinivasakannan & Balasubramaniam, 2003).

Literature suggest that agglomeration and bed quenching all have the same initial stages. Becher & Schlunder (1998) suggest that all growth mechanisms and bed quenching start in the exact same way; liquid bonds form between colliding particles, the liquid bonds will dry and form solid bridges between these particles, or redistribution will take place in which either the liquid- or solid bridges will break. This in turn will depend on two aspects of fluidised bed granulation, namely the (i) binding mechanism and the (ii) abrasive action and

circulation of solids within the bed which prevents the formation of agglomerates. These two factors will depend on the liquid feed physical properties and quality, the fluidised bed characteristics, size and type of particles as well as the fluidising air velocity.

The particle growth rate can be determined using equation 2.4, where d_{pm} and d_{pi} refer to the mean and initial particle size respectively (Hemati *et al.*, 2003).

$$X = 100\frac{d_{pm} - d_{pi}}{d_{pi}} \qquad [2.4]$$

The mean diameter is calculated using equation 2.5 where f_i refers to particle mass fraction.

$$d_{pm} = \frac{\sum_i f_i d_{pi}}{\sum_i f_i} \qquad [2.5]$$

Variables that have an impact on the particle growth rate can be seen in Table 2.5. A positive effect indicates an increase in the variable will result in an increase in particle growth rate and a decrease in the variable will result in the decrease of the particle growth rate. A negative effect indicates an increase in the variable will result in a decrease in the particle growth rate and vice versa.

Table 2.5 Variables that influence particle growth rate (summarised from various sources)

Variable	Effect	Source
Binder Spray Rate	Positive	(Srinivasakannan & Balasubramaniam, 2003) (Tan *et al.*, 2005)
Binder Concentration	Positive	(Srinivasakannan & Balasubramaniam, 2003)
Seed Particle size	Negative	(Srinivasakannan & Balasubramaniam, 2003) (Saleh *et al.*, 2003)
Bed Temperature	Positive	(Tan *et al.*, 2005)
Droplet Size	Positive	(Tan *et al.*, 2005)
Fluidising Air Velocity	Negative	(Tan *et al.*, 2005)

Tan *et al.* (2006) determined that fluidising air velocity is one of the factors that has the largest effect on the particle growth rate. The particle growth rate decreases at higher fluidising air velocities. This is attributed to the escalation in liquid bridge breakages due to more agitation which leads to less binder being picked up by particles in a certain time frame due to increased air velocity. This produces higher chances of failed aggregation due to increased kinetic energy and less binder being available for aggregation due to improved heat transfer conditions.

2.4 Process variables

2.4.1 Physicochemical properties

2.4.1.1 Binder concentration

According to trials done by Smith & Nienow (1983) an increase in the binder concentration will result in faster particle growth. Dadkhah & Tsotsas (2014) agreed and also saw an increase in the formation of agglomerates and higher agglomerate porosity with an increase of binder concentration. Different binders would, however, react differently in granulation systems due to a difference in material properties. A change in concentration can affect certain liquid properties such as viscosity and surface tension.

Viscosity and surface tension influences the distribution of the binder liquid on the surface of the granules. Smith & Nienow (1983) and Pont *et al.*, (2001) concluded that a higher binder viscosity would prohibit the binder from covering the entire surface of the particle, making layered growth less feasible than with a lower viscosity binder. Schæfer (2001) also indicated that a higher viscosity would change the wettability of the particles and determined that this influenced the particle growth mechanism as well as the particle shape, decreasing particle sphericity. Iveson *et al.* (2001) also concluded that the governing growth mechanism may be altered by a change in binder viscosity.

Pont *et al.* (2001) used surfactant to induce a decrease of surface tension; the results obtained indicating that a decrease in surface tension leads to less particle growth.

2.4.1.2 Binder spray rate

Tan *et al.* (2006) established that different binder spray rates had little effect on size of the granules they produced, but the amount of binder injected into the system, by mass, showed a visible effect on granule size and was identified as the rate determining step of this process. In order to compare various amounts of binder injected into the system Tan *et al.* (2006) defined a binder to particle ratio defined by equation 2.6.

$$\frac{B}{P} = \frac{t \times Sprayrate}{Particle\ Mass} \qquad [2.6]$$

Mort & Tardos (1999) suggested that the final granule size distribution is dependent on the degree of binder distribution within the fluidised bed, where well distributed binder will result in the homogeneous distribution of granule properties.

The moisture content in the fluidised bed influences the overall performance of the process and is therefore a critical parameter to control (Faure et al., 2001). It was established that a higher binder spray rate increased particle growth due to an increase in both moisture content and droplet size. One method to control the moisture content is by adjusting the nozzle spray rate during granulation. Närvänen et al. (2008) determined that pulsed spray would be an effective way of controlling the granulation process. This allows a regular drying and rewetting sequence which minimises humidity in the bed.

2.4.1.3 Binder temperature

The effects of bed temperature and fluidising air temperature are discussed widely in literature, while the effect of binder temperature on granule properties and the granulation system is not. Possible explanations could be that the overall process temperature or

fluidising air temperature has such a large effect that the binder temperature seems negligible.

2.4.1.4 Initial particle shape and size

Becher & Schlunder (1998) experimented by using both a strong and weak agglomerating system. When starting off with a smaller initial particle size in a strong agglomerating system, larger agglomerates were formed than when larger initial sized particles were used. Zhai *et al.* (2009) also studied the effect of initial particle size and saw an increase in granule growth rate with a smaller starting particle size. A decrease in final granule size was also observed.

The strength of agglomerated particles depend on the shape of the solid particles before agglomeration. Irregular shaped particles can interlock, increasing particle strength and reducing the amount of binder required for agglomeration, while round particles will decrease agglomerate strength (Schæfer, 2001)

As the particle shape factor (an indication of the closeness of a particle shape to that of a perfect sphere) increases, the capillary tension or adhesion strength decreases as observed by the term/symbol ϕ in equation 2.3. Pont *et al.* (2001) compared the growth of glass beads and hydrophobic sand particles, and determined that in the initial operating time the growth kinetics for these two particle were the same. After a while, the glass beads had a slower growth rate than that of the sand particles. Non-spherical particles have a larger contact area which promotes growth, which also explains why an increase in shape factor can decrease growth rate.

During a study by Pont *et al.* (2001), contact angle was examined by using a chemical surface treatment with hydrophobic and partly hydrophobic particles to increase the contact angle. A decrease in contact angle was found to favour agglomeration.

2.4.1.5 Atomizing air pressure

Liu *et al.* (2013) determined that an increase in atomising air pressure caused a decrease in granule size and attributed it to a decrease of spray droplet size with an increase in atomising air pressure. A faster initial particle growth stage is seen when smaller droplets are injected into the system, which can be attributed to the higher collision rate between particles and smaller but more droplets, while a faster secondary particle growth stage occurs with larger droplets. This is due to the formation of successful aggregates when larger droplets dampen kinetic energy more successfully. The overall granule size and growth rate is seen to increase with a larger droplet size (Tan *et al.*, 2006).

Atomising air pressure not only influences droplet size but also the spray angle and speed of these droplets. In addition, Zhai *et al.* (2009) concluded that an increase in droplet size can influence the particle shape factor and particle density.

2.4.2 Particle properties

2.4.2.1 Particle size

Närvänen *et al.* (2008), Kukec *et al.* (2012) and Veliz Moraga *et al.* (2015) constructed cumulative particle size distributions in order to model granule size. Närvänen *et al.* (2008) used the relative width (RW), dictated by equation 2.7, of the granule size distribution to model granule size.

$$RW = \frac{d_{90} - d_{10}}{d_{50}} \quad [2.7]$$

With d_{10}, d_{50} and d_{90} referring to the particle diameter at the 10%, 50% and 90% points of the cumulative distribution. Mean granule diameter, the d_{50} value, was also used by various authors to compare different size distributions for fluidised bed granulation (Aleksić *et al.*, 2015; Behzadi *et al.*, 2005; Wong *et al.*, 2013).

2.4.2.2 Particle shape

Dadkhah & Tsotsas (2014) suggested characterising agglomerate particle shape by investigating circularity, roundness or aspect ratio. Authors such as Abberger *et al.* (2002), Bodhmage (2006) and Talu *et al.* (2000) all used particle circularity to characterise particle shape with the use of image analysis software.

Circularity, also called shape factor, gives an indication of sphericity with a value of one indicating perfect sphericity and lower values associated with less perfect sphericity (Parikh, 2009). Circularity is calculated using equation 2.8.

$$Circularity = \frac{4\pi A}{P^2} \quad [2.8]$$

Where A denotes the projected area and P the particle perimeter.

2.4.2.3 Particle flowability

Both the Carr Index, shown by equation 2.9, and the Hausner Ratio, shown by equation 2.10, are used to characterise particle flow and are calculated using bulk and tapped density (Patel *et al.*, 2010).

Carr's Index

$$CI = \frac{(TD - BD)}{TD} \times 100 \quad [2.9]$$

Hausner Ratio

$$HR = \frac{TD}{BD} \quad [2.10]$$

The flowability for various Hausner ratios and compressibility indices can be seen in Table 2.6. For this study the Carr's index will be used to characterise flowability.

Table 2.6 Flowability scale for Hausner ratio and compressibility Index (Taken from Patel et al., 2010)

Flow Characteristic	Compressibility Index (%)	Hausner Ratio
Excellent	≤10	1.00 – 1.11
Good	11 – 15	1.12 – 1.18
Fair	16 – 20	1.19 – 1.25
Passable	21 – 25	1.26 – 1.34
Poor	26 – 31	1.35 – 1.45
Very Poor	32 – 37	1.46 – 1.59
Very, Very Poor	>38	>1.60

2.4.2.4 Porosity

Granule Porosity refers to the ratio of void space to the total granule mass or volume. Various methods to determine granule porosity is mentioned in literature, e.g. X-ray micro-tomography was used by both Rajniak *et al.* (2007) and Rieck *et al.* (2015), while Walker *et al.* (2005) used density measurements to calculate porosity and Petrovic *et al.* (2011) made use of a mercury porosimeter. Porosity in this study is determined with an oil absorption technique, as detailed in Chapter 3.

2.4.2.5 Granule strength

According to Mort & Tardos (1999) a granule can suffer from various methods of breakage and the degree to which breakage occurs will depend on material properties such as hardness, particle shape and impact conditions inside the bed. One method to quantify the granules' tendency to succumb to breakage is to determine the granules' abrasion resistance. Rutland (1986) defines abrasion resistance as a granule's resistance to form fines and powder due to the contact granules have with equipment as well as with each other. This is done by exposing the granules to abrasive actions and establishing the the amount of formed powders and fines. Table 2.7 gives the value of the abrasion resistance of various fertilisers, with a low degradation percentage indicating a high particle abrasion resistance.

Table 2.7 Abrasion resistance of various fertilizer including ammonium nitrate (Taken from Rutland, 1986)

Type of fertilizer	Abrasion Resistance (% degradation)
Prilled urea	21.0
Granular Urea	0.4
Prilled Ammonium nitrate	7.8
Granular potassium chloride	1.4

Jansens (2000) states that granules formed by granulation have a higher abrasion resistance than particles formed by prilling. Therefore we can expect lower degradation values for granules produced by granulation than granules produced by prilling.

2.5 Modelling of the fluidised bed granulation process

There are various methods to model any process, especially granulation, ranging from mechanistic or white box modelling to empirical or black box modelling (Cameron *et al.*, 2005).

2.5.1 Different modelling approaches

2.5.1.1 Mechanistic models

Typically mechanistic models combine the most basic forms of chemistry and physics into creating a model. Cameron *et al.* (2005) identified two key aspects that make up mechanistic models; 1) conservation, which includes thermodynamic fundamentals for mass, momentum and energy and population balances and 2) constitutive, referring to the development of relationships to establish valuable properties or mechanisms throughout systems.

According to Iveson *et al.* (2001) three main mechanisms need to be considered when modelling granulation. These include nucleation, particle growth and breakage. Developing mechanistic models are more time consuming and complex than using an empirical approach and will need some form of data fitting, which necessitates an adequate amount of data. With this being said, these models can yield a lot of insight into the process. (Cameron *et al.*, 2005).

A variety of mechanistic modelling techniques used in modelling a FBG is summarised in Table 2.8

Table 2.8 Mechanistic modelling techniques used on FBGs (summarised from various sources)

Author	Modelling Technique	Description
(Nagaiah *et al.*, 2008)	Three-dimensional continuum model	Developed from earlier derived models for mass and energy transfer of particles, liquid film and air, and solved using the Euler and finite method.
(Goldschmidt *et al.*, 2003)	Discrete Element modelling	Developed from the discrete hard-sphere particle model for fluidised beds to describe particle to droplet coalescence and agglomeration
(Saleh *et al.*, 2003)	Population balance model	A mathematical model based on the various rate processes with the assumption that layering and agglomeration are size dependent and solved using a fourth order Runge-Kutta-Merson algorithm.
(Hussain *et al.*, 2015)	Monte-Carlo Simulation	A constant number Monte-Carlo used as a virtual fluidised bed granulator implemented with various rate processes and compared to one-dimensional population balance.

2.5.1.2 Empirical or statistical models

Empirical models are created from a real series of input (x) and output (y) plant data where the model parameters are adjusted to have the best fit of the collected data (Cameron *et al.*, 2005). In the granulation process the selected input variables refer to material properties and process conditions and the output variables to product granule properties (Faure *et al.*, 2001).

This method is ideal for control applications in situations where no substantial understanding of the model is needed. One of the drawbacks of this method is that the model is restricted to the data range used (Cameron *et al.*, 2005). Table 2.9 gives a few examples of empirical modelling work done on FBGs.

Table 2.9 Empirical modelling techniques used on FBG

Author	Modelling Technique	Description
(Liu *et al.*, 2013)	Box-Behnken Design	Three factor, three level design to construct second order polynomial models and quadratic response surface methodology.
(Närvänen *et al.*, 2008)	Central Composite Design	Three factor, three level face-centred central composite design, with three midpoint repetitions, to obtain second order polynomial models, simplified by a backwards multi-linear regression method.
(Albuquerque *et al.*, 2010)	Granule Quality Index	Parameters are selected for the index, standardisation and aggregation of these parameters are done. Centre of gravity design used for design of experiments.

2.5.2 Statistical modelling

This study was conducted on an actual production plant with real input and output values, with the aim of controlling and predicting granule quality and thus a statistical approach to modelling was chosen. Using a statistical approach assists in determining the effects of the variables chosen for this study without having to investigate all variables associated with the fluidised bed. In the following section the statistical modelling techniques used in this study are discussed.

2.5.2.1 Design of experiments

A wide variety of experimental designs exist such as a full factorial and fractional factorial design, central composite design, mixture design and a saturated design. The choice of design depends on the objective of the study. Lazic (2004) states that if the optimum and shape of the response surface is unknown before experimental work is conducted it is important to choose an experimental design that will give the largest amount of information for the least amount of design points, called optimal designs. One such design which allows the collection of the most data with the least amount of design points is the central

composite design (Ferreira *et al.*, 2007) and is therefore used as the experimental design method for this study.

Central composite design is a popular design of experiments method presented by Box and Wilson in 1951 and is primarily used in the estimation of second order response surfaces. The design comprises of three parts: a centre point (n_o), factorial design points (n_f) and axial points (n_α). The factorial design points are used to estimate linear models with or without variables interactions and can either be fractional or full factorial. Full factorial consists of all possible variables and level combinations while fractional factorial only uses certain variable and level combinations resulting in less experimental work. The centre point indicates if the system contains any curvature while the axial points allows for the estimation of the curvature in a second order model (Lazic, 2004; Park *et al.*, 2003; Phan-Tan-Luu & Sergent, 2009). A schematic representation of the design is shown in Figure 2.5.

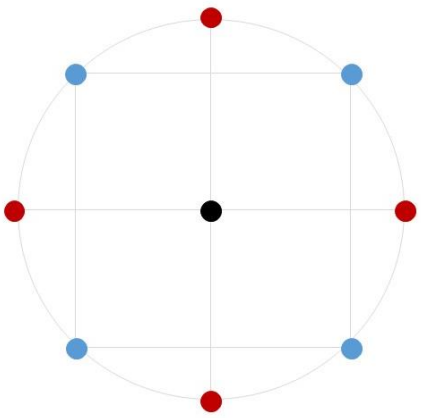

Figure 2.5 Central composite design with ● centre points ● axial points ● factorial points adapted from Ferreira et al. (2007)

Using these various sections of the design, the number of design points *N*, in a central composite design can be calculated using equation 2.11 and is simplified for a 2 level fractional factorial design in equation 2.12 with k referring to the number of factors used during the experiments.

$$N = n_f + n_\alpha + n_o \quad [2.11]$$

$$N = 2^{k-1} + 2k + n_o \quad [2.12]$$

There are two basic design considerations when it comes to a central composite design, namely the rotatability and orthogonality. A design is considered rotatable when any rotation of the design allows the user to collect the same amount of data (Park *et al.*, 2003).

The distance from the centre point to the axial points, α, for a rotatable design is calculated using equation 2.13.

$$\propto = {n_f}^{(k-1)/4} \qquad [2.13]$$

An orthogonal design allows the estimation of main and interaction effects that are independent of one another. An added benefit of using an orthogonal design is the ease of the calculations (Park *et al.*, 2003). Equation 2.14 presents the calculation of α for this design.

$$\propto = \left\{ \left[\left(n_f + n_\alpha + n_o\right)^{\frac{1}{2}} - {n_f}^{\frac{1}{2}} \right]^2 \times \frac{n_f}{4} \right\}^2 \qquad [2.14]$$

In order to obtain a design close to both a rotatable and orthogonal design, α is calculated using equation 2.15 for a rotatable design and centre points have to be added to adhere to the following condition:

$$n_0 \gg 4{n_f}^{1/2} + 4 - 2k \qquad [2.15]$$

Using all of the information above a design matrix can be obtained. The design matrix is then used to perform the experimental investigation, as outlined in Table 3.5 and 3.6 in Section 3.3.1.2.

2.5.2.2 Spearman's correlation matrix

The Spearman's rho value, r_s, is used to identify the strength and the direction of a monotonic relationship between two variables from a data set. A monotonic relationship suggests that, as the value of one variable increases, the value of another variable will either increase or decrease. Spearman's rho is calculated using the rank of the data and the average of the position in ascending order of data values, rather than the data itself as can be seen in equation 2.16 (Zhang *et al.*, 2016).

$$r_s = \frac{\sum_{i=1}^{n}\{(x_i - \bar{x})(y_i - \bar{y})\}}{\sqrt{\sum_{i=1}^{n}(x_i - \bar{x})^2}\sqrt{\sum_{i=1}^{n}(y_i - \bar{y})^2}} \qquad [2.16]$$

In this equation x_i is the rank of X_i, y_i the rank of Y_i, and $\bar{x}$ and $\bar{y}$ the average rank values of X and Y. This calculation will present a value of $-1 \leq r_s \leq 1$, where a negative r_s value for two variables indicates that a lower value of one variable is linked to higher value of the other variable, and a positive r_s value that a high value of one variable is linked to higher value in the other variable (Puth *et al.*, 2015). According to Prion & Haerling, (2014) the rule

of thumb when it comes to r_s values is that any value below 0.21 indicates a negligible effect, values between 0.21 and 0.40 are classified as weak, values between 0.41 and 0.60 are moderate, values of 0.61 to 0.80 is classified as strong and values of 0.81 and up are considered as very strong.

2.5.2.3 Regression analysis

Regression is a technique used to develop a numerical relationships between independent and dependent variables using experimental data, and showcases the influence of these independent variables on the dependent variable. In engineering applications regression is applied to a wide variety of situations including complex engineering systems (Lazic, 2004).

2.5.2.3.1 Multiple linear regression

In the event where a relationship of the effect of multiple independent variables on a dependent variable is needed, multiple linear regression is used. The general form of a multiple linear regression model can be seen in equation 2.17.

$$Y = b_0 + b_1X_1 + b_2X_2 + \cdots + b_pX_p + \varepsilon \quad [2.17]$$

In this equation Y denotes the dependent variable and X_i the independent variables at a specific index number in a data set. The regression coefficients are denoted by β_0 and β_i. The regression coefficients are unknown and have to be determined. The random error or residual is represented by ε and refers to the variation of dependent variable Y not accounted for by the linear relationship. The magnitude of a regression coefficient gives a clear indication of the influence associated with a particular factor, a coefficient with a positive sign indicates an increase in response with an increase in the factor (Lazic, 2004).

2.5.2.3.2 Linear regression with interactions

A linear regression model consists of regression coefficients and a bias coefficient b_0. The general form of a linear regression model can be seen in equation 2.18 (Lazic, 2004).

$$\hat{Y} = b_0 + \sum_i^k b_iX_i + \sum_i^k b_{ij}X_iX_j + \varepsilon \quad [2.18]$$

Here, $\hat{Y}$ refers to the response value, b_i to linear regression coefficients and b_{ij} to regression coefficients associated with interactions. From the design matrix and operational matrix an arithmetic matrix can be constructed, transforming the real x_i values into coded X_i values as seen in equation 2.19.

$$X_i = \frac{x_i - x_{i0}}{\Delta x}$$

[2.19]

X_i denotes the calculated coded value for the i^{th} factor, x_{i0} the real factor null value, x_i the real factor current value and Δx the value of the variation factor interval. The method of least squares is then used to obtain the regression coefficients, as shown by the following equations:

$$b_0 = \frac{\sum_1^N \bar{Y}_u}{N}$$

[2.20]

$$b_i = \frac{\sum_1^N X_{iu}\bar{Y}_u}{\sum_1^N X_{iu}^2} = \frac{\sum_1^N X_{iu}\,\bar{Y}_u}{N}$$

[2.21]

$$b_{ij} = \frac{\sum_1^N X_{iu}X_{ju}\bar{Y}_u}{\sum_1^N X_{iu}^2} = \frac{\sum_1^N X_{iu}X_{ju}\bar{Y}_u}{N}$$

[2.22]

Here, X_{iu} and $\bar{Y}_u$ are the values of factor X_i, the response average at the u^{th} design point, N the total number of design points and u the current design point number. Both the statistical significance and the lack of fit the regression coefficients should be determined in order to verify the linear model obtained (Lazic, 2004).

2.5.2.3.3 Second order regression

The general form of a second order regression model can be seen in equation 4.23 (Lazic, 2004).

$$\hat{Y} = b_0 + \sum_i^k b_i X_i + \sum_i^k b_{ij} X_i X_j + \sum_i^k b_{ii} X_{ii}^2 + \varepsilon$$

[2.23]

In addition to basic variable regression coefficients and two-way variable interaction regression coefficients, this model consist of a second order term $b_{ii}X_{ii}^2$. When a rotatable second order design is used, the regression coefficients can be obtained using equations 2.24 – 2.27.

$$b_0 = a_1 \sum_{1}^{N} Y_u - a_2 \sum_{1}^{k} \sum_{1}^{N} X_{iu}^2 \times Y_u$$

[2.24]

$$b_i = a_3 \sum_{1}^{N} X_{iu} \times Y_u$$

[2.25]

$$b_{ij} = a_4 \sum_{1}^{n_j} X_{iu} X_{ju} Y_u$$

[2.26]

$$b_{ii} = a_5 \sum_{1}^{N} X_{iu}^2 \times Y_u + a_6 \sum_{1}^{k} \sum_{1}^{N} X_{iu}^2 \times Y_u - a_7 \sum_{1}^{N} Y_u$$

[2.27]

The values for a_1 to a_7 for five factors full and fractional factorial designs can be seen in Table 2.10.

Table 2.10 Coefficient values of a1 - a7 (taken from Lazic, 2004)

Number of Factors	**Coefficients**						
	a_1	a_2	a_3	a_4	a_5	a_6	a_7
5*	0.1591	0.0341	0.0417	0.0625	0.0312	0.0028	0.0341
5	0.0988	0.0191	0.0231	0.0312	0.0156	0.0015	0.0191

The design matrix for a second-order central composite design is transformed to provide orthogonality and to ease regression coefficient calculations (Lazic, 2004). This transformation is done by using equation 2.28.

$$(X'_{iu})^2 = X_{iu}^2 - \bar{X}_{iu}^2$$

[2.28]

With $\bar{X}_{iu}^2$ calculated using the following equation:

$$\bar{X}_1^2 = \frac{\sum_1^N X_1^2}{N}$$

[2.29]

The regression coefficients b_i and bij are calculated using equations 2.21 and 2.22 in section 2.6.2.3.2. Coefficient b_{ii}, the second order regression coefficient, is calculated using equation 2.30.

$$b_{ii} = \frac{\sum_1^N (X'_{iu})^2 \bar{Y}_u}{\sum_1^N \left(X'_{iu}\right)^2}$$

[2.30]

The regression coefficient b_0 can then be determined using equation 2.31.

$$b_0 = b'_0 - b_{11}\bar{X}_1^2 - b_{22}\bar{X}_2^2 - \cdots b_{kk}\bar{X}_k^2$$

[2.31]

With b'_0 calculated by:

$$b'_0 = \frac{\sum_1^N \bar{Y}_u}{N}$$

[2.32]

2.5.2.4 Model quality

2.5.2.4.1 Analysis of variance

Analysis of variance (ANOVA) is used to test the variations observed in a regression model and also to provides the basis for determining significance (Lazic, 2004). ANOVA uses the sum of squared ratios of different variances to determine if a significant variation exists in the mean of different observational groups. The different variations and their calculations can be seen in Table 2.11.

Table 2.11 ANOVA Calculations adapted from Ferreira *et al.* (2007)

Variation Source	Degrees of freedom	Sum of Square Calculation		Mean Square Calculation	
Regression	p - 1	$SS_R = \sum_i^m \sum_j^{n_i} (\hat{y}_i - \bar{y})^2$	[2.33]	$MS_R = \frac{SS_R}{(p-1)}$	[2.34]
Residual	n - p	$SS_r = \sum_i^m \sum_j^{n_i} (y_{ij} - \hat{y}_i)^2$	[2.35]	$MS_r = \frac{SS_r}{(n-p)}$	[2.36]
Lack of fit	m - p	$SS_{lof} = \sum_i^m \sum_j^{n_i} (\hat{y}_i - \bar{y}_i)^2$	[2.37]	$MS_{lof} = \frac{SS_{lof}}{(m-p)}$	[2.38]
Pure Error	n - m	$SS_{pe} = \sum_i^m \sum_j^{n_i} (y_{ij} - \bar{y}_i)^2$	[2.39]	$MS_{pe} = \frac{SS_{pe}}{(n-m)}$	[2.40]
Total	n - 1	$SS_T = \sum_i^m \sum_j^{n_i} (y_{ij} - \bar{y})^2$	[2.41]		

Here, $\hat{y}_i$,y_{ij}, $\bar{y}_i$ and $\bar{y}$ denotes the predicted response, the real response, the average response value at that level and the average of all the responses respectively. The degrees of freedom is also calculated in order to determine the mean square, with p, the number of coefficients in the model, n, the total number of observations, m, the number of levels used for the independent variables and n_i the number of repeats at that level.

2.5.2.4.2 Regression coefficient significance

A test of significance for regression coefficients are done in order to define the confidence interval they fall in. Insignificant statistical regression coefficients can be omitted from regression models which provides reproducible results from a simplified model. A regression coefficient is said to be statistically significant when the absolute value of the coefficient is higher than the selected confidence interval (Lazic, 2004). For a 95% confidence interval a regression coefficient is said to be significant if it falls in the following interval:

$$b_i - 2S_{b_i} \leq \beta_i \leq b_i + 2S_{b_i} \quad [2.42]$$

With b_i, the calculated value of the regression coefficient, β_i the real value and S_{b_i} the variance in the calculation of the regression coefficient, calculated in the following equation:

$$S_{b_i}{}^2 = \frac{S_y{}^2}{n - n_i}$$

[2.43]

Here, $S_y{}^2$ is the reproducibility variance as calculated by equation 2.44.

$$S_y{}^2 = \frac{SS_T}{n(n_i - 1)}$$

[2.44]

2.5.2.4.3 Coefficient of determination

The coefficient of determination or R^2 gives an indication of the amount of variation the model accounts for. Lee *et al.* (2015) states that R^2 can overestimate the fit of the model in the presence of a lot of predictors and suggest using adjusted R^2, which takes all independent variables into account and only increase when an independent variable has a positive effect on the response. The value of both R^2 and adjusted R^2 is between 0 and 1, with 1 indication a very good fit and zero a total lack of fit. Equations 2.45 and 2.46 represent the calculations for both coefficients.

$$R^2 = 1 - \frac{SS_r}{SS_T}$$

[2.45]

$$R_a^2 = 1 - \frac{(1 - R^2)(n - 1)}{n - P - 1}$$

[2.46]

2.5.2.4.4 Lack of fit

Ficher's criterion or the F-test, as it is more commonly known, is used to test regression models for their lack of fit. The F value is calculated using equation 2.47 and then compared to its tabulated value at the corresponding degrees of freedom and level of significance. If the calculated value is below the associated tabulated value, it is accepted that there is no lack of fit in the model (Lazic, 2004).

$$F = \frac{MS_R}{MS_r}$$

[2.47]

2.5.3 Previous modelling work

A lot of work was previously done on fluidised bed granulation using a central composite design and regression analysis. Kukec *et al.* (2012) used a three factor central composite design with five levels, a triplicate centre point repeat and response surface methodology (RSM) to determine the influence of independent variables (x), binder content, fluidising air temperature and process end temperature, on response variables (y), particle size distributions and particle dissolving rate.

A non-linear quadratic model was used to model the response surfaces for the factors. A significance value of p = 0.10 was chosen for the study. The correlation between the independent and response variables were illustrated using response surface plots. These plots were constructed using one fixed response variable and two independent variables, keeping the third variable at a level of zero.

Aleksić *et al.* (2015) investigated the effect of binder concentration and atomising air pressure on the response variables particle mean diameter, Carr's index, particle size distribution, aspect ratio, yield and projection sphericity using a randomized central composite design and a significance level of 0.05. The data acquired was modelled using the response surface methodology, the partial least squares method and an artificial neural network.

Wong *et al.* (2013) did a two part investigation. Part one used a randomised central composite design with six centre points to assess the influence of binder spray rate, amount of binder and spray distance on yield, mean particle size, amount of fines, amount of lumps, PSD span, roundness and Hausner ratio. The response variables were modelled using a quadratic regression analysis and then optimised. In part two the optimised values were used to investigate the interaction of the next set of variables, fluidising air flow, atomising air pressure and spray distance on the same set of response variables using a Box-Behnken design, a three factor, three level design with six centre point repeats.

Närvänen *et al.*(2008) made use of a face centred, three level, central composite design with three centre point repeats in order to determine the effect granulation spray rate, inlet air relative humidity and granulation pulsing feed might have on the particle size obtained using three different PSD analysis methods.

2.6 Summary

This aim of this study is to model the influence of the physicochemical feed properties of AN on granule quality of a real production plant. A statistical approach was chosen because

only certain variables are investigated and not the complete system, real plant data can be collected, the ability of statistical models to predict and provide interaction effects and its use throughout literature in modelling FBG. The central composite design was used because of its capability to provide the most amount of information with the least amount of experimental work. The data obtained by the central composite experimental design is then subjected to regression analysis in order obtain predictive models.

3. Experimental Procedure

3.1 Introduction

Chapter 3 contains the experimental procedure section of this study. Section 3.2 provides information on the experimental setup for the various experimental runs including the various materials used and a process flow diagram which describes the different sections of the plant with regards to the experimental work done. Section 3.3 focuses on the experimental phases together with the various measurement methods used.

3.2 Experimental setup

3.2.1 Materials used

All materials used during the experimental runs can be seen in Table 3.1.

Table 3.1 Materials used during experimental runs

Material	Description
Ammonium Nitrate (l)	Diluted ammonium nitrate solution at 90 wt% and 130 °C
Ammonium Nitrate (s)	Seed material as fine particles for the fluidised bed granulator
Water	Water used in the process
Galoryl AT Plus	Additive used to help with the crystallisation of the AN

All these materials were supplied by Omnia and are used during normal plant operation.

3.2.2 Process flow diagram

The research for this study was conducted on a Porous Granular Ammonium Nitrate Plant (PGAN). The PGAN plant consists of two identical production lines. All experimental work was conducted on one of these production lines.

3.2.2.1 Premixing tank

The premixing tank is the first section in the PGAN process. Here fresh liquid ammonium nitrate, at a temperature of 130 °C and a concentration of 90 wt%, is mixed with scrubber liquid, a weak ammonium nitrate solution produced from the PGAN scrubber at a temperature of 70 °C, and additives. The additives aid in the crystallisation of ammonium

nitrate, increasing the particle strength and porosity of the final product. This section is schematically represented in Figure 3.1. After the liquid ammonium nitrate is acceptably agitated, it is drawn from the premixing tank into the falling film evaporator.

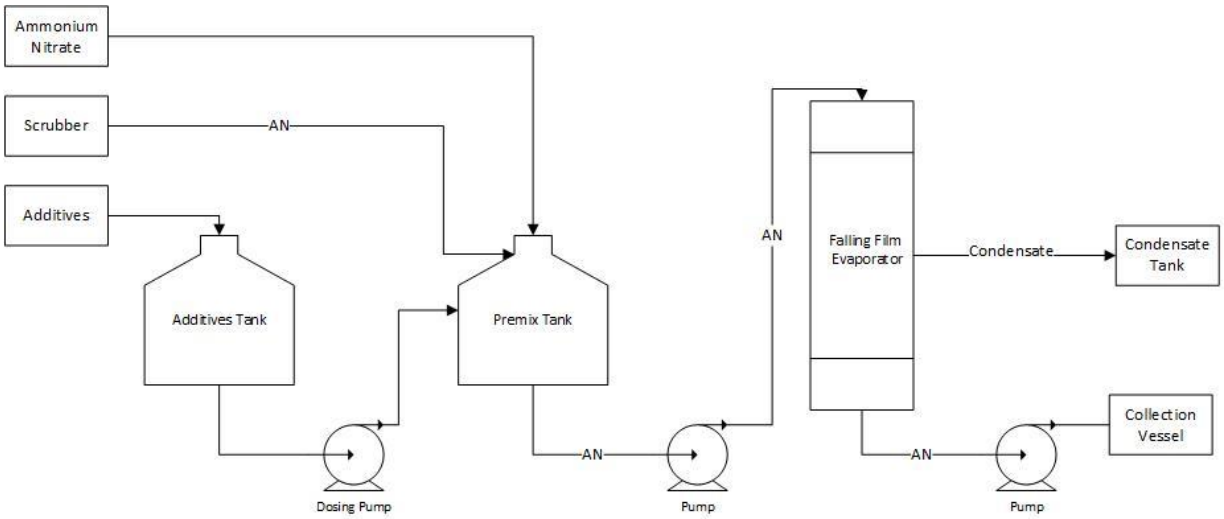

Figure 3.1 Additive, premixing and falling film evaporator section

3.2.2.1 Falling film evaporator (FFE)

The liquid ammonium nitrate feed from the premixing tank enters the falling film evaporator tubes, as shown in Figure 3.1. Steam is applied to the shell side of the evaporator to induce the evaporation of water and thus increase the concentration of ammonium nitrate up to a maximum of 96 wt % at a temperature of 135 °C.

The concentrated ammonium nitrate is collected in a liquid chamber at the bottom of the evaporator from where it is pumped to the collection vessel. In the collection vessel the temperature of the concentrated ammonium nitrate is maintained between 115 °C and 135 °C by internal steam coils. From the collection vessel the ammonium nitrate liquid is pumped to the fluidised bed granulator.

The concentration of the ammonium nitrate is measured by using the boiling point elevation (BPE) of the AN leaving the falling film evaporator. This value is used to control the heat applied to the evaporator. The BPE is calculated using the AN liquid temperature and saturated vapour pressure temperature which gives a differential temperature as seen in equation 3.1. The steam pressure to the heater is then controlled using the differential temperature.

$$BPE\ (°C) = BP\ of\ AN\ exiting\ the\ FFE\ (°C) - BP\ of\ water\ at\ pressure\ in\ the\ FFE\ (°C) \quad [3.1]$$

3.2.2.2 Fluidised bed granulator

The Porous Granular Ammonium Nitrate (PGAN) vessel is divided into two regions, the granulation section and the cooling section as shown in Figure 3.2. Each of these regions has its own unique characteristics. In the PGAN fluidised bed granulator section the ammonium nitrate solution is sprayed into the granulator through ten side spraying nozzles onto recycled granules (seed particles). Granule growth happens at this point as the mean particle size of the particles increases as it travels through the fluidised bed.

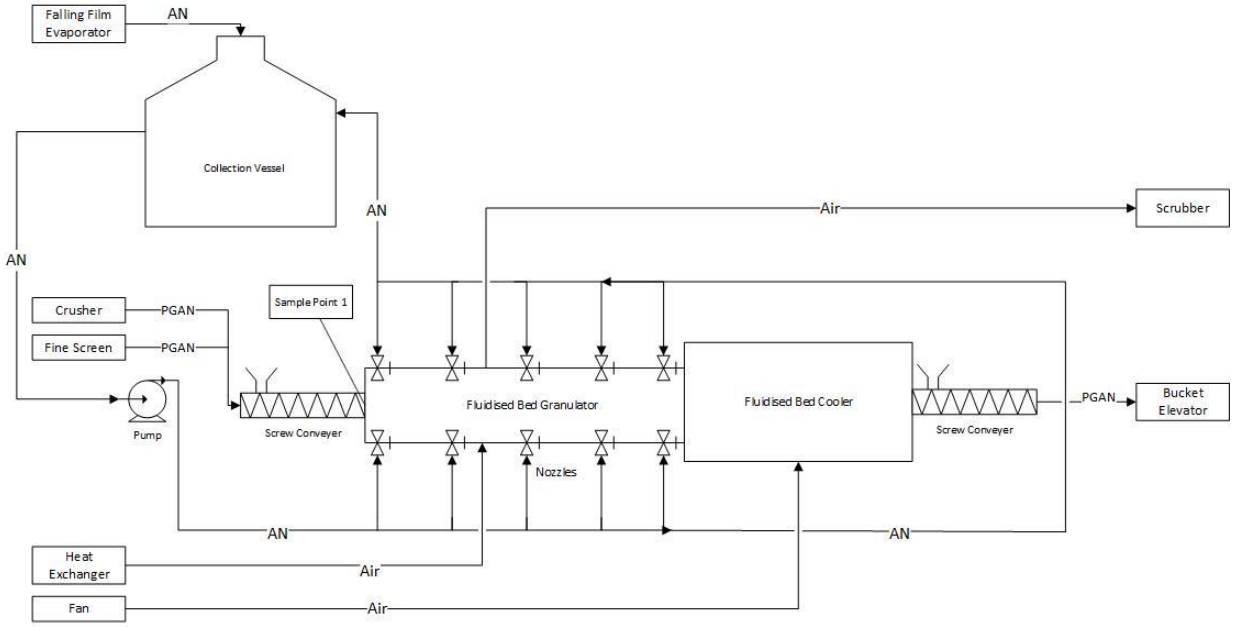

Figure 3.2 FBG section

The AN liquid is atomised by the nozzles using heated plant air at 95 °C to 120 °C. The ammonium nitrate not sprayed into the bed by the nozzles is recycled to the collection vessel. The liquid flow rate to the bed is controlled by opening or closing one or more nozzles. The effective atomisation of ammonium nitrate depends largely on the pressure of the ammonium nitrate and thus the pressure of the ring main. The ring main refers to the AN piping from the collection vessel around the granulator which branches out to the various nozzles and recycles the excess AN back to the collection vessel as seen in Figure 3.2. The pressure is this ring main is controlled in order to create back pressure. The atomising air pressure to the nozzle is maintained equal to that of the back pressure in the ring main. In order to vary the atomising air pressure a difference is initiated between the atomising air pressure and the back pressure.

The ammonium nitrate seed material is fed to the granulator by a screw conveyer. The particulate feed to the granulator is composed of recycled fines, particles from the crusher and a portion of the on-size granules. The feed from the screw conveyor into the bed is the

location of sample point 1, as indicated on Figure 3.2. The samples taken here were analysed for size in order to determine the feed particle d_{50} to the bed.

The fluidising air, at a temperature ranging between 100 °C and 125 °C enters the bed through three dampers beneath the bed of seed material and flows vertically up through a perforated plate and the bed and exits the granulator at the top. The fluidising air velocity is adjusted by the dampers to ensure sufficient fluidisation and mixing of particles. The fluidising air in the granulator and cooler is pre-treated to reduce its relative humidity. The granules are fluidised from the granulator to the cooling section where chilled air, which enters through five dampers at the bottom of the bed at a temperature of 15 °C, is used to reduce the temperature of the granules to 55 °C.

From the cooling section of the fluidised bed the cooled granules are transported into the bucket elevator for screening by means of a screw feeder. The speed of the screw feeder is determined by the bed material level in the granulator.

3.2.2.3 Crusher and screening

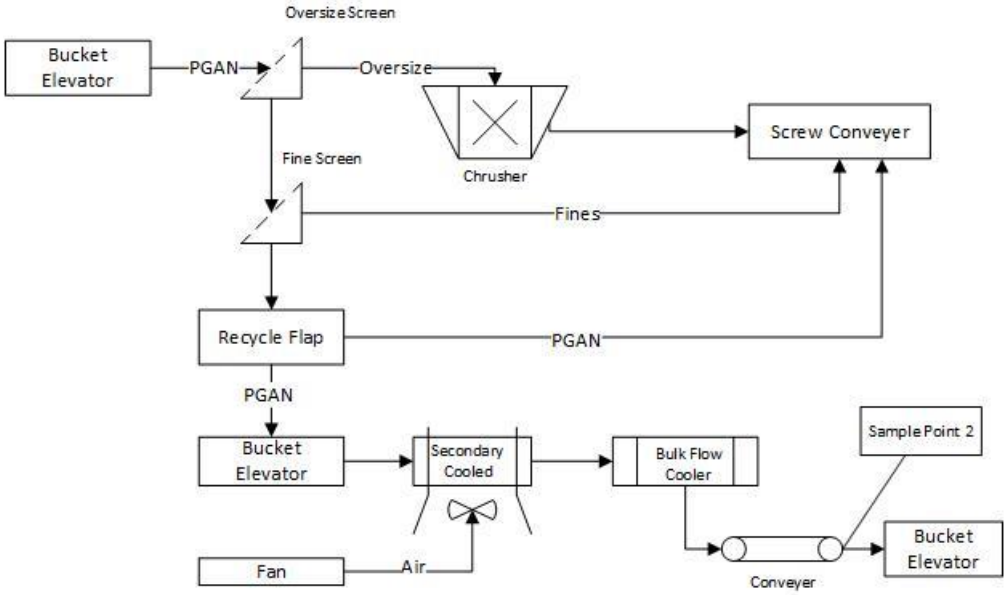

Figure 3.3 Crusher and cooler section

In the screening section depicted in Figure 3.3, the primary screen separates the granules into on-size and oversize particles. On-size granules include fines and particles smaller than 3 mm and oversize particles refers to particles larger than 3 mm. All oversize particles are transported to the crusher through a chute before being recycled back to the granulator as seed material. Spacers are inserted into the crusher in order to change the crushing size.

On-size particles, particles with a size in the range of 1 – 3 mm, and fines, particles smaller than 1mm, are transported to a secondary screen where they are separated. The fines are

recycled to the granulator with a portion of the on-size granules also as seed material, depending on various plant conditions, while the rest of the on-size granules are sent for final screening by the polishing screens. During final screening, particle size is double checked and fines are again removed from on-size granules and recycled to the granulator. All recycle streams are mixed and sent back into the granulator by the recycle screw feeder.

The final on-size granules are transported from the polishing screen to the secondary cooler for additional cooling and also to remove excess dust stuck to the granules. The granules are cooled to 45 ^{o}C and then either sent to the bulk flow cooler or allowed to bypass it. The conveyer belt leaving the bulk flow cooler is used as sampling point two. Samples taken here were used to determine product size, porosity, degree of abrasion, circularity and both bulk and tapped densities.

3.3 Experimental

3.3.1 Experimental program

The experimental program was divided into three phases. Phase one consisted of a broad experimental range which was used to give a broad process overview before commencing with phase two. Phase two focused on the physicochemical specific variables while phase three consisted of experimental runs with the purpose of collecting data for validating the models obtained in phase two.

3.3.1.1 Phase one

Phase one consisted of exploratory experimental work to establish variable ranges, main effects and plant responses. A summary of the variables, ranges and response variables measured for this phase is presented in Table 3.2.

Table 3.2 Experimental phase one: independent and response variables

Independent Variables	**Range**	**Response Variables**
Fluidising Air Flow (FAF)	11 000 - 13 000 Nm^3/hr	Porosity True Density Product d_{50} Circularity
Fluidising Air Temperature (FAT)	90 – 135 °C	
Spray Liquid Temperature (SLT)	120 – 133 °C	
Spray Liquid Concentration (SLC)	88 – 69 wt%	

Spray Liquid Flow Rate (SLF)	3.5 – 13 ton/hr	
Atomising Air Pressure (AAP)	250 – 375 kPa	
Atomising Air Temperature (AAT)	110 - 150°C	
Feed Particle Size (FPS)	1.0 – 1.4 mm	

All process related variables were included in the experimental work done during phase one with the widest ranges possible in order to get a broad overview of the process. The experimental design for phase one is found in Table 3.3. Ten runs were conducted with all the independent variables randomised. Experimental run one was repeated (as denoted with the letter R) with the aim of determining the repeatability of the experimental runs.

Table 3.3 Experimental design for phase one

	FAF	**FAT**	**SLF**	**SLT**	**SLC**	**FPS**	**AAP**	**AAT**
1 R	13000	112.5	8.5	126.5	92	1.0	375	130
2	13000	90.0	8.5	133.0	92	1.2	250	110
3	11000	112.5	13.5	126.5	88	1.2	500	150
4	13000	112.5	8.5	120.0	88	1.4	375	130
5	9000	135.0	8.5	126.5	88	1.0	375	110
6 R	13000	112.5	8.5	126.5	92	1.0	375	130
7	9000	135.0	3.5	133.0	92	1.4	500	110
8	11000	90.0	13.5	120.0	92	1.2	250	150
9 R	13000	112.5	8.5	126.5	92	1.0	375	130
10	9000	135.0	3.5	133.0	94	1.4	500	110

For each run the independent variables were changed to their respective settings and samples were taken from the granulator feed as well as the product conveyer an hour after the settings were adapted. Thereafter three more samples were taken in half-hour intervals at the same settings. After the fourth and final samples were taken the following set of independent variables were implemented and the sampling procedure commenced in the same manner.

3.3.1.2 Phase two

Phase two, the main experimental phase, focused only on the physicochemical material feed properties of ammonium nitrate. This included variables that had a physical or chemical relation to ammonium nitrate. Physical properties include ammonium nitrate temperature, spraying rate, atomising air pressure and seed particle size while chemical properties refer to ammonium nitrate concentration.

A summary of the variables, ranges and response variables measured for phase two can be seen in Table 3.4.

Table 3.4 Experimental phase two independent and response variables

Independent Variables	**Range**	**Response Variables**
Spray Liquid Temperature	120 - 155°C	Porosity (%) Abrasion (%) Product Size (mm) Circularity Carr Index (%)
Spray Liquid Concentration	90 - 93.5 wt%	
Spray Liquid Flow Rate	3.5 – 9.5 ton/hr	
Atomising Air Pressure	250 - 375	
Seed Particle Size	1.0 – 1.4 mm	

During experimental phase two, variables such as the fluidising air temperature, fluidising air flow rate as well as atomising air temperature were held constant. The bed temperature was closely monitored and maintained at a temperature of 77°C to ensure that the product granules have the same crystal structure across all the experimental runs.

A five level central composite design for five variables was used for the experimental design of phase two. The axial distance was calculated as 2 using equation 2.13, this is the maximum distance from the centre point and thus the levels of the various factors would lie between 2 and -2. The highest value assigned to a variable with fall at level 2 and the lowest variable value will be assigned to level -2. The ranges of each of the independent variables were divided into five levels. The levels assigned to the various variables and their corresponding values are seen in Table 3.5.

Table 3.5 Central composite design levels

	Level	AAF	SLF	SLC	SLT	SPS
Maximum	2	30	9.5	93.5	155	1.4
	1	15	8.0	93.0	135	1.3
	0	0	6.5	92.0	130	1.2
	-1	-10	5.0	91.0	125	1.1
Minimum	-2	-15	3.5	90.0	120	1.0

The values in the AAF column refer to the difference induced between these two variables and is represented by Equation 3.2.

$$New\ AAF\ pressure = Backpressure - pressure\ in\ AFF\ column \quad [3.2]$$

A number of 30 runs were conducted including three centre point repeats, denoted with an R. The experimental design for phase two was obtained using STATISTICA® and is provided in Table 3.6.

Table 3.6 Experimental design for phase two

	Atomizing Air Pressure	Spray Liquid Flowrate	Spray Liquid Concentration	Spray Liquid Temperature	Feed Particle d_{50}
1	-1	-1	-1	-1	1
2	-1	-1	-1	1	-1
3	-1	-1	1	-1	-1
4	-1	-1	1	1	1
5	-1	1	-1	-1	-1
6	-1	1	-1	1	1
7	-1	1	1	-1	1

8	-1	1	1	1	-1
9	1	-1	-1	-1	-1
10	1	-1	-1	1	1
11	1	-1	1	-1	1
12	1	-1	1	1	-1
13	1	1	-1	-1	1
14	1	1	-1	1	-1
15	1	1	1	-1	-1
16	1	1	1	1	1
17	-2	0	0	0	0
18	2	0	0	0	0
19	0	-2	0	0	0
20	0	2	0	0	0
21	0	0	-2	0	0
22	0	0	2	0	0
23	0	0	0	-2	0
24	0	0	0	2	0
25	0	0	0	0	-2
26	0	0	0	0	2
27	0	0	0	0	0
27 R	0	0	0	0	0
27 R	0	0	0	0	0
27 R	0	0	0	0	0

A complete experimental design including the boiling point elevations and vacuum pressures used to obtain the various concentrations and the coinciding calculations are detailed in Appendix A.

For each run the independent variables were changed to their respective settings followed by samples taken from the granulator feed as well as the product conveyer half an hour after the process stabilised to ensure the sample points were representative of the variables' settings. After the samples were taken, the next set of variable settings were implemented. The data obtained during this phase was used to model the granulator.

3.3.1.3 Phase three

Experimental phase three consisted of 11 randomised runs of the same variables and the same ranges as used during phase two (refer to section 3.3.1.2). No experimental design

was used, different variables and level combinations were chosen than those used in the experimental design in phase two. The experimental design for phase three is seen in Table 3.7.

Table 3.7 Experimental design for phase three

Run	Atomizing Air Pressure	Spray Liquid flowrate	Spray Liquid Concentration	Spray Liquid Temperature	Seed Particle Size (mm)
1	-10	5	90	125	1,1
2	-10	5	91	135	1,3
3	-15	6,5	90	125	1,2
4	-10	6,5	91	135	1,1
5	15	3,5	90	125	1,2
6	15	5	91	135	1,2
7	10	8	90	125	1,3
8	15	8	92	135	1,3
9	-10	8	92	135	1,1
10	-10	8	93	135	1,2
11	15	6,5	92	140	1,3

As in phase two the independent variables were changed to their respective settings and samples were taken from the granulator feed as well as the product conveyer half an hour after the process stabilised to ensure representativeness of the variable set. Subsequently all variables were altered to the new set, as detailed in Table 3.7. The data obtained during this phase was used to validate the models obtained in phase two.

3.3.2 Measurement procedures

3.3.2.1 Oil absorption

An oil absorption technique based on a set standard was used to determine granule porosity. The experimental setup for the oil absorption is presented in Figure 3.4.

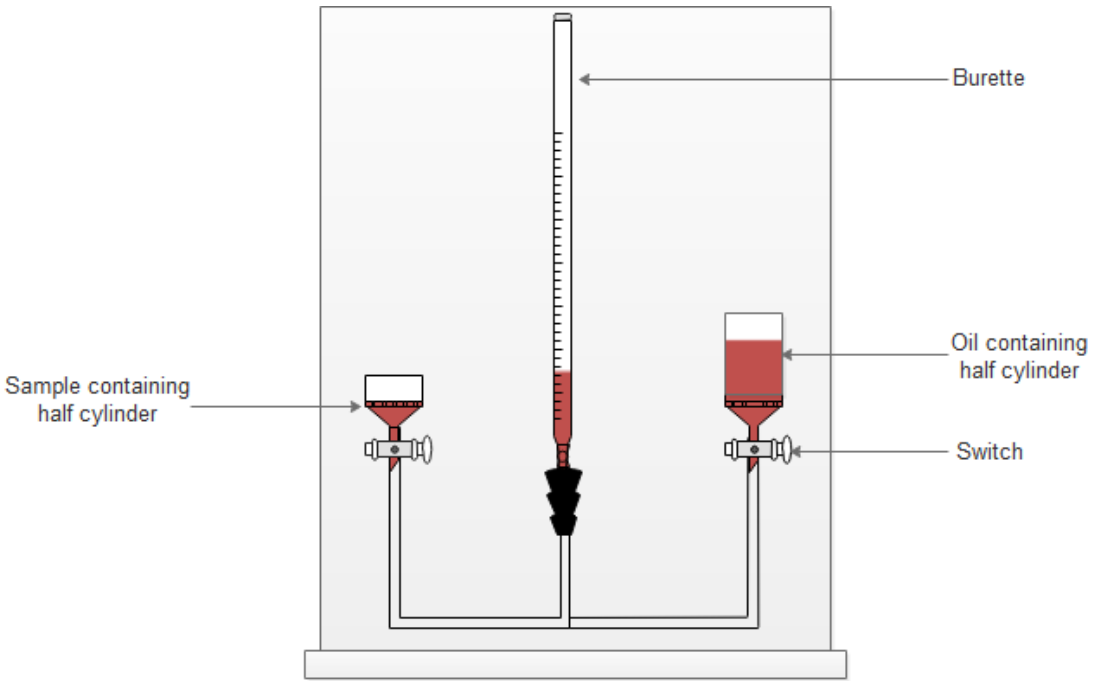

Figure 3.4 Oil Absorption Setup

The setup contained two half cylinders and a burette. Before the oil absorption measurement procedure is commenced, the sample was screened to remove fines and lumps in order to ensure that the sample is representative of the mean size. The valve of the oil containing cylinder was opened until the oil level in the burette reached the marked level and then closed. A 2.5 g portion of the sieved sample was placed into the sample cylinder and the valve of the sample containing half cylinder opened. After ten minutes this valve was closed and the sample removed and weighed again. The porosity was then calculated using the following equations:

$$V_{oil} = \frac{M_{oil}}{\rho_{oil}} \quad [3.3]$$

$$V_{AN} = \frac{M_{AN}}{\rho_{AN}} \quad [3.4]$$

$$Porosity\ (\%) = \frac{V_{oil}}{V_{oil} + V_{AN}} \quad [3.5]$$

Where V refers to the volume of oil and AN respectively, M to the mass of oil and AN respectively and ρ to the density of the oil and the AN granules respectively.

3.3.2.2 Abrasion resistance testing

The abrasion resistance testing was done in order to determine the granules' resistance to dust and fines formation due to attrition. The setup consisted of a rotary drum and a motor as presented in Figure 3.5.

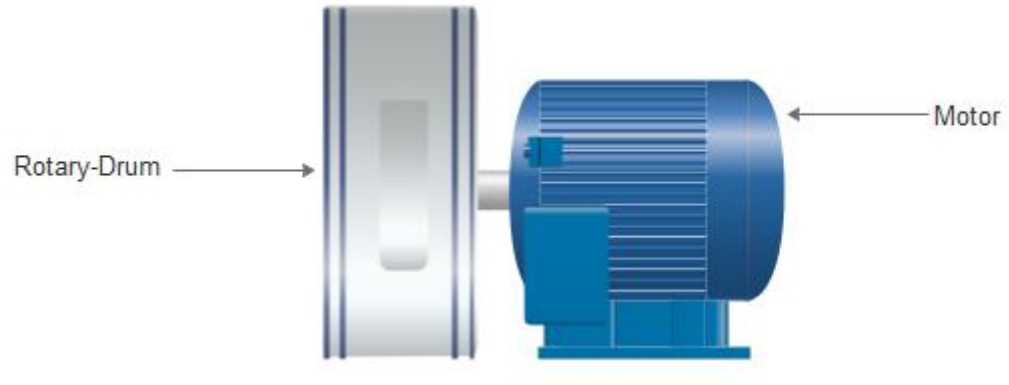

Figure 3.5 Abrasion Testing Setup

Before the abrasion testing was done the sample was sieved to eliminate fines and lumps to ensure the sample used was representative of the particle size range stated in the operational standard. A 100 cm^3 portion of the sample was measured off, weighed and then placed in the rotary-drum along with 50 stainless steel balls with a diameter of 7.9 mm and a combined weight of 100 g. The drum was subsequently rotated for 5 minutes at a speed of 30 rpm. After the 5 minute time period the sample was removed and hand screened to remove the steel balls. The sample was then screened on a 1 mm sieve using a sieve shaker and the sample portion remaining on the 1 mm sieve was weighed. The percentage degradation was calculated using Equation 3.6.

$$Degradation\,\% = 100 - 100 \times \frac{Wt\ of\ +1.00\ mm\ fraction\ recovered}{Wt\ of\ +1.00\ mm\ fraction\ charged} \quad [3.6]$$

3.3.2.3 Particle size distribution and circularity

The particle size distribution and circularity of the various samples were determined using a HAVER CPA 2-in-1 computerised particle analyser. A 150 g sample was placed into the feeding section of the particle size analyser and the program started. The vibrating feeder moved the particles past the optical camera lens. After all the particles were analysed the results of the size distribution and circularity was delivered by the software. The analyser was calibrated at a maximum and minimum particle size of 5 mm and 0.05 mm.

3.3.2.4 Bulk and tapped density

The bulk density, ρ_B, was determined by filling a 250 ml measuring cylinder with granules, which is then weighed. The experimental setup can be seen in Figure 3.6. The bulk density was calculated using Equation 3.7 where M denotes the mass of the sample and V_B the bulk volume.

$$\rho_B = \frac{M}{V_B} \quad [3.7]$$

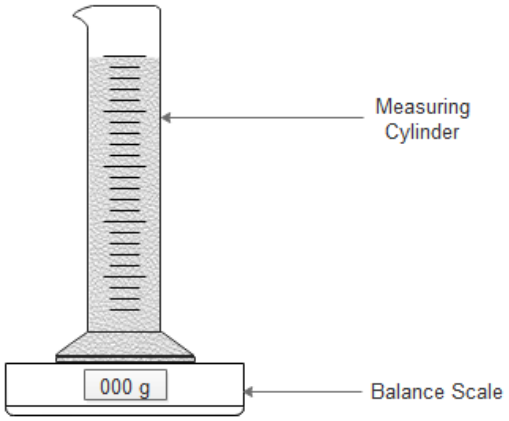

Figure 3.6 Bulk density setup

The same measuring cylinder filled with granules was subsequently hand tapped until no further volume change was noted. The new volume was then read and used to calculate the tapped density, ρ_T, using Equation 3.8 with V_T referring to the tapped volume.

$$\rho_T = \frac{M}{V_T} \quad [3.8]$$

3.3.2.5 Measurement error

The calculated measurement error for the various quality parameters can be seen in Table 3.8. The full set of error calculations can be seen in Appendix B.

Table 3.8 Experimental error for the various quality parameters

	Standard Deviation	Standard Error	Margin of Error (95% confidence)	Experimental Error (%)
Abrasion Resistance (%)	0,199	0,089	0,248	7,03
Particle Size (mm)	0,089	0,04	0,111	5,35
Particle Shape	0,002	0,0008	0,002	0,25
Porosity (%)	1,993	0,891	2,478	30,67
Flowability (%)	1,025	0,458	1,274	18,17

In Table 3.8 the standard deviation, standard error and the margin of error at a 95% confidence interval is reported. The abrasion resistance reports a ±0.248 % margin of error which is high if considering that the abrasion results obtained fell between 0.25 and 2.06 %. The margin of error obtained for porosity and flowability was ± 2.478% and ±1.274% respectively, which is also a high margin of error considering the range in which the porosity, 33.43 to 42.22%, and flowability, 2.85 to 10%, values fall.

Particle size produced a ±0.111mm margin of error which can be considered low when the particle size ranges from 1.812 and 2.433 mm. The particle shape produced a ±0.002 margin error, which is high for a circularity range that falls between 0.888 and 0.910

In the following section, the data obtained during experimental phase two will be used to develop models to describe the influence of the physicochemical material feed properties on the AN product quality.

4. Model Development

4.1 Introduction

In this chapter the development of the regression models expressing the influence of the physicochemical material feed properties on each of the quality parameters is presented. This was done by using the data obtained during phase two, which is presented in Appendix C, Table C.0.1. Models were developed using the regression results for the various quality parameters. The different models include (i) multiple linear regression models, (ii) multiple linear regression with two way variable interactions models and (iii) second order regression models in the general forms presented in section 2.5.2.3. All regression results were obtained using STATISTICA® software.

It is important to note that the significance value of the regression coefficients only gives the statistical reliability of the coefficient and does not consider the field of study nor the theoretical background. From literature and the phase one results, presented in Appendix D, it was established that all the physicochemical AN properties do in fact have an influence on the granulation quality parameters, whether they are reported significant or not. The size and direction of the effect can, however, vary from system to system. For the purpose of this study the significant regression terms will give an indication of what effects can be reported with statistical certainty, while the complete regression model describes the system as a whole.

The coefficient of determination, the F-test and significance values, discussed in section 2.5.2.4.3, 2.5.2.4.4 and 2.5.2.4.2 respectively, are mentioned throughout this chapter.

4.2 Models for particle abrasion resistance

Table 4.1 reports the regression coefficients and significance values of the process variables for multiple linear regression, multiple linear regression with two-way variable interactions and second order regression analysis for the particles resistance to abrasion.

Table 4.1 Regression results for particle abrasion resistance

	Multiple linear regression		**Multiple linear regression with interaction**		**Second-order regression**	
	Coefficient	P-Value	Coefficient	P-Value	Coefficient	P-Value
Mean	11.532	0.128	-250.351	0.162	-760.956	0.607
DP	0.006	0.293	-1.296	0.122	-2.811*	0.043
SLF	-0.124*	0.028	-5.499	0.458	-0.503	0.962
SLC	-0.196*	0.046	2.824	0.236	10.622	0.773
SLT	0.062*	0.002	2.422*	0.012	4.044	0.414
Fd50	-0.235	0.725	-26.556	0.719	8.646	0.956
DP*SLF	-	-	-0.002	0.677	-0.011	0.172
DP*SLC	-	-	0.016	0.120	0.034*	0.045
DP*SLT	-	-	0.0003	0.828	-0.002	0.360
DP*Fd50	-	-	-0.093	0.222	0.034	0.754
SLF*SLC	-	-	-0.019	0.851	-0.217	0.193
SLF*SLT	-	-	0.015	0.439	0.086	0.058
SLF*Fd50	-	-	3.028*	0.010	6.312*	0.015
SLC*SLT	-	-	-0.024*	0.021	-0.102	0.160
SLC*Fd50	-	-	0.260	0.783	-0.867	0.618
SLT*Fd50	-	-	-0.128	0.565	0.347	0.317
DP^2	-	-	-	-	0.0003	0.699
SLF^2	-	-	-	-	-0,148	0.121
SLC^2	-	-	-	-	0.032	0.894
SLT^2	-	-	-	-	0.016*	0.041
$Fd50^2$	-	-	-	-	-4.769	0.637
R^2	0.434		0.719		0.875	
F- value	3.680*	P=0.013	2.388	P=0.056	3.137*	P=0.041

All regression coefficients that are statistically significant and significant F values, thus having P<.05, are indicated with an asterisk.

4.2.1 Multiple linear regression model for abrasion resistance

The linear model obtained in the regression analysis is reported in the following equation.

$$A = 11.532 + 0.006\mathrm{DP} - 0.124\mathrm{SLF} - 0.196\mathrm{SLC} + 0.062\mathrm{SLT} - 0.235\mathrm{Fd}_{50} \qquad [4.1]$$

In the above mentioned model the spray liquid flowrate, concentration and feed particle size have negative coefficients, indicating an increase in these variables will result in a decrease in the particle degradation. As mentioned in section 2.2.1, the degradation is inversely proportional to the abrasion resistance. The spray liquid temperature has a positive constant suggesting an increase in spray liquid temperature will result in a larger degradation value. This model revealed a R^2 value of 0.434, and a significant F-test value. The overall model thus explains 43.4% of the variance in this system with the significant F-test value revealing that all the variables in the model jointly describe the abrasion resistance.

In Table 4.1 the only statistically significant regression coefficients obtained were the spray liquid flowrate, spray liquid concentration and the spray liquid temperature. It can be reported with statistical certainty that an increase in spray liquid flowrate and concentration will result in a decrease in percentage degradation, while an increase in spray liquid temperature will result in an increase. A comparison of the observed and predicted values can be seen in the following graph.

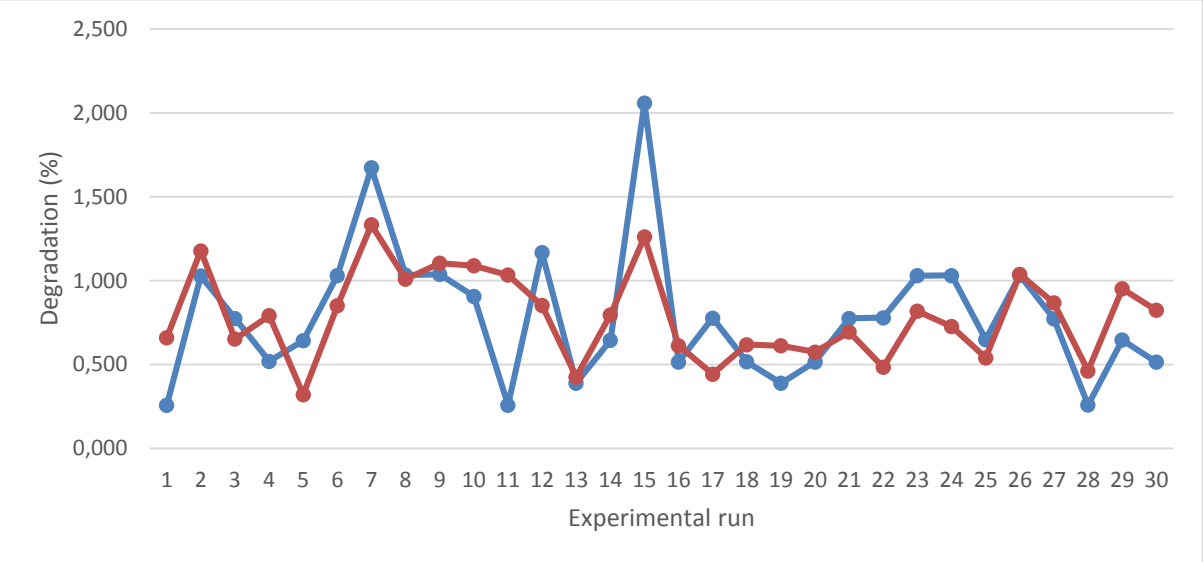

Figure 4.1 Comparison of the observed and predicted values of particle abrasion resistance ●observed ●predicted

In Figure 4.1 it can be seen that the predicted values fall in range of the observed values but doesn't closely follow the trend of the observed values. This model provides inadequate prediction of the observed values.

4.2.2 Multiple linear regression with two-way interactions for abrasion resistance

Equation 4.2 presents the linear regression model with two-way interactions included.

$$A = -250.351 - 1.296\mathrm{DP} - 5.499\mathrm{SLF} + 2.824\mathrm{SLC} + 2.422\mathrm{SLT} - 26.556\mathrm{Fd}_{50} - 0.002\mathrm{DP} \times \mathrm{SLF} + 0.016\mathrm{DP} \times \mathrm{SLC} + 0.0003\mathrm{DP} \times \mathrm{SLT} - 0.093\mathrm{DP} \times \mathrm{Fd}_{50} - 0.019\mathrm{SLF} \times \mathrm{SLC} + 0.015\mathrm{SLF} \times \mathrm{SLT} + 3.028\mathrm{SLF} \times \mathrm{Fd}_{50} - 0.024\mathrm{SLC} \times \mathrm{SLT} + 0.260\mathrm{SLC} \times \mathrm{Fd}_{50} - 0.128\mathrm{SLC} \times \mathrm{Fd}_{50} \quad [4.2]$$

In equation 4.2 it can be seen that the regression coefficients for the spray liquid flowrate, temperature and feed particle size remain positive with the addition of interaction terms, while the effect of the atomising air pressure difference and spray liquid concentration changed. A positive regression coefficient for an interaction term implies that an increase of one of the variables in the interaction term will increase the effect of the other variable in the interaction term. The opposite is true for a negative interaction term regression coefficient. The linear regression model with interactions has a R^2 value of 0.719, explaining 71.9% of the variance in the system. This value is higher than the R^2 values obtained in the multiple linear regression without interactions section. This is expected due to the fact that interaction terms explain a little more variance in the system. An insignificant F-test value expresses a lack of fit in the model.

The only variable seen to be statistically significant in Table 4.1 was the spray liquid temperature, and the only significant interaction terms the (i) spray liquid flowrate and feed particle size and (ii) spray liquid concentration and spray liquid temperature. The positive regression coefficient of the spray liquid flowrate and the feed particle size interaction term suggests an increase in the spray liquid flowrate will increase the effect of the feed particle size while the negative coefficient of the spray liquid concentration and temperature interaction term indicates that a rise in spray liquid concentration will decrease the effect of the spray liquid temperature. The difference in atomising air pressure shows no statistically significant effect on the abrasion resistance. An evaluation of the observed and predicted values can be seen in Figure 4.2.

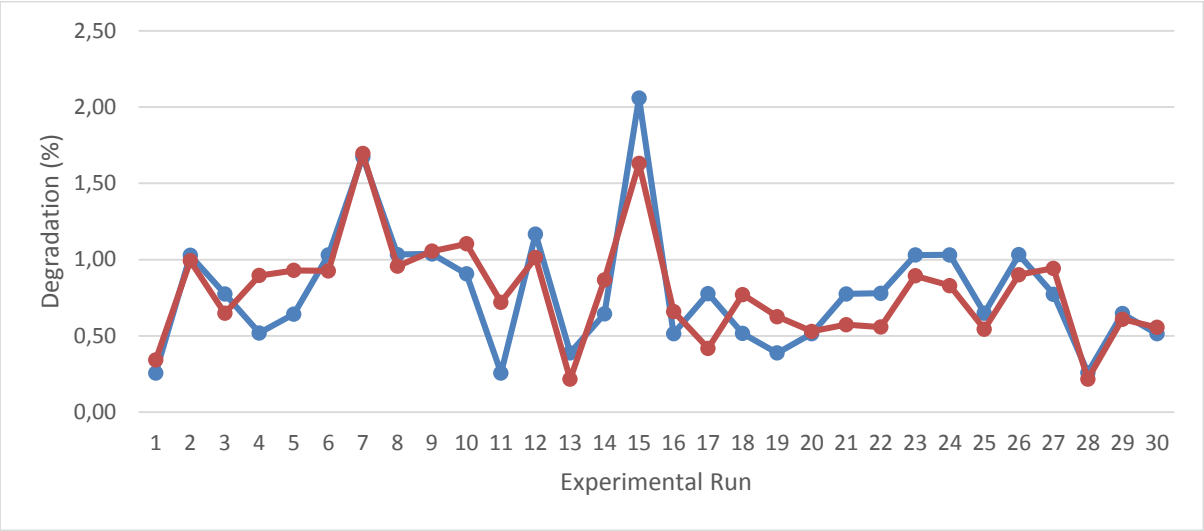

Figure 4.2 Comparison of the observed and predicted values of particle abrasion resistance ●observed ●predicted

In the figure above it can be seen that the overall model produces values in range with the observed values and in some sections following the trend of the observed values. This model displays better results than the linear regression model without interactions.

4.2.3 Second order regression model for particle abrasion resistance

The second order regression model is presented in the following equation.

$$A = -760.956 - 2.811\text{DP} - 0.503\text{SLF} + 10.622\text{SLC} + 4.044\text{SLT} + 8.646\text{Fd}_{50} - 0.011\text{DP} \times \text{SLF} + 0.034\text{DP} \times \text{SLC} - 0.002\text{DP} \times \text{SLT} + 0.034\text{DP} \times \text{Fd}_{50} - 0.217\text{SLF} \times \text{SLC} + 0.086\text{SLF} \times \text{SLT} + 6.312\text{SLF} \times \text{Fd}_{50} - 0.102\text{SLC} \times \text{SLT} - 0.867\text{SLC} \times \text{Fd}_{50} + 0.347\text{SLT} \times \text{Fd}_{50} + 0.0003\text{DP}^2 - 0{,}148\text{SLF}^2 + 0.032\text{SLC}^2 + 0.016\text{SLT}^2 - 4.769\text{Fd}_{50}^2 \quad [4.3]$$

The second order regression model obtained produced a R^2 value of 0.875 which is higher than any of the previously mentioned models, explaining 87.5% of the variation in the system. This is expected since the addition of second order terms will describe more variance in the system. Jointly all the variables in this equation are adequate in describing the abrasion resistance, seen by the significant F- test value.

The only statistically significant effects observed for the particle abrasion resistance were the (i) difference in atomising pressure, the interaction between the (ii) difference in atomising air pressure and spray liquid concentration, (iii) spray liquid flowrate and feed particle size and then the only second order term, (iv) the spray liquid temperature. The difference in atomising air pressure has a significant effect here unlike the two previously

obtained models while a new interaction effect is added between the atomising air pressure and the spray liquid concentration. Figure 4.3 presents the observed and predicted results.

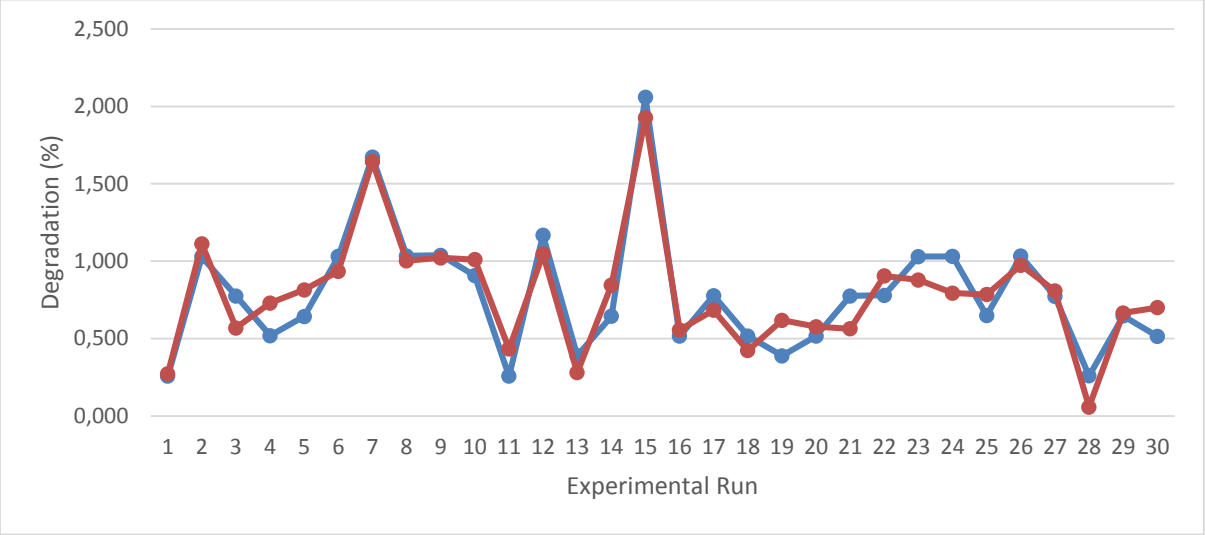

Figure 4.3 Comparison of the observed and predicted values of particle abrasion resistance ●observed ●predicted

In the figure above the second order model produced values in range and close to that of the observed values, which is expected with the high R^2 value obtained, and is observed to adequately describe the particle degradation.

4.3 Models for product d_{50}

The various regression results obtained for particle mean diameter can be seen in Table 4.2.

Table 4.2 Regression results for particle size

	Multiple linear regression		**Multiple linear regression with interaction**		**Second order regression**	
	Coefficient	P-Value	Coefficient	P-Value	Coefficient	P-Value
Mean	1.948	0.348	-124.395*	0.018	814.663	0.110
DP	-0.001	0.568	-0.513*	0.037	-0.497	0.227
SLF	0.004	0.790	1.089	0.617	-0.209	0.951
SLC	-0.004	0.891	2.019*	0.004	-20.094	0.115
SLT	-0.008	0.128	0.164	0.564	2.281	0.167
Fd50	0.844*	0.000	23.330	0.283	-53.590	0.305
DP*SLF	-	-	-0.002	0.278	-0.001	0.634
DP*SLC	-	-	0.006*	0.036	0.007	0.180
DP*SLT	-	-	-0.0003	0.473	-0.001	0.448
DP*Fd50	-	-	0.0001	0.998	-0.027	0.446
SLF*SLC	-	-	-0.045	0.119	-0.036	0.484
SLF*SLT	-	-	0.013*	0.021	0.015	0.281
SLF*Fd50	-	-	0.791*	0.022	1.175	0.116
SLC*SLT	-	-	-0.006	0.053	-0.025	0.270
SLC*Fd50	-	-	-0.564*	0.042	0.353	0.530
SLT*Fd50	-	-	0.178*	0.006	0.060	0.585
DP^2	-	-	-	-	0.0001	0.725
SLF^2	-	-	-	-	-0.029	0.317
SLC^2	-	-	-	-	0.126	0.122
SLT^2	-	-	-	-	-0.001	0.795
$Fd50^2$	-	-	-	-	1.811	0.579
R^2	0.628		0.794		0.890	
F- value	8.092*	P=137E-04	3.598*	P=0.010	3.636*	P=0.025

All statistically significant regression coefficients, i.e. with P<.05, are indicated with an asterisk. The significant F-values are indicated in the same manner.

4.3.1 Multiple linear regression model for product particle size

The linear product size model can be seen in equation 4.4.

$$Pd_{50} = 1.948 - 0.001\mathrm{DP} + 0.004\mathrm{SLF} - 0.004\mathrm{SLC} - 0.008\mathrm{SLT} + 0.844\mathrm{Fd}_{50} \qquad [4.4]$$

The difference in atomising air pressure, spray liquid concentration and temperature all have inverse relationships with the mean particle size while the spray liquid flowrate and feed particle sizes all have positive effects. The overall regression model obtained for particle mean size produced and R^2 value of 0.628 and a significant F-test value, which suggests that this model is 62.8% accurate in predicting particle size. Only the feed particle size was reported as statistically significant. This indicates that an increase in feed particle mean size will result in an increase in product mean size. This agrees with the Spearman's correlation discussed in Appendix E, which found a strong positive correlation between the feed particle mean size and the product mean size. A graphical comparison of the predicted and compared particle size values can be seen in Figure 4.4.

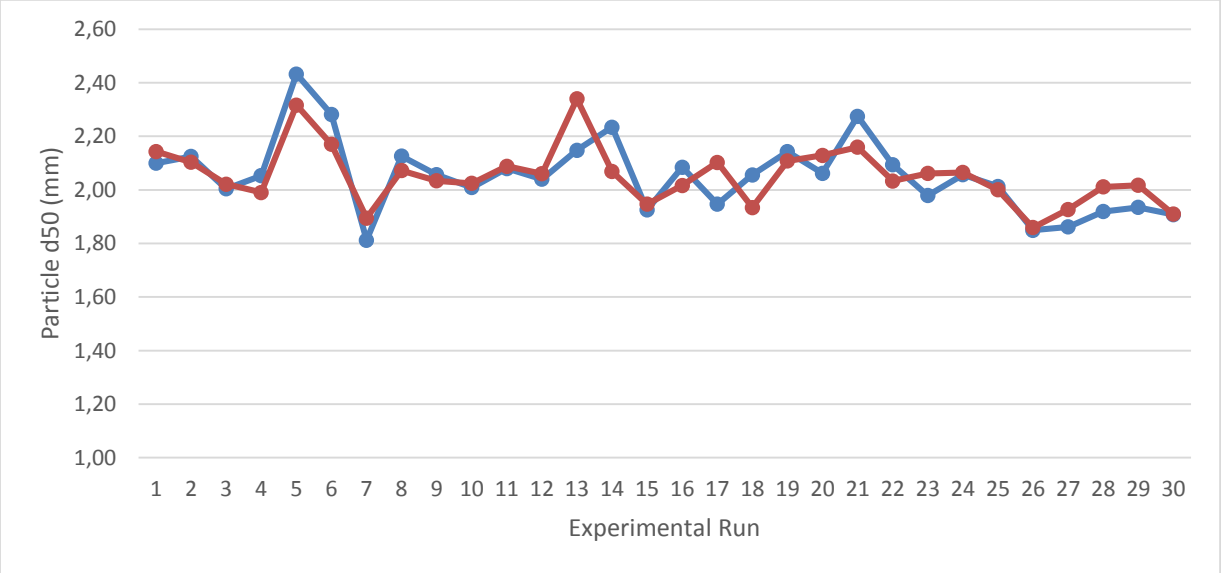

Figure 4.4 Comparison of the observed and predicted values of particle size ●observed ● predicted

From Figure 4.4 it is visible that the linear regression model provided a good prediction ability of the observed values, almost following the same trend.

4.3.2 Multiple linear regression with two-way interactions model for the product size

Equation 4.5 presents the linear model with interaction terms for the product size.

$$Pd_{50} = -124.395 - 0.513\mathrm{DP} + 1.089\mathrm{SLF} + 2.019\mathrm{SLC} + 0.164\mathrm{SLT} + 23.330\mathrm{Fd}_{50} - 0.002\mathrm{DP} \times \mathrm{SLF} + 0.006\mathrm{DP} \times \mathrm{SLC} - 0.0003\mathrm{DP} \times \mathrm{SLT} + 0.0001\mathrm{DP} \times \mathrm{Fd}_{50} - 0.045\mathrm{SLF} \times \mathrm{SLC} + 0.013\mathrm{SLF} \times \mathrm{SLT} + 0.791\mathrm{SLF} \times \mathrm{Fd}_{50} - 0.006\mathrm{SLC} \times \mathrm{SLT} - 0.564\mathrm{SLC} \times \mathrm{Fd}_{50} + 0.178\mathrm{SLT} \times \mathrm{Fd}_{50} \quad [4.5]$$

The direction of influence of the atomising air pressure difference, spray liquid flowrate and feed particle size remains the same with the addition of interaction terms while the effects of the spray liquid concentration and temperature changed. The multiple linear regression model with interactions revealed a R^2 value of 0.794, and thus accounts for 79.4% of the variance observed in the product mean size. This value is higher than the R^2 value obtained for the linear regression without interactions model, which implies that more variance is predicted using a model with interactions.

The (i) difference in atomising air pressure and the (ii) spray liquid concentration were found to be statistically significant as well as the interaction between the (iii) atomising air pressure difference and spray liquid concentration, (iv) spray liquid flowrate and temperature, (v) spray liquid temperature and feed particle size and lastly the (vi) spray liquid temperature and feed particle size. It can be said that a positive atomising air pressure difference will result in a decrease in particle size and an increase in spray liquid concentration will cause an increase in particle size. The regression coefficients for the significant interaction terms are all positive implying that an increase in the difference in atomising air pressure while increase the effect of the spray liquid concentration, and vice versa. This applies to the spray liquid flowrate and temperature, spray liquid flowrate and feed particle size and the spray liquid temperature and feed particle size. A comparison of the various predicted and observed results can be seen in Figure 4.5.

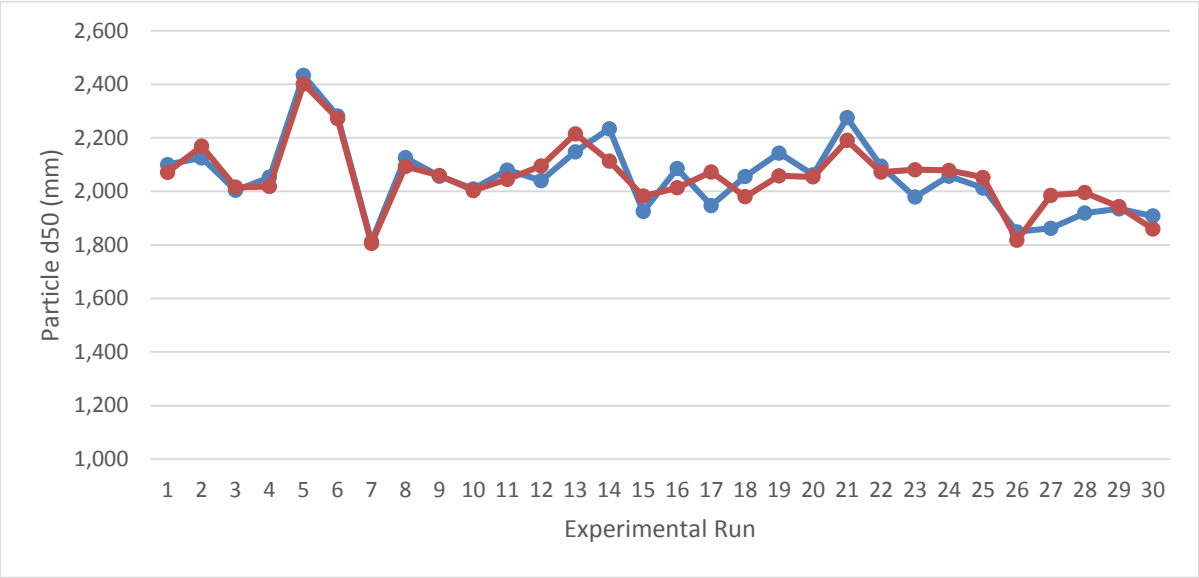

Figure 4.5 Comparison of the observed and predicted values of particle size ●observed ● predicted

As expected from a high coefficient of determination, the regression model produced values close to that of the observed values and followed the trend closely.

4.3.3 Second-order regression model for product size

The second order regression model for the product size is presented in the following equation.

$$Pd_{50} = 814.663 - 0.497\text{DP} - 0.209\text{SLF} - 20.094\text{SLC} + 2.281\text{SLT} - 53.590\text{Fd}_{50} - 0.001\text{DP} \times \text{SLF} + 0.007\text{DP} \times \text{SLC} - 0.001\text{DP} \times \text{SLT} - 0.027\text{DP} \times \text{Fd}_{50} - 0.036\text{SLF} \times \text{SLC} + 0.015\text{SLF} \times \text{SLT} + 1.175\text{SLF} \times \text{Fd}_{50} - 0.025\text{SLC} \times \text{SLT} + 0.353\text{SLC} \times \text{Fd}_{50} + 0.060\text{SLT} \times \text{Fd}_{50} + 0.0001\text{DP}^2 - 0.029\text{SLF}^2 + 0.126\text{SLC}^2 - 0.001\text{SLT}^2 + 1.811\text{Fd}_{50}^2 \quad [4.6]$$

The second order regression model obtained produced an R^2 value of 0.890, indicating that this model explains 89% of the variance in the system. This value is higher than any of the R^2 values obtained thus far for the product size, even though no statistically significant regression coefficients were obtained for the second order regression, as observed in Table 4.2. Figure 4.6 presents the observed and predicted values for the second order model.

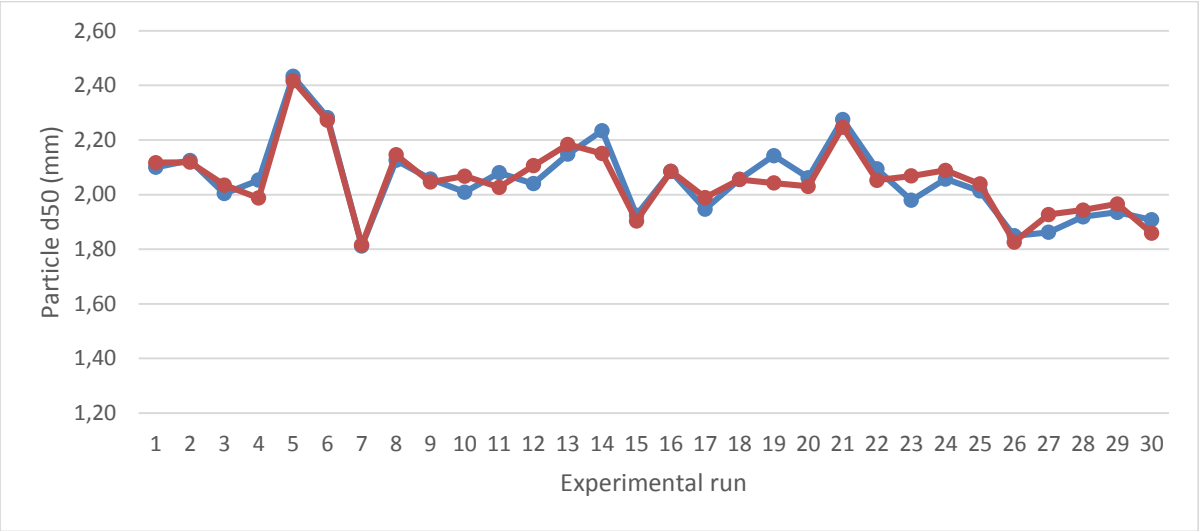

Figure 4.6 Comparison of the observed and predicted values of particle size ●observed ● predicted

From the figure it is visible that the values obtained from the second order regression model closely follow the observed values, which is expected form a regression model with a high coefficient of determination. This model provided a significant F-value meaning the variables within the model is jointly adequate in describing the product size.

4.4 Models for particle shape

A model predicting the particle shape, or particle circularity, is discussed in this section. Table 4.3 summarises the results of the various regression analyses.

Table 4.3 Regression results for particle shape

	Multiple linear regression		**Multiple linear regression with interaction**		**Second order regression**	
	Coefficient	P-Value	Coefficient	P-Value	Coefficient	P-Value
Mean	1.240*	0.000	4.523	0.064	4.854	0.850
DP	0.0001	0.088	0.032*	0.005	0.023	0.298
SLF	-0.0001	0.859	-0.060	0.555	-0.073	0.691
SLC	-0.004*	0.001	-0.068*	0.037	-0.103	0.872
SLT	0.0005*	0.040	-0.016	0.231	0.009	0.911
Fd50	-0.001	0.886	1.090	0.280	0.656	0.812

DP*SLF	-	-	0.0001	0.512	0.00002	0.854
DP*SLC	-	-	-0.0004*	0.002	-0.0003	0.233
DP*SLT	-	-	0.00004	0.065	0.00004	0.385
DP*Fd50	-	-	0.0004	0.725	0.001	0.527
SLF*SLC	-	-	0.003*	0.040	0.002	0.536
SLF*SLT	-	-	-0.001*	0.004	-0.0002	0.768
SLF*Fd50	-	-	-0.057*	0.000	-0.029	0.452
SLC*SLT	-	-	0.0003*	0.019	-0.0004	0.758
SLC*Fd50	-	-	0.001	0.954	-0.006	0.850
SLT*Fd50	-	-	-0.006	0.053	-0.002	0.734
DP^2	-	-	-	-	-0.00002	0.226
SLF^2	-	-	-	-	-0.001	0.568
SLC^2	-	-	-	-	0.001	0.845
SLT^2	-	-	-	-	0.0001	0.372
Fd50^2	-	-	-	-	0.097	0.583
R^2	0.430		0.692		0.775	
F- value	3.620*	P=0.014	2.096	P=0.087	1.550	P=0.253

Statistically significant regression coefficients and F-test values, P<.05, are indicated with an asterisk.

4.4.1 Multiple linear regression models for particle shape

Equation 4.7 presents the linear regression model for the particle shape.

$$C = 1.240 + 0.0001\mathrm{DP} - 0.0001\mathrm{SLF} - 0.004\mathrm{SLC} + 0.0005\mathrm{SLT} - 0.001\mathrm{Fd}_{50} \quad [4.7]$$

In the abovementioned equation all the variables were seen to have a negative effect on the particle shape except for the spray liquid temperature and the difference in atomising pressure. For the particle shape the regression model containing all the regression

coefficients revealed a R^2 value of 0.430 and a significant F- value indicating a model with prediction ability of 43% of the variance in the particle shape data.

The spray liquid concentration as well as the spray liquid temperature were determined to be statistically significant suggesting that an increase in spray liquid concentration will result in a decrease in circularity while an increase in spray liquid temperature will result in an increase of particle circularity. The negative effect of the spray liquid concentration agrees with the Spearman's correlation obtained and shown in Appendix E. Figure 4.7 presents the observed and predicted particle shape values for the various experimental runs.

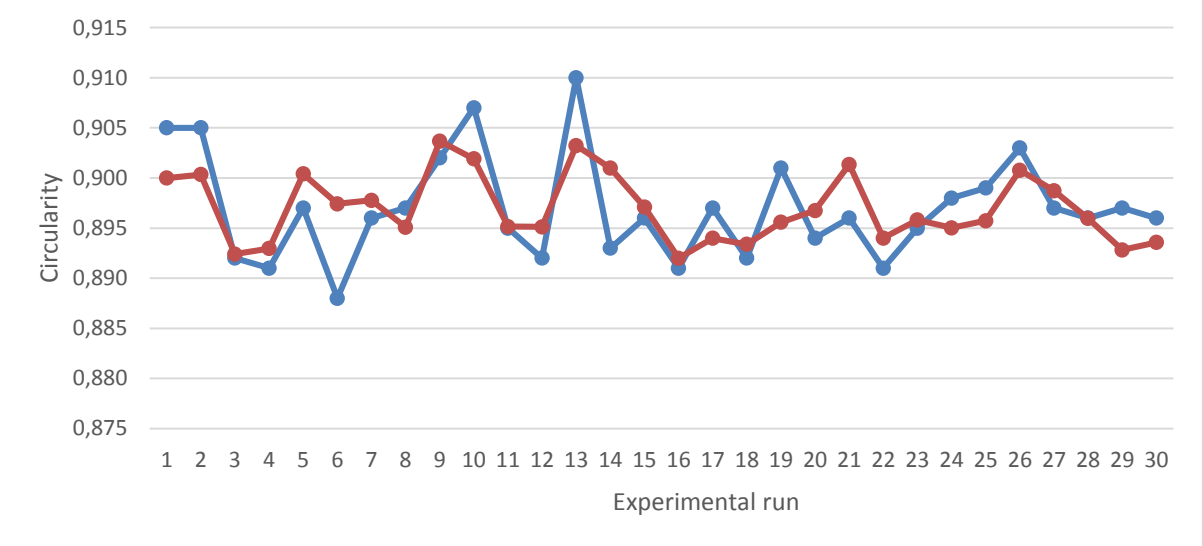

Figure 4.7 Comparison of the observed and predicted values of particle shape ●observed ● predicted

In Figure 4.7 the regression model is seen to predict values within the range of the observed values but does not closely predict the observed values as seen in the difference in drifts of the two lines.

4.4.2 Multiple linear regression with two way interactions model for particle shape

The linear regression model with interactions is presented in the following equation.

$$C = 4.523 + 0.032\mathrm{DP} - 0.06\mathrm{SLF} - 0.068\mathrm{SLC} - 0.016\mathrm{SLT} + 1.090\mathrm{Fd}_{50} + 0.0001\mathrm{DP} \times \mathrm{SLF} - 0.0004\mathrm{DP} \times \mathrm{SLC} + 0.00004\mathrm{DP} \times \mathrm{SLT} + 0.0004\mathrm{DP} \times \mathrm{Fd}_{50} + 0.003\mathrm{SLF} \times \mathrm{SLC} - 0.001\mathrm{SLF} \times \mathrm{SLT} - 0.057\mathrm{SLF} \times \mathrm{Fd}_{50} + 0.0003\mathrm{SLC} \times \mathrm{SLT} + 0.001\mathrm{SLC} \times \mathrm{Fd}_{50} - 0.006\mathrm{SLT} \times \mathrm{Fd}_{50} \quad [4.8]$$

The addition of interaction effects changed the influence direction of the atomising air pressure difference, spray liquid temperature and feed particle size. This regression model

produced a coefficient of determination value of 0.692. This relatively high R^2 value indicates the model explains 69.2% of the variance in the system which is significantly higher than the R^2 values obtained by regular linear regression.

In Table 4.3 it can be seen that the atomising air pressure and spray liquid concentration were found to be significant. Interaction terms that were found to be statistically significant were the interaction between the (i) atomising air pressure difference and spray liquid concentration, (ii) spray liquid flowrate and concentration, (iii) spray liquid flow rate and temperature, (iv) spray liquid flowrate and feed particle size as well as the interaction between the (v) spray liquid concentration and temperature. An increase in the atomising air pressure difference will result in an increase of circularity while an increase in spray liquid concentration will result in a lower particle circularity. The effect of the atomising air pressure difference and spray liquid concentration interaction term as well as the spray liquid flow rate and temperature and spray liquid flowrate and feed particle size interaction terms are negative, signifying that an increase in any one of the combinations in the interaction term will decrease the effect of the other variable in the interaction term. The interaction between spray liquid flowrate and concentration and the interaction between the spray liquid concentration and temperature has a positive effect which indicated an increase in the effect of one of the variable in the interaction term as the other one increases. A comparison of the observed and predicted particle shape values can be seen in Figure 4.8.

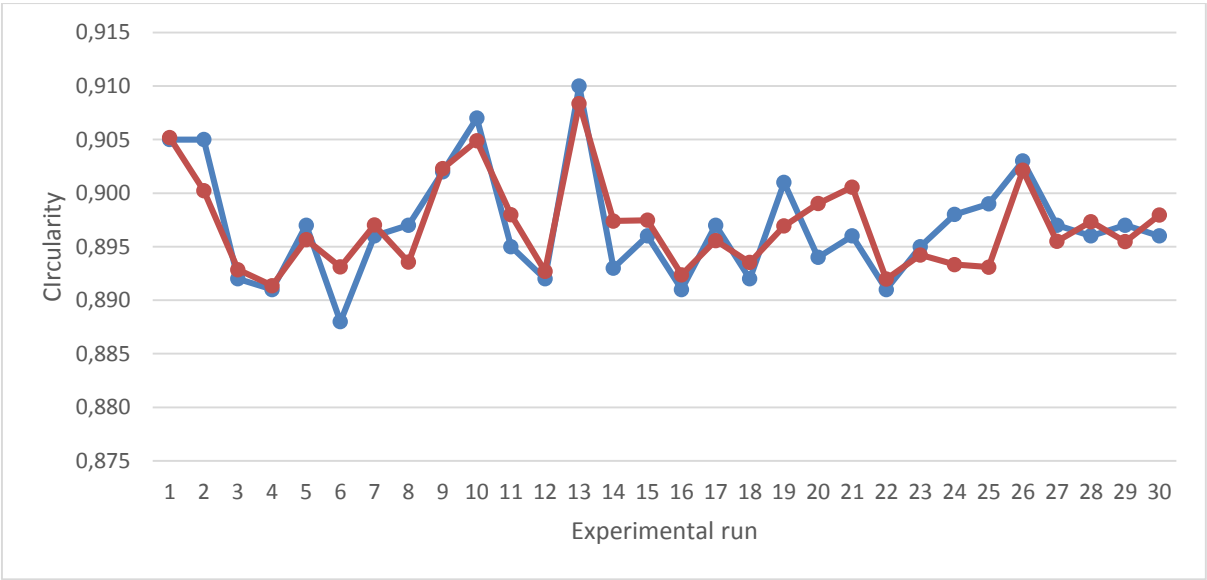

Figure 4.8 Comparison of the observed and predicted values of particle shape ●observed ● predicted

In the figure above it is visible that the values calculated by the regression model fall in range of the observed values and mostly follows the direction of the trend associated with the observed values.

4.4.3 Second-order regression model for particle shape

The following equation displays the second order regression model for the particle shape.

$$C = 4.854 + 0.023\mathrm{DP} - 0.073\mathrm{SLF} - 0.103\mathrm{SLC} + 0.009\mathrm{SLT} + 0.656\mathrm{Fd}_{50} + 0.00002\mathrm{DP} \times \mathrm{SLF} - 0.0003\mathrm{DP} \times \mathrm{SLC} + 0.00004\mathrm{DP} \times \mathrm{SLT} + 0.001\mathrm{DP} \times \mathrm{Fd}_{50} + 0.002\mathrm{SLF} \times \mathrm{SLC} - 0.0002\mathrm{SLF} \times \mathrm{SLT} - 0.029\mathrm{SLF} \times \mathrm{Fd}_{50} - 0.0004\mathrm{SLC} \times \mathrm{SLT} - 0.006\mathrm{SLC} \times \mathrm{Fd}_{50} - 0.002\mathrm{SLT} \times \mathrm{Fd}_{50} - 0.00002\mathrm{DP}^2 - 0.001\mathrm{SLF}^2 + 0.001\mathrm{SLC}^2 + 0.0001\mathrm{SLT}^2 + 0.097\mathrm{Fd}_{50}^2 \quad [4.9]$$

A R^2 value of 0.775 was calculated for the overall second order regression model obtained in Table 4.3. This implies the model accounts for 77.5% of the variation in the system, and account for more variation in the system than the linear regression with interaction. The F-test, however, revealed an insignificant F-value suggesting a lack of fit associated with this model. No statistically significant regression coefficients were obtained from the regression results. An evaluation of the predicted and observed circularities can be seen in Figure 4.9.

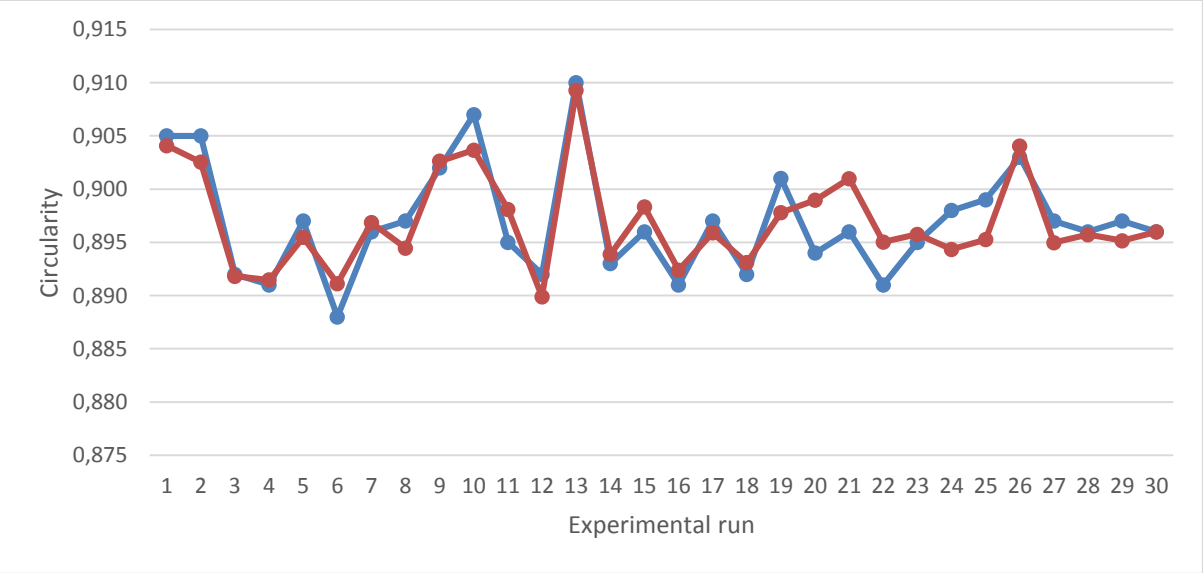

Figure 4.9 Comparison of the observed and predicted values of particle shape ●observed ● predicted

In Figure 4.9 the regression model provides values in range with the observed values and correlates moderately well with the observed values.

4.5 Models for particle porosity

The regression coefficients and significance values for the various regression analyses can be seen in Table 4.4. Statistically significant regression coefficients and F-test values, P<.05, are indicated with an asterisk.

Table 4.4 Regression results for particle porosity

	Multiple linear regression		**Multiple linear regression with interaction**		**Second-order regression**	
	Coefficient	P-Value	Coefficient	P-Value	Coefficient	P-Value
Mean	31.979	0.531	1742.96	0.151	-20397.03	0.075
DP	-0.019	0.657	11.01	0.052	7.42	0.403
SLF	0.025	0.946	-110.46*	0.028	-46.09	0.542
SLC	0.248	0.703	-36.15*	0.025	512.91	0.074
SLT	-0.093	0.445	16.81*	0.010	-40.63	0.256
Fd50	-3.178	0.491	-1081.97*	0.031	-248.56	0.824
DP*SLF	-	-	0.024	0.535	-0.003	0.952
DP*SLC	-	-	-0.109	0.109	-0.069	0.527
DP*SLT	-	-	0.008	0.462	0.003	0.852
DP*Fd50	-	-	-1.286*	0.013	-0.893	0.266
SLF*SLC	-	-	1.543*	0.021	0.533	0.637
SLF*SLT	-	-	-0.199	0.128	0.019	0.947
SLF*Fd50	-	-	-2.345	0.768	-1.431	0.925
SLC*SLT	-	-	-0.057	0.424	0.511	0.310
SLC*Fd50	-	-	21.37*	0.001	7.942	0.522
SLT*Fd50	-	-	-6.31*	0.000	-3.907	0.127
DP^2	-	-	-	-	0.004	0.516
SLF^2	-	-	-	-	-0.271	0.668
SLC^2	-	-	-	-	-3.262	0.076
SLT^2	-	-	-	-	0.0005	0.992
$Fd50^2$	-	-	-	-	19.76	0.782
R^2	0.053		0.545		0.778	
F- value	0.268	P=0.930	1.118	P=0.415	1.574	P=0.246

4.5.1 Multiple linear regression model for product porosity

The linear regression model obtained for the porosity is presented in the following equation.

$$P = 31.979 - 0.019\mathrm{DP} + 0.025\mathrm{SLF} + 0.248\mathrm{SLC} - 0.093\mathrm{SLT} - 3.178\mathrm{Fd}_{50} \qquad [4.10]$$

In his model, the difference in atomising air pressure difference, spray liquid temperature and feed particle size all have negative effects on the porosity, while the spray liquid concentration and flowrate is seen to have positive effects. From the regression model a R^2 value of 0.053 was obtained suggesting this model provides little to no explanation of the variation in the system. An insignificant F-test value was obtained for this model indicating a complete lack of fit. No statistically significant regression model coefficients were obtained. The observed and predicted results for the various experimental runs can be seen in Figure 4.10.

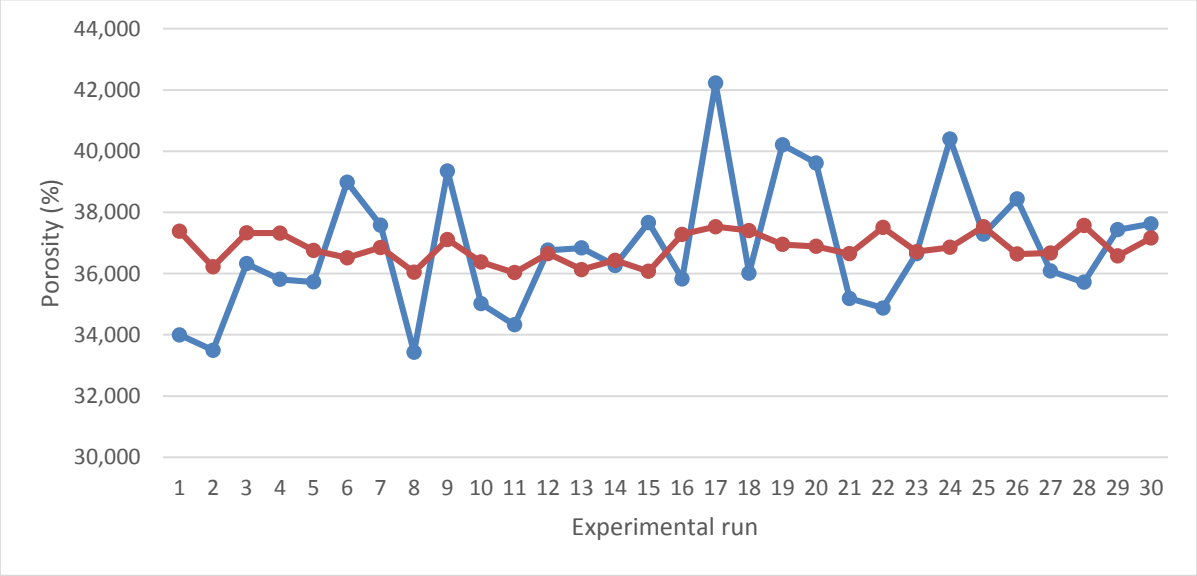

Figure 4.10 Comparison of the observed and predicted values of particle porosity ●observed ● predicted

In Figure 4.10 it is visible that the regression model does not predict any variation in the system as can be expected from such an extremely low coefficient of determination. The linear regression model is thus concluded incapable of describing the particle porosity.

4.5.2 Multiple linear regression with two-way interactions model for product porosity

Equation 4.11 presents the linear regression model with interaction terms for particle porosity.

$$P = 1742.96 + 11.01\mathrm{DP} - 110.46\mathrm{SLF} - 36.15\mathrm{SLC} + 16.81\mathrm{SLT} - 1081.97\mathrm{Fd}_{50} + 0.024\mathrm{DP} \times \mathrm{SLF} - 0.109\mathrm{DP} \times \mathrm{SLC} + 0.008\mathrm{DP} \times \mathrm{SLT} - 1.286\mathrm{DP} \times \mathrm{Fd}_{50} + 1.543\mathrm{SLF} \times \mathrm{SLC} - 0.199\mathrm{SLF} \times \mathrm{SLT} - 2.345\mathrm{SLF} \times \mathrm{Fd}_{50} - 0.057\mathrm{SLC} \times \mathrm{SLT} + 21.37\mathrm{SLC} \times \mathrm{Fd}_{50} - 6.31\mathrm{SLT} \times \mathrm{Fd}_{50}$$

[4.11]

The direction of the effects of the all the variables except for the feed particle size changed with the addition of the interaction terms. The multiple linear regression with two-way interactions model obtained in Table 4.4 delivered a R^2 value 0.545, a significant improvement from the value obtained for multiple regression only, and indicates that this model will account for 54.5% of the variation in the system. This model also obtained an insignificant F-test value suggesting a lack of fit.

The spray liquid flowrate, concentration, temperature and feed particle size were seen to be statistically significant. Statistically significant interaction effects were found between the (i) feed particle size and the atomising air pressure difference, (ii) spray liquid flowrate and concentration, (iii) spray liquid concentration and feed particle size and lastly between the (iv) spray liquid temperature and feed particle size. It can be seen that an increase in the spray liquid flowrate, concentration and feed particle size will result in a decrease in particle porosity, while an increase in spray liquid temperature will result in an increase in particle porosity. The interaction between the atomising air pressure difference and feed particle size as well as the interaction between the spray liquid temperature and feed particle size have negative effects suggesting that an increase in any one of the interactions will decrease the effect of the other. The interaction between spray liquid flowrate and concentration and the interaction between spray liquid concentration and feed particle size has a positive effect indicating that an increase in any one of these interactions will increase the effect of the other. A comparison of the observed and predicted values can be seen in Figure 4.11.

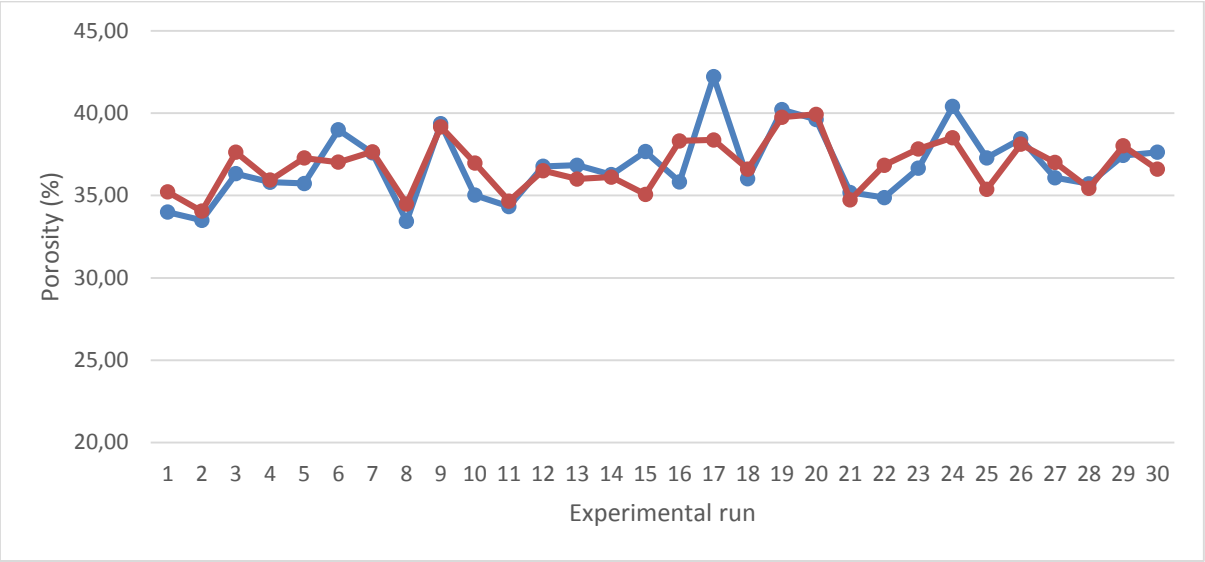

Figure 4.11 Comparison of the observed and predicted values of particle porosity ●observed ● predicted

In the figure above the values calculated by the regression model falls in the same range as the observed values and is seen to moderately follow the trend of the observed value.

4.5.3 Second-order regression model for product porosity

The second order regression model is displayed in the following equation.

$$P = -20397.03 + 7.42\mathrm{DP} - 46.09\mathrm{SLF} + 512.91\mathrm{SLC} - 40.63\mathrm{SLT} - 248.56\mathrm{Fd}_{50} - 0.003\mathrm{DP} \times \mathrm{SLF} - 0.069\mathrm{DP} \times \mathrm{SLC} + 0.003\mathrm{DP} \times \mathrm{SLT} - 0.893\mathrm{DP} \times \mathrm{Fd}_{50} + 0.533\mathrm{SLF} \times \mathrm{SLC} + 0.019\mathrm{SLF} \times \mathrm{SLT} - 1.431\mathrm{SLF} \times \mathrm{Fd}_{50} + 0.511\mathrm{SLC} \times \mathrm{SLT} + 7.942\mathrm{SLC} \times \mathrm{Fd}_{50} - 3.907\mathrm{SLT} \times \mathrm{Fd}_{50} + 0.004\mathrm{DP}^2 - 0.271\mathrm{SLF}^2 - 3.262\mathrm{SLC}^2 + 0.0005\mathrm{SLT}^2 + 19.76\mathrm{Fd}_{50}^2 \quad [4.12]$$

The regression model obtained in Table 4.4 provided a R^2 value of 0.778 indicating the overall regression model explains 77.8% of the variation in the system. This value is much larger than the R^2 values obtained for the previous porosity regression models. The F-value was determined to be statistically insignificant showing a lack of fit associated with the model. No statistically significant regression coefficients were found for the second order regression model. A comparison of the predicted an observed values is presented in Figure 4.12.

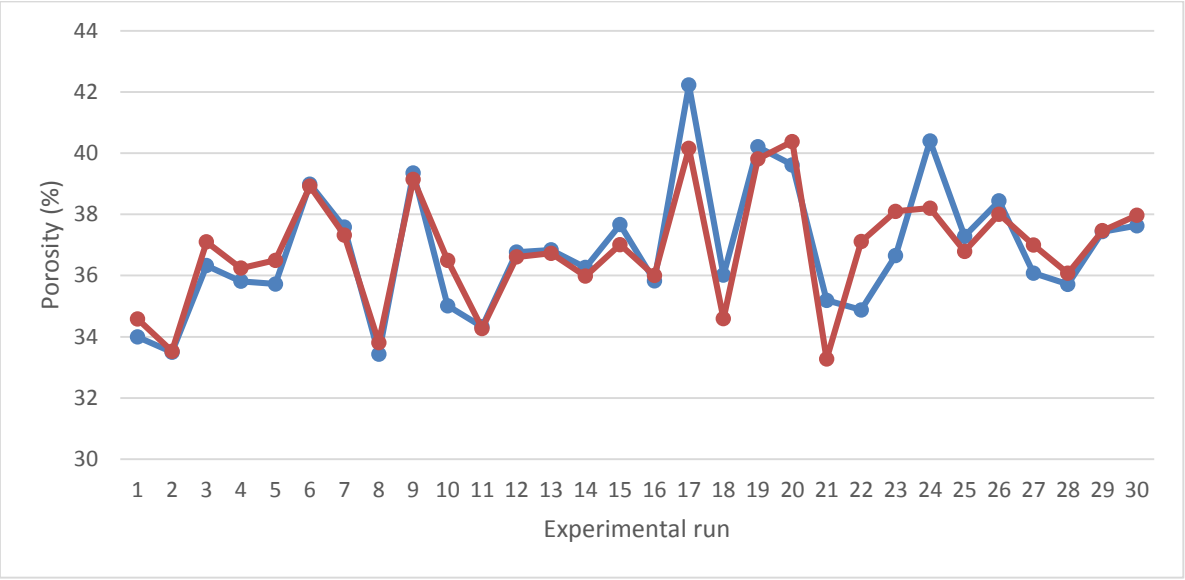

Figure 4.12 Comparison of the observed and predicted values of particle porosity ●observed ● predicted

In the figure above the overall regression model can be seen to produce values within a close range to that of the observed values.

4.6 Models for flowability

The various regression results for particle flowability can be seen in Table 4.5.

Table 4.5 Regression results for particle flowability

	Multiple linear regression		**Multiple linear regression with interaction**		**Second-order regression**	
	Coefficient	P-Value	Coefficient	P-Value	Coefficient	P-Value
Mean	62.475	0.145	817.25	0.471	5421	0.656
DP	0.026	0.450	3.113	0.557	-2.383	0.813
SLF	-0.466	0.134	110.85*	0.018	135.44	0.143
SLC	-0.549	0.308	-10.485	0.487	-127.02	0.677
SLT	0.071	0.478	-10.246	0.095	3.351	0.933
Fd50	-7.115	0.069	65.11	0.889	-229.45	0.860
DP*SLF	-	-	0.023	0.517	-0.004	0.954
DP*SLC	-	-	-0.016	0.796	0.068	0.589
DP*SLT	-	-	-0.014	0.153	-0.032	0.145

DP*Fd50	-	-	0.106	0.826	0.281	0.755
SLF*SLC	-	-	-1.121	0.074	-1.851	0.178
SLF*SLT	-	-	0.093	0.447	0.335	0.332
SLF*Fd50	-	-	-13.13	0.077	-1.255	0.944
SLC*SLT	-	-	0.114	0.085	-0.147	0.796
SLC*Fd50	-	-	0.875	0.884	4.207	0.768
SLT*Fd50	-	-	-0.523	0.711	-0.272	0.922
DP^2	-	-	-	-	0.006	0.447
SLF^2	-	-	-	-	-0.762	0.311
SLC^2	-	-	-	-	0.821	0.674
SLT^2	-	-	-	-	0.031	0.584
Fd50^2	-	-	-	-	-36.160	0.664
R^2	0.217		0.514		0.634	
F- value	1.330	P=0.285	0.988	P=0.510	0.780	P=0.694

Regression coefficients and F-test values that are statistically significant are indicated with an asterisk.

4.6.1 Multiple linear regression model for product flowability

Equation 4.13 presents the linear regression model based on the observations in Table 4.5.

$$CI = 62.48 + 0.026\mathrm{DP} - 0.466\mathrm{SLF} - 0.549\mathrm{SLC} + 0.071\mathrm{SLT} - 7.115\mathrm{Fd}_{50} \quad [4.13]$$

The spray liquid concentration, flowrate and the feed particle size all have negative effects on the flowability while the atomising air pressure difference and spray liquid temperature have positive effects. A R^2 value of 0.217 was obtained for the regression model above, revealing that this model contributes little in predicting the variance in the flowability. An insignificant F-test value was obtained implying this model exhibits a lack of fit. No statistically significant regression coefficients were obtained from Table 4.5. A comparison of the predicted and observed values can be seen in Figure 4.13.

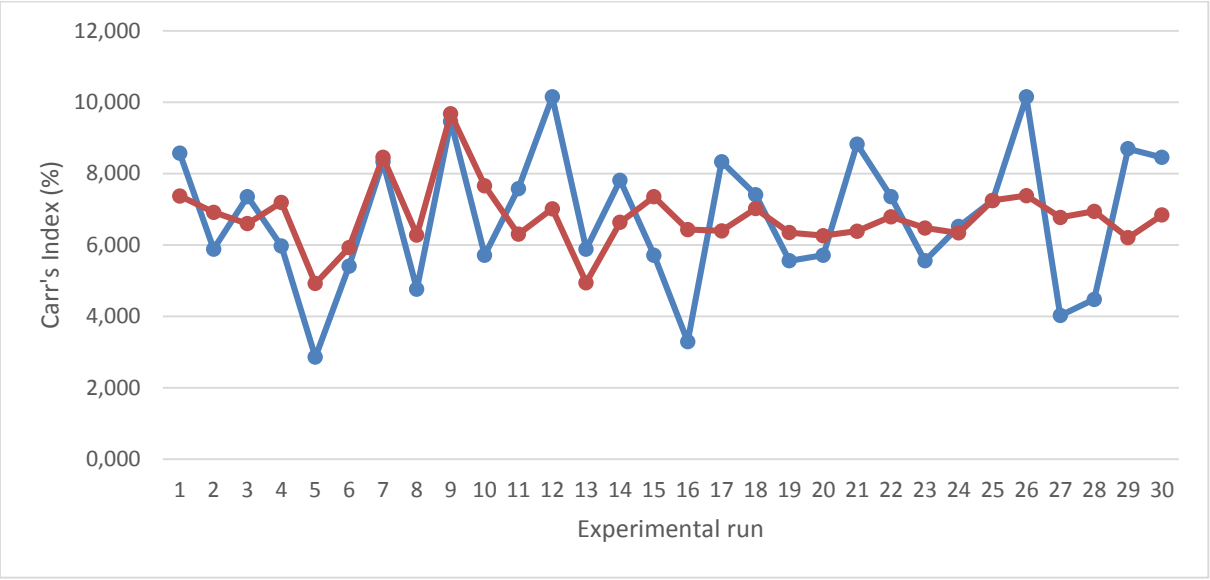

Figure 4.13 Comparison of the observed and predicted values of particle flowability ●observed ● predicted

From the figure above it is clear that there is a substantial difference between the predicted and observed values, thus indicating an incapability in the prediction efficiency of the model obtained.

4.6.2 Multiple linear regression with two-way interactions model for product flowability

In the following equation the linear regression model with interactions is presented.

$$CI = 817.25 + 3.113\text{DP} + 110.85\text{SLF} - 10.485\text{SLC} - 10.246\text{SLT} + 65.11\text{Fd}_{50} + 0.023\text{DP} \times \text{SLF} - 0.016\text{DP} \times \text{SLC} - 0.014\text{DP} \times \text{SLT} + 0.106\text{DP} \times \text{Fd}_{50} - 1.121\text{SLF} \times \text{SLC} + 0.093\text{SLF} \times \text{SLT} - 13.135\text{SLF} \times \text{Fd}_{50} + 0.114\text{SLC} \times \text{SLT} + 0.875\text{SLC} \times \text{Fd}_{50} - 0.523\text{SLT} \times \text{Fd}_{50} \quad [4.14]$$

The addition of interaction terms changes the direction of the effects of the spray liquid flowrate, temperature and feed particle size. The regression model with interactions provided a coefficient of determination value of 0.514, indicating that this model accounts for 51.4% of the variation in the system. A lack of fit was identified by an insignificant F-value. From Table 4.5 it can be seen that only the spray liquid flow rate was calculated to be significant suggesting that an increase in spray liquid concentration will result in an increase in particle flowability. Figure 4.14 presents a comparison of the observed and predicted results for the various experimental results.

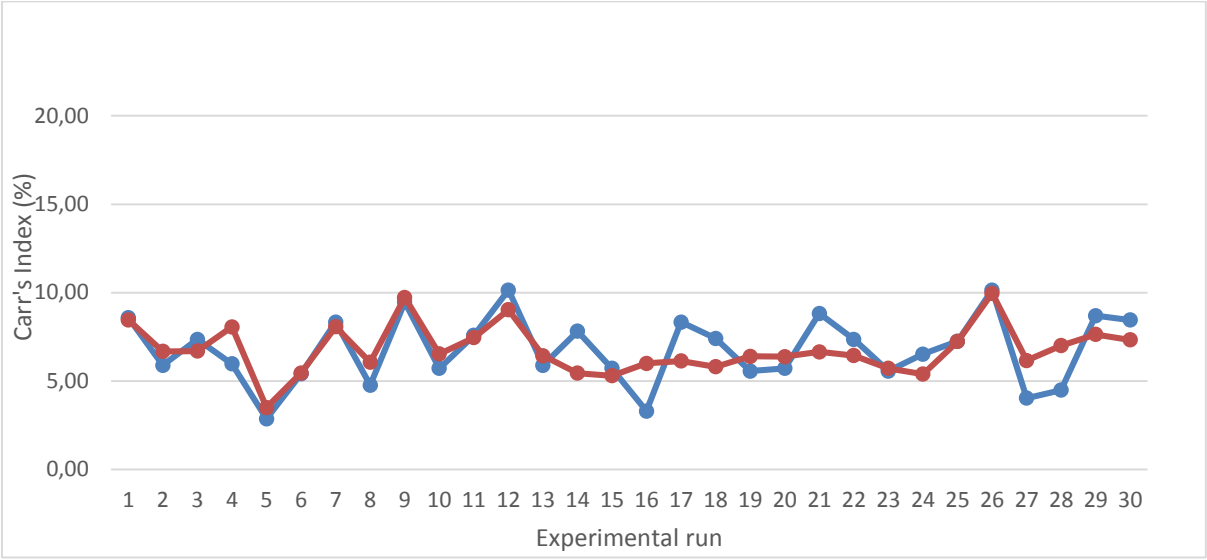

Figure 4.14 Comparison of the observed and predicted values of particle flowability ●observed ● predicted

This regression model provided values within the range of the observed values, but with a lot of variance.

4.6.3 Second-order regression model for product flowability

The second order regression model is presented in the following equation.

$$\begin{aligned} CI = {} & 5421 - 2.383\mathrm{DP} + 135.44\mathrm{SLF} - 127.02\mathrm{SLC} + 3.351\mathrm{SLT} - 229.45\mathrm{Fd}_{50} - 0.004\mathrm{DP} \times \mathrm{SLF} \\ & + 0.068\mathrm{DP} \times \mathrm{SLC} - 0.032\mathrm{DP} \times \mathrm{SLT} + 0.281\mathrm{DP} \times \mathrm{Fd}_{50} - 1.851\mathrm{SLF} \times \mathrm{SLC} \\ & + 0.335\mathrm{SLF} \times \mathrm{SLT} - 1.255\mathrm{SLF} \times \mathrm{Fd}_{50} - 0.147\mathrm{SLC} \times \mathrm{SLT} + 4.207\mathrm{SLC} \times \mathrm{Fd}_{50} \\ & - 0.272\mathrm{SLT} \times \mathrm{Fd}_{50} + 0.006\mathrm{DP}^2 - 0.762\mathrm{SLF}^2 + 0.821\mathrm{SLC}^2 + 0.031\mathrm{SLT}^2 \\ & - 36.160\mathrm{Fd}_{50}^2 \end{aligned} \quad [4.15]$$

The second order regression model suggested in Table 4.5 produces a coefficient of determination value of 0.634, resulting in the 63.4% explanation for the variation in the flowability data. This value is only a little higher than the values obtained from linear regression and linear regression with two-way interactions. A lack of fit for this model was concluded by an insignificant F value. A comparison of the predicted and observed results is shown in Figure 4.15.

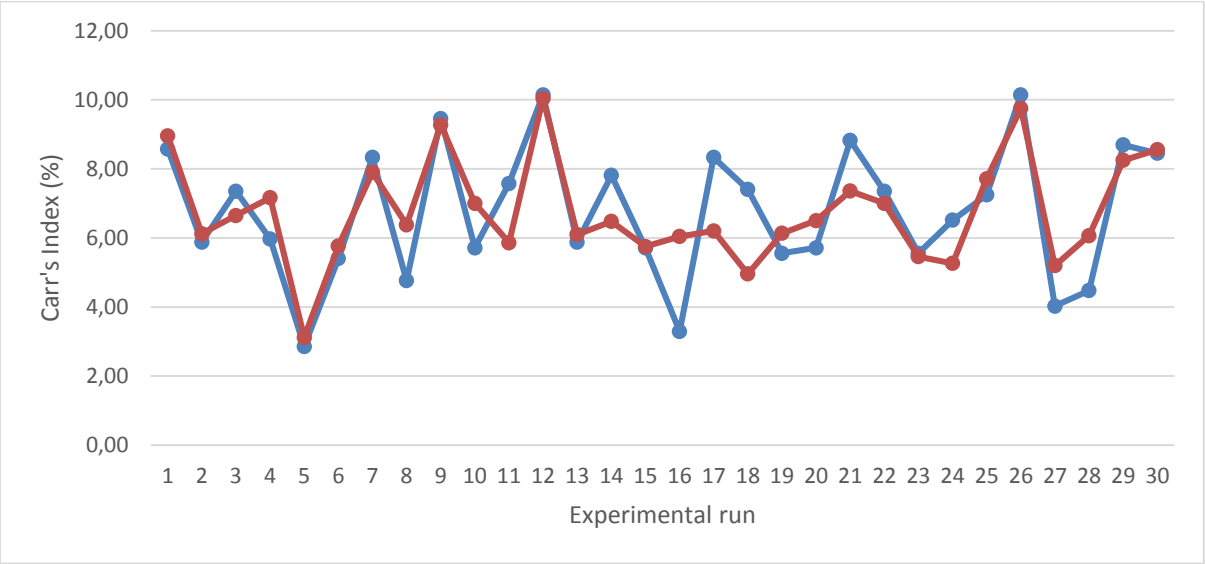

Figure 4.15 Comparison of the observed and predicted values of particle flowability ●observed ● predicted

In the figure above it can be seen that the values obtained from the regression model falls within the range of the observed values, but with limited overlapping, indicating a lack of predictive capability.

All models obtained in this chapter will be evaluated, compared and validated in the following chapter.

5. Results and Discussion

5.1 Introduction

In this chapter the regression models obtained in chapter 4 are evaluated and then validated using the validation results obtained during experimental phase three. The models are evaluated according to three criteria: (i) the R^2 value which is the measure of how good variance in the data is predicted, (ii) the mean square error (MS_r), which gives the error associated with the predicted and observed values and (iii) the F-test value, which indicates a model's lack of fit or the ability of the variables within the model to describe the quality parameter. The ideal would be to have a high R^2 value, low MS_r value and significant F-test value.

In order to validate the model, the data obtained during experimental phase three is inserted into the two most statistically reliable models of each of the quality parameters and then the predicted results are compared to the observed validation results. The validation data was obtained using the same variable levels as used during the development phase, but with different variable and level combinations. The validation data can be seen in Appendix F.

5.2 Evaluation of regression models

5.2.1 Particle abrasion resistance

A comparison of the various coefficients of determination, mean square residuals and F-test values for the various models can be seen in Table 5.1.

Table 5.1 Abrasion resistance model comparison

Model	R^2	MS_r	F
Multiple linear regression model	0.434	0.108	3.680*
Multiple linear regression with interactions model	0.719	0.092	2.388
Second order regression model	0.875	0.064	3.137*

In Table 5.1 the coefficient of determination, the mean square error (MS_r) and the F-test value, are compared for the various models. F-values that were determined to be statistically significant are marked with an asterisk.

By firstly looking at the coefficient of determination, it is visible that the linear regression model provides a weak explanation for the variation in the system while the linear regression model with interactions and the second order regression model produce the highest R^2 values.

R^2, however, gives no indication of the error associated with a model and therefore the MS_r is used to compare the error values associated with the regression models. All the regression models yield low error values with the second order model having the lowest error value. The only models having a significant F-test value are the linear and second order models, suggesting the variables presented in these models are jointly capable of describing the abrasion resistance. This doesn't suggest a model is sufficient or correct, only that it is statistically reliable.

From Table 5.1 it can be concluded that the overall second order model has the lowest MS_r and the highest R squared values and that the variables within the model have a statistically reliable relationship with the abrasion resistance. This makes this model most statistically adequate in describing the abrasion resistance. Figure 5.1 presents the values produced by the overall second order model and the experimentally obtained values with the addition of experimental error bars.

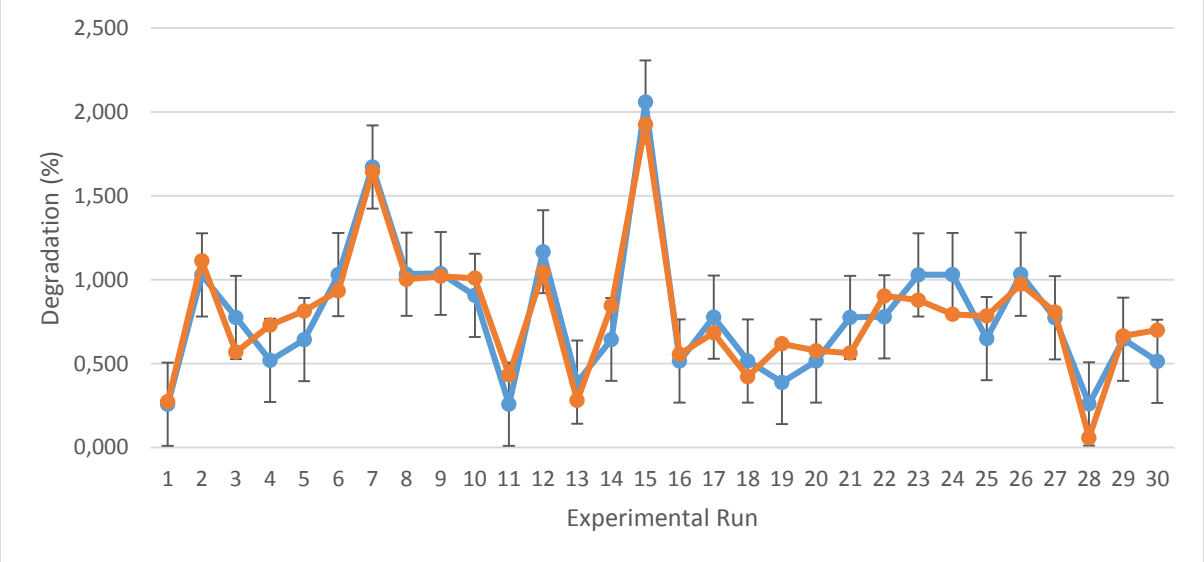

Figure 5.1 Comparison of the predicted and observed values for abrasion resistance with experimental error
observed predicted

From the figure above it is visible that the overall second order model predicts the percentage degradation values within the experimental error band determined for abrasion resistance in section 3.3.2.5. This model is thus concluded adequate in describing the particles' resistance to abrasion.

5.2.2 Product size

A comparison of the statistical performance indicators for the various models is displayed in Table 5.2.

Table 5.2 Particle size models comparison

Model	R^2	MS_r	F
Multiple linear regression	0.628	0,008	8,092*
Multiple linear regression with interaction	0.794	0,008	3,598*
Second order regression	0.890	0,007	3.636*

Table 5.2 presents the coefficients of determination, the mean square errors and the F-test values for the various models discussed in chapter 4 for the product size. Statistically significant F-values are indicated with an asterisk.

From the R^2 values in Table 5.2 it can be observed that the second order regression model produces the highest R^2 values with the multiple linear regression with interactions following. All the regression models obtained produced very low error values, with the second order model only just yielding the lowest MS_r value indicating the smallest difference between the predicted and observed values. All the regression models have a statistical reliable relationship with the variables within the regression model as seen by the significant F-test value in Table 5.2.

The second order regression model has the lowest error values and the highest explanation for the variance in the system in comparison with the other models. It also has a significant F-value. In the following figure a comparison of the values predicted by the second order regression model and the observed values can be seen along with the experimental error value determined for the particle size analysis.

In Figure 5.2 the values predicted by the overall second order regression model sit well in range of the experimental error for particle size analysis. From Figure 5.2 and Table 5.2 Particle size models comparison it can be determined that the second order regression model is suitable to describe the product mean particle diameter.

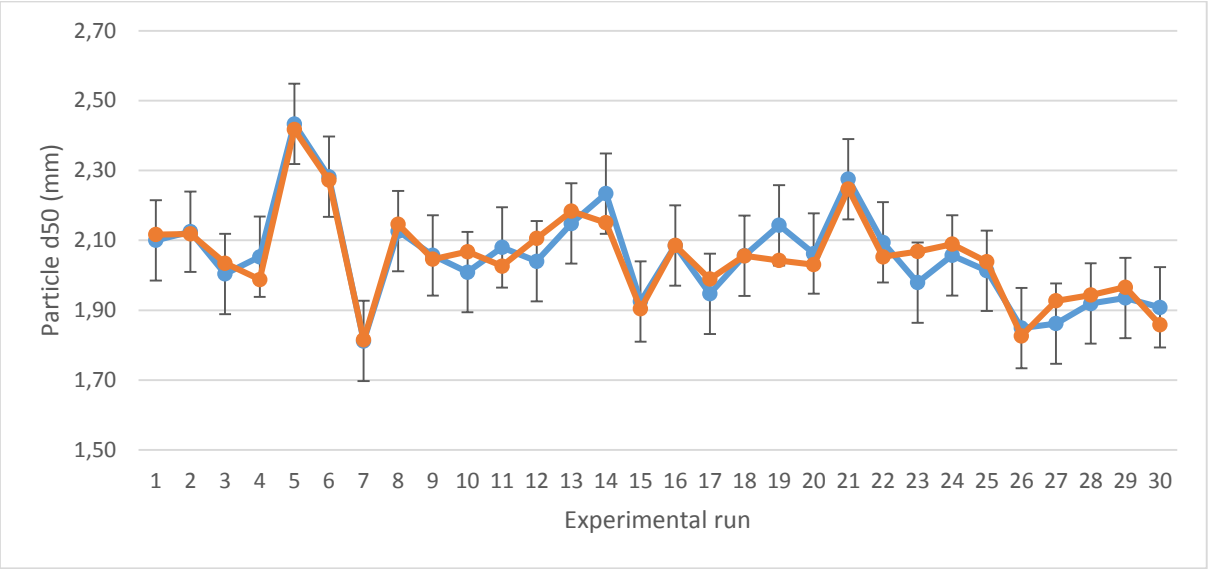

Figure 5.2 Comparison of the predicted and observed values for particle size with experimental error
observed predicted

5.2.3 Particle shape

In the following table a comparison of the various particle shape regression models is displayed.

Table 5.3 Particle shape models comparison

Model	R^2	MS_r	F
Multiple linear regression	0.434	1.86E-05	3.620*
Multiple linear regression with interaction	0.719	1.72E-05	2.096
Second order regression	0.775	1.95E-05	1.550

The R^2 value, the mean square error and the F- values for the different regression models are reported in Table 5.3. The F-values that were found to be statistically significant are indicated with an asterisk.

The linear regression model produced a moderately low R^2 value while both the linear regression with interactions and the second order regression reporting the highest explanation for variance in the system. The lowest error value was reported by the linear regression model with interaction terms, followed by the linear regression and second order models respectively. The only model that obtained a significant F-test values was the linear regression model. On further Investigation it was determined that the confidence intervals

associated with the F-values for the linear model with interaction terms and second order models are 91% and 75% respectively.

For the purpose of the finding the most capable model, the overall linear regression model with interaction terms has the lowest error, a reasonable R- squared value and an acceptable F-test value significance of 91% and is therefore acknowledged as the most adequate model in describing the circularity data values obtained in phase two.

In the following figure the linear regression with interactions model is presented together with the observed values and experimental errors.

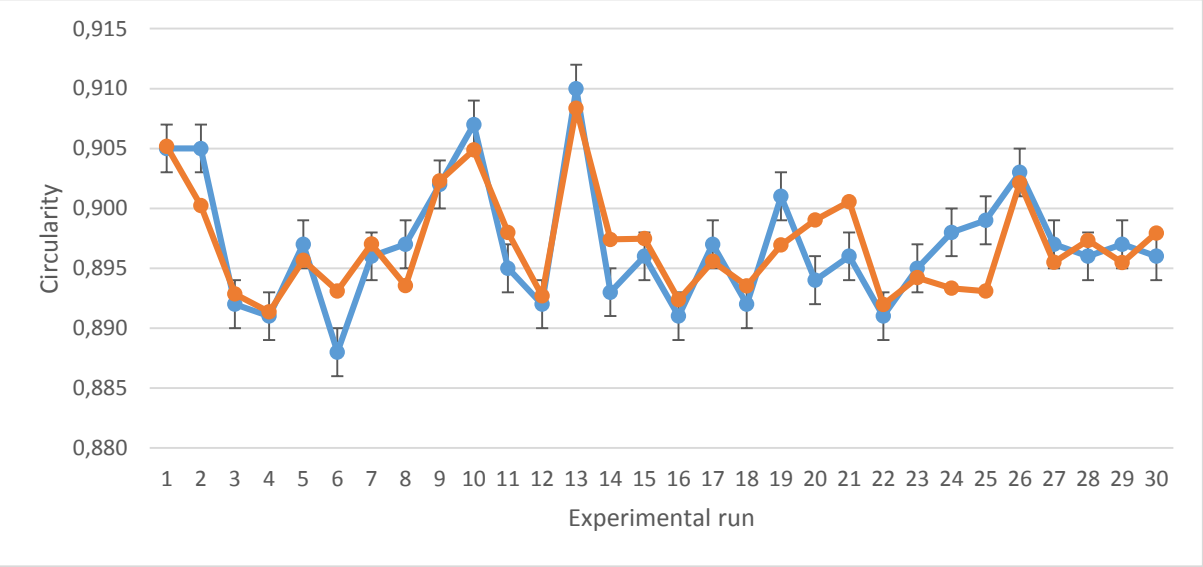

Figure 5.3 Comparison of the predicted and observed values for particle shape with experimental error
observed predicted

In Figure 5.3 it can be seen that the model does not always describe the particle circularity within the experimental error. This model, in comparison with the rest of the models obtained for particle shape, provides the best statistical explanation for the particle shape.

5.2.4 Porosity

A comparison of the various models for describing particle porosity can be seen in Table 5.4.

Table 5.4 Particle porosity models comparison

Model	R^2	MS_r	F
Multiple linear regression	0.053	5.138	0.268
Multiple linear regression with interaction	0.545	4.232	1.118
Second order regression	0.778	3.216	1.574

In Table 5.4 the coefficient of determination, the mean square error and the F- value are compared for the various models. The F-values that were calculated to be statistically significant are indicated by means of an asterisk.

The linear model produced the lowest R^2 value, describing little to no variation within the system. The second order model obtained the highest R squared value and the linear regression model with interactions the second highest R-squared value. The linear models both produced relatively high errors, with the second order model yielding the lowest error value.

None of these models produces a significant F-test value, or a F-value close to the significance value chosen for this study. Based on the R^2 and mean square error values the overall second order model appears to have the best description of the particle porosity. A comparison of the predicted and observed values with the measurement error can be seen in Figure 5.4

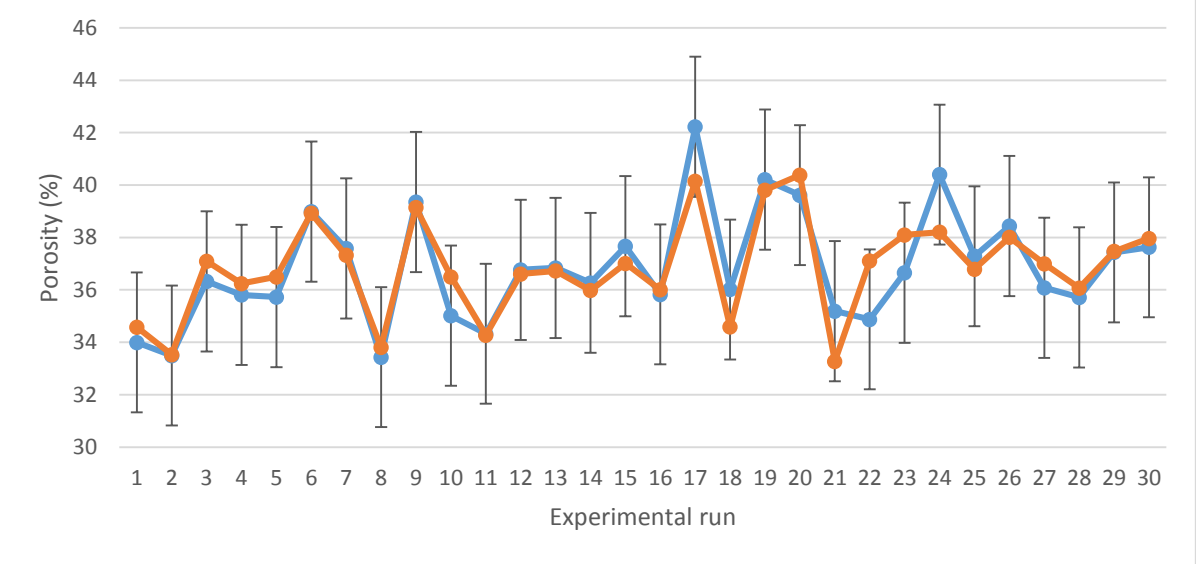

Figure 5.4 Comparison of the predicted and observed values for particle porosity with experimental error
observed predicted

In the figure above it is visible that the porosity measurement has an extremely large experimental error and that the second order regression model predicts the porosity values fairly well within this experimental error, and is statistically speaking the most adequate in describing the particle porosity.

5.2.5 Flowability

A comparison of the various coefficients of determination, mean square residuals and F values for the various flowability models can be seen in Table 5.5. The F-values that were found to be statistically significant are indicated with an asterisk.

Table 5.5 Particle flowability models comparison

Model	R^2	MS_r	F
Multiple linear regression	0.217	3.478	1.330
Multiple linear regression with interaction	0.514	3.698	0.989
Second order regression	0.634	4.333	0.780

The linear obtained the lowest R^2 values while the largest R squared values were obtained by the linear model with interactions and the second order models, with the highest value obtained by second order model.

The mean square error for all the regression models fall within the same range, with the overall linear model producing the lowest error value of all the models. None of the model obtained a significant F-value or an F-value close to the chosen confidence interval chosen for this study.

Due to the close mean square error values between the overall linear model with interactions and the second order model, the higher R^2 value gives the overall second order model the edge. In Figure 5.5 the values predicted by the second order model and the observed values are compared.

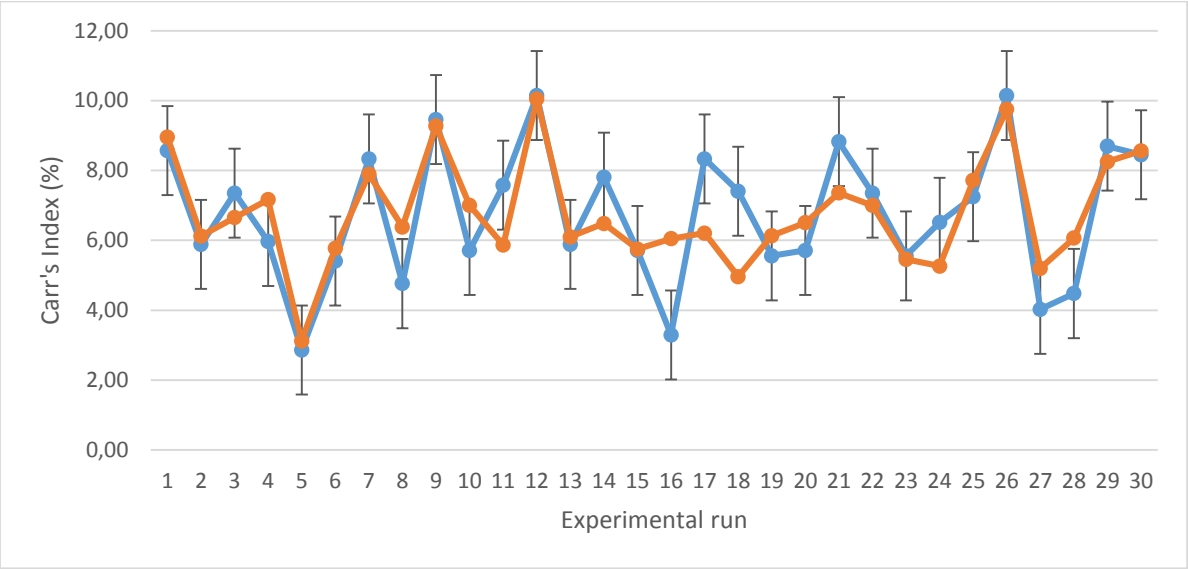

Figure 5.5 Comparison of the predicted and observed values for particle flowability with experimental error
observed predicted

In Figure 5.5 a large measurement error is visible. The second order model is seen to fall in range with the observed model and to mostly predict the particle flowability within the experimental error, but there are quite a few values that are not well predicted; even significantly outside the experimental error range. Although this model doesn't provide the best prediction, it does have the best statistical reliability of the three obtained models.

5.3 Model Validation

5.3.1 Particle abrasion resistance

The second order regression model was found to be the most statistically reliable in describing the abrasion resistance of the product granules in section 5.2.1. Figure 5.6 presents the observed versus predicted graph of this model using the validation data.

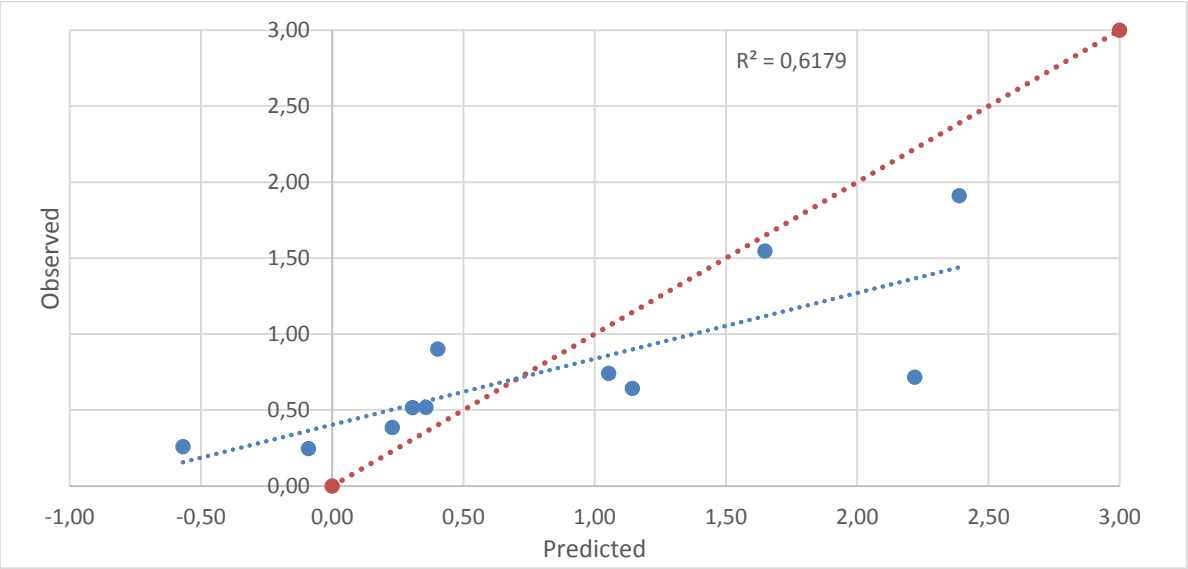

Figure 5.6 Observed versus predicted validation values for the second order abrasion resistance regression model ●observed versus predicted ●identity line

In Figure 5.6 the observed versus predicted values are presented with the trend line for this comparison as well as the identity line, a line through the origin with a slope of one. Ideally the observed and predicted values would lie on this line in indicating a perfect fit. In Figure 5.6 the model can be seen to provide values within range of the observed values between the values of range of 0.00 and 0.50. Between the values of 1.00 and 2.5 the model essentially overestimates the observed values. This graph produced an R^2 value of 0.618, explaining that 61.8% of the variance in the system is predicted. The model also produced negative values and can occur as a result of the different variable and level combinations chosen for the validation phase. This model does not provide an ideal fit.

The linear model with interactions produces the second-best statistical reliability in section 5.2.1. The observed versus predicted values for this model using the validation can be seen in Figure 5.7.

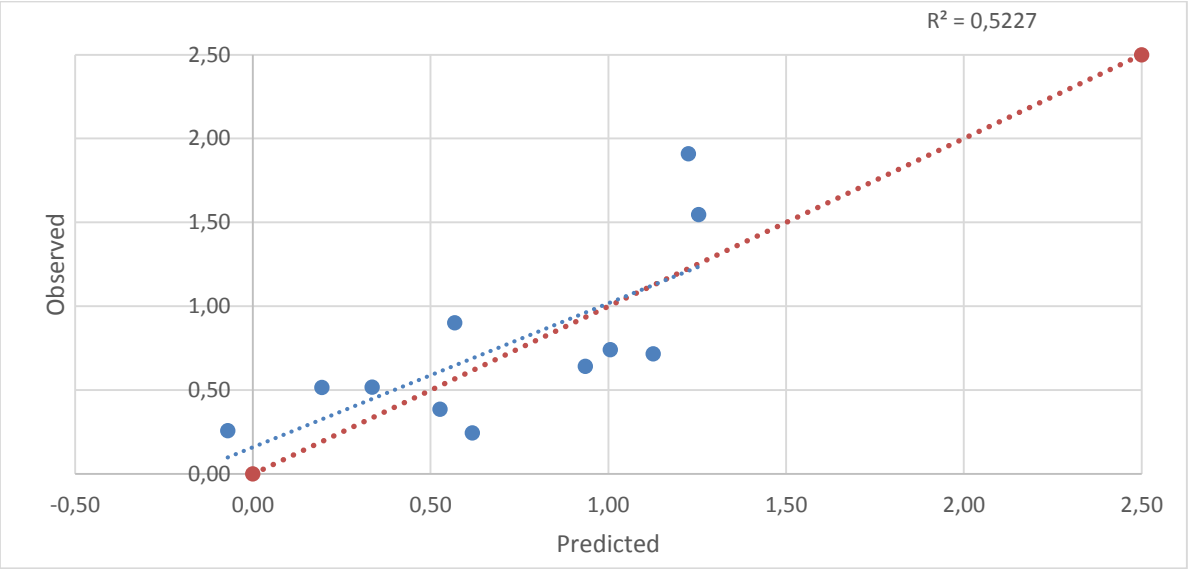

Figure 5.7 Observed versus predicted validation values for the linear model with interaction terms abrasion resistance regression model ●observed versus predicted ●identity line

In the figure above, the predicted values can be seen to fall within range of the identity line. Although the R^2 value for this graph is 0.523, which accounts for less variance in the system than the second order model, the predicted values are scattered more closely to the identity line suggesting a better predictive fit. A comparison of the R^2 and MSr values of these two models for the validation data can be seen in Table 5.6.

Table 5.6 Comparison of validation models for particle abrasion resistance

Model	**MS_r**	**R^2**
Linear model with interactions	0.099	0.523
Second order model	0.443	0.618

In the table above it can be seen that the linear regression with interaction model provides the lowest error value suggesting it is better suited to describe the validation data than the second order regression model due to the closeness in R^2 values. A schematic comparison of the values predicted by these two models and the observed validation values are presented in Figure 5.8.

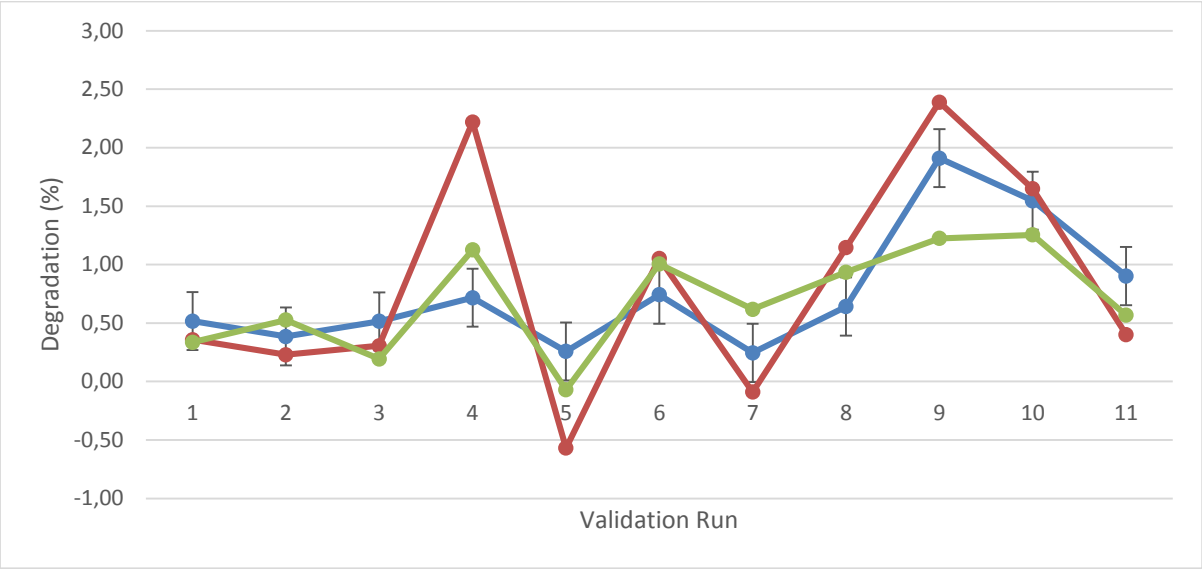

Figure 5.8 Comparison of the predicted and observed values for the validation of the abrasion resistance models ●observed ● linear with interactions ● second order model

In the Figure 5.8 error bars were added to the observed data values, and presented for the various validation runs. In this figure it is visible that both of these models predict values in range of the observed values, but both of these models produce values not always within the experimental error of the data obtained. The linear model with interactions produced more values within range of the experimental error than the second order regression model. The second order model is also seen to overestimate the values to a larger extent than the linear model.

Although the second order model better predicted the abrasion resistance values during the model development phase it did not perform as well during the validation phase in comparison with the linear regression model with interactions. This can be attributed to over fitting of the experimental data using a second order regression model. It can therefore be concluded that the linear regression model with two-way interactions provides better prediction capability that the second order regression model.

5.3.2 Product d_{50}

The observed and predicted values for the second order particle size regression model is displayed in Figure 5.9.

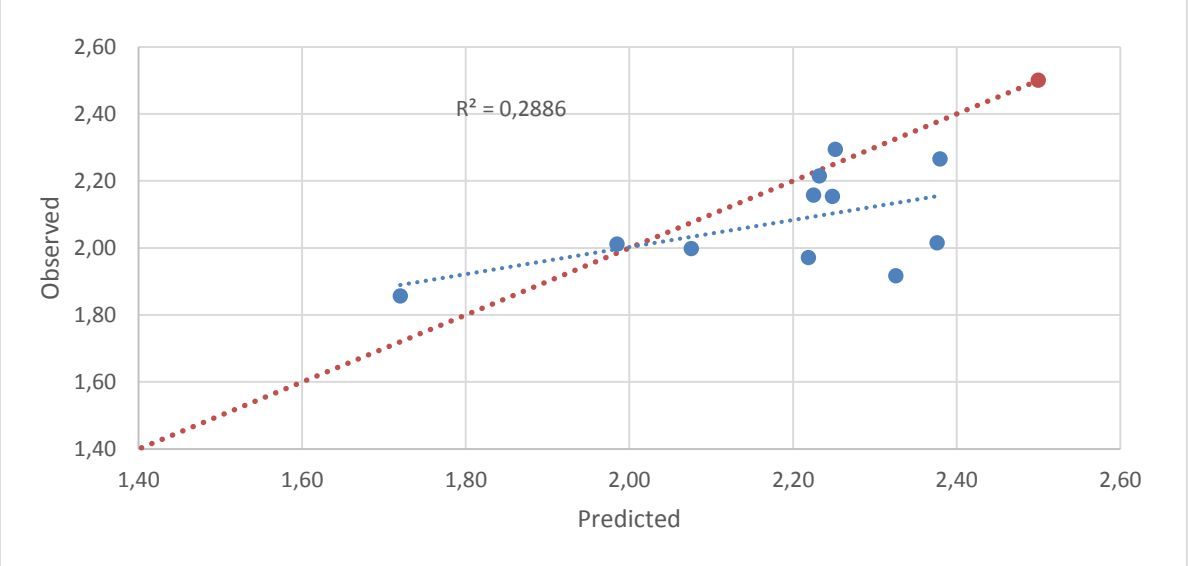

Figure 5.9 Observed versus predicted validation values for the overall second order product size regression model ●observed versus predicted ●identity line

From this figure it is visible that the model essentially overestimates the product size from point 2.20 to 2.40 where most of the data points are seen. It is also visible that the relationship between the model and the data is random, which is confirmed by the R^2 value of 0.289. This indicates a large discrepancy within the second order model. The linear model with interaction terms model was determined to be the second best statistically reliable model and in the following figure, the observed versus predicted values for this model are presented.

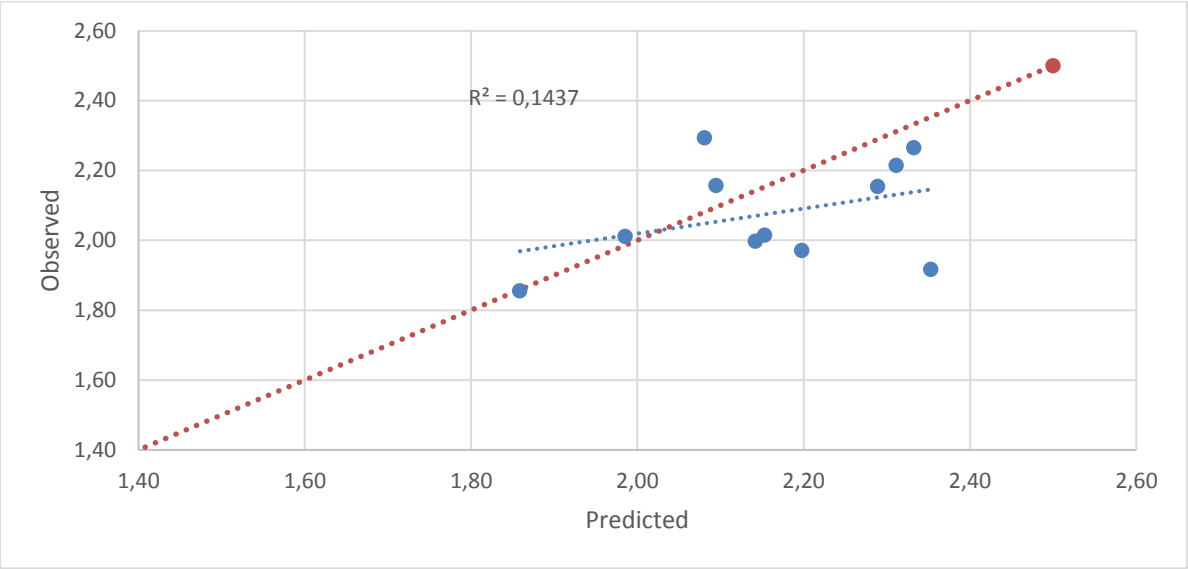

Figure 5.10 Observed versus predicted validation values for the overall linear model with interaction terms product size regression model ●observed versus predicted ●identity line

In Figure 5.10 the same situation is observed as with the second order model. The relationship between the model and the data is random and is again confirmed by a R^2 value of 0.144, indicating the model only explain 14.45% of the variation in the system. Both of these models exhibit a poor fit and not capable of accurately predicting the mean particles size. A comparison of the R^2 and MSr values of these two models for the validation data can be seen in in the following table.

Table 5.7 Comparison of validation models for particle size

Model	**MS_r**	**R^2**
Linear model with interactions	0.026	0.289
Second order model	0.046	0.144

A seen in Table 5.7, the R^2 values are extremely low showing that both these models can't explain a lot of variance in the system. The error values for both of these models are high in comparison to those obtained during the model evaluation in section 5.2.2. This indicates that neither of these models provides adequate prediction of the validation values. In Figure 5.11 a visual comparison of the two models over the various validation runs is presented.

Figure 5.11 Comparison of the predicted and observed values for the validation of the product size models ●observed ● linear with interactions ● second order model

In the above mentioned figure both of the models are seen to produce values within range of the observed values until validation run number eight. From validation run eight to ten the models predicted values completely out of range. This could be attributed to the different variable and level combinations used during the validation experimental design.

Although both these models were found to be statistically acceptable in section 5.2.2, neither of them were able to predict the particle size well enough during validation. Expanding the number of experimental runs and variable level combinations could assist in solving this deficiency.

5.3.3 Particle shape

Figure 5.12 presents the observed versus predicted result for the second order regression model.

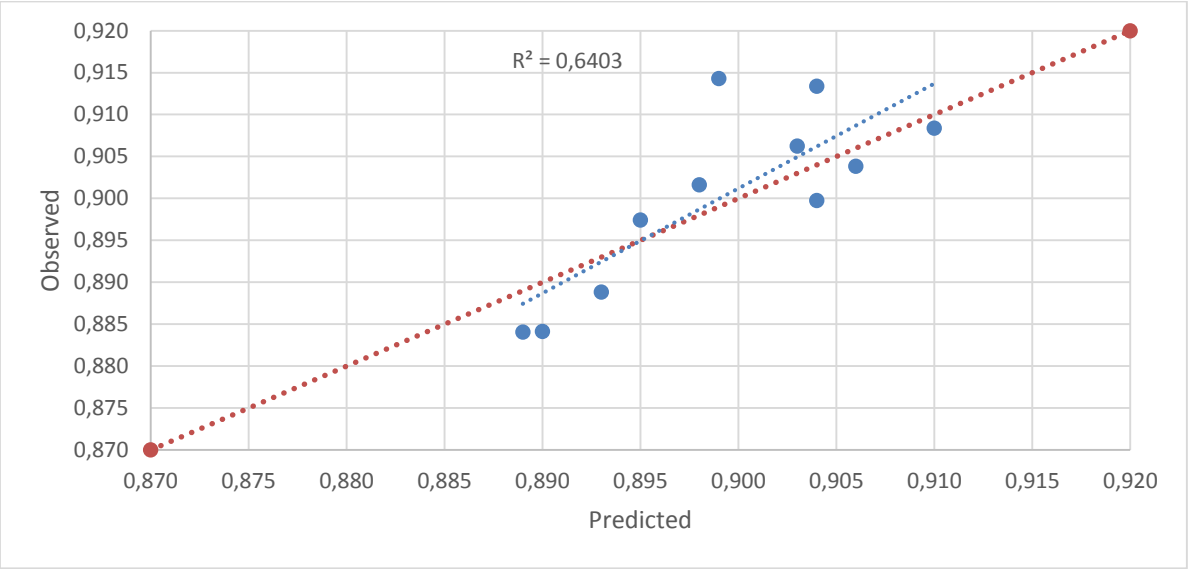

Figure 5.12 Observed versus predicted validation values for the second order product shape regression model ●observed versus predicted ●identity line

In Figure 5.12 the values are distributed around the identity line, suggesting the predicted and observed values are well within range of each other, with the circularity slightly underestimated from point 0.898 to 0.905. This model brought about an R^2 value of 0.640, indicating a moderate goodness of fit.

The linear model with interaction terms was the second best statistically reliable model. The observed and predicted values are compared in the following figure.

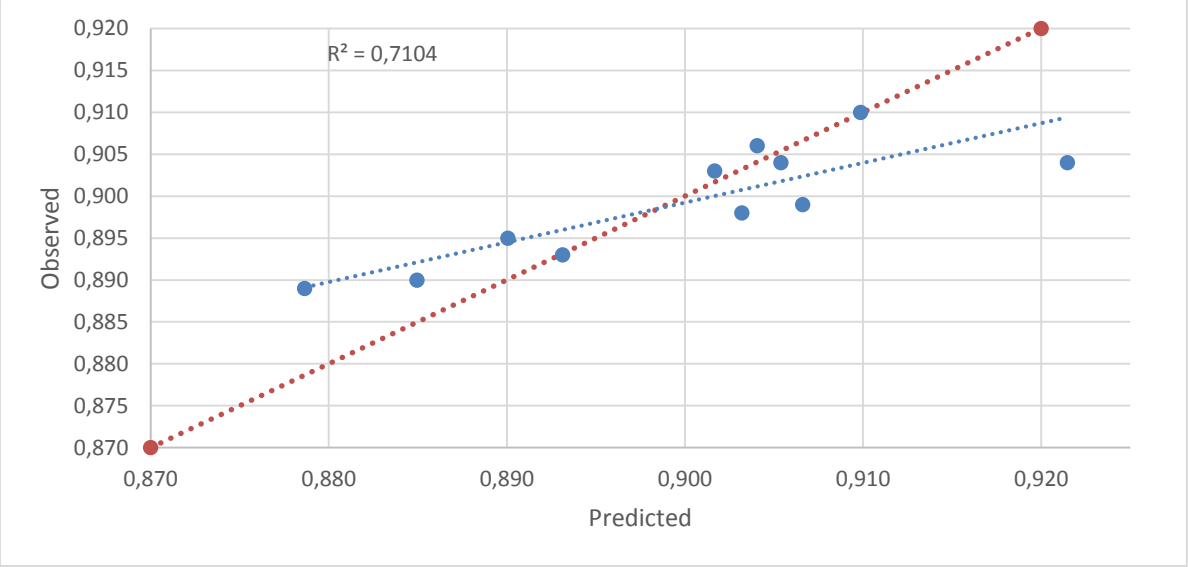

Figure 5.13 Observed versus predicted validation values for the linear model with interaction terms product shape regression model ●observed versus predicted ●identity line

Form Figure 5.13 it is visible that the predicted values are scattered around the identity line. This model underestimated values from point 0.876 to 0.890 with a visible over estimation of a values just past the point 0.920. With the observed R^2 value of 0.710, the model may

look good, but by carefully considering the data points in the figure above, it is concluded that this model does not have an ideal fit. A comparison of the R^2 and MSr values of these two models for the validation data can be seen in in the following Table 5.8.

Table 5.8 Comparison of validation models for particle shape

Model	**MS_r**	**R^2**
Linear model with interactions	3.96E-05	0.710
Second order model	5.03E-05	0.640

In the table above it can be seen that the linear model with interactions provides the smallest error value and the highest R^2 indicating that this model is better suited to describe the validation results than the second order model. Figure 5.14 presents a comparison of the predicted values of both models along with the observed values.

Figure 5.14 Comparison of the predicted and observed values for the validation of the product shape models
observed *linear with interactions* *second order model*

In the figure above the two models can be seen to follow the exact same trend as the observed data. Both of these models predicted most of the values within the experimental error range, with the linear model providing a little more accuracy.

Although the second order model was found to be more statistically acceptable in section 5.2.3, the linear model provided better prediction of the validation results. Again, this can

be attributed to over fitting associated by the use of a second order regression model. It can thus be concluded that the linear model with interactions provides the best predictive capability.

5.3.4 Particle porosity

The observed versus predicted values for the second order model can be seen in the following figure.

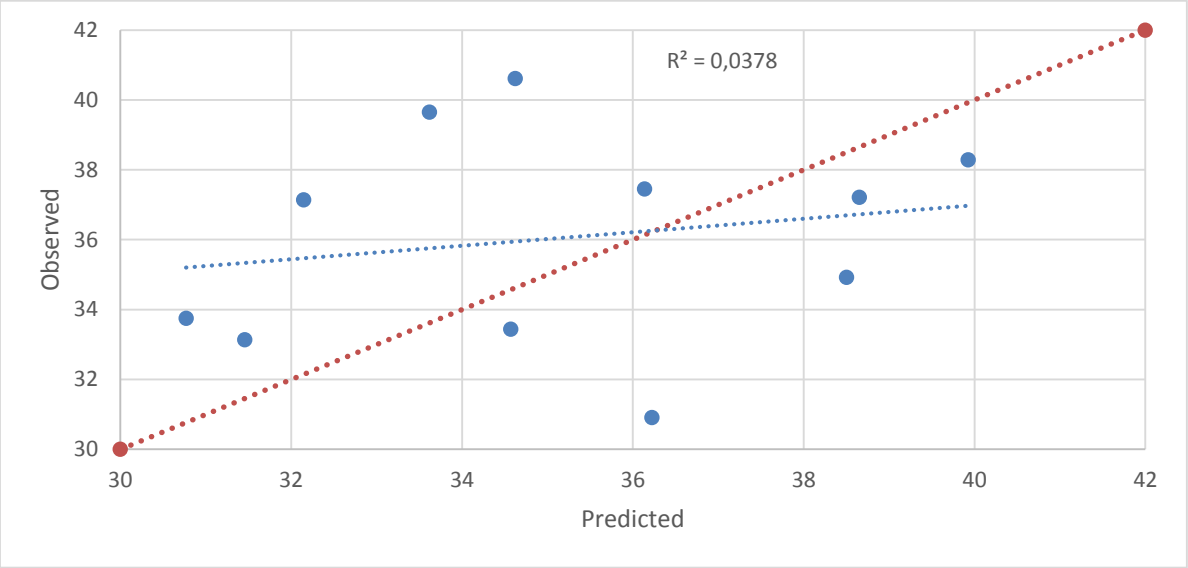

Figure 5.15 Observed versus predicted validation values for the second order product porosity regression model ●observed versus predicted ●identity line

In Figure 5.15 it is visible that the model has a random relationship with the validation data. The model is underestimating the data from values 31 to 35 and then overestimating the data from values 36 to 40. The R^2 value obtained for this fit is 0.038, indicating that this model accounts for almost none of the variance in system. This agrees with the lack of statistical reliability in all of the models obtained in section 4.3.

The observed versus predicted values for the overall linear with interaction terms model is displayed in Figure 5.16.

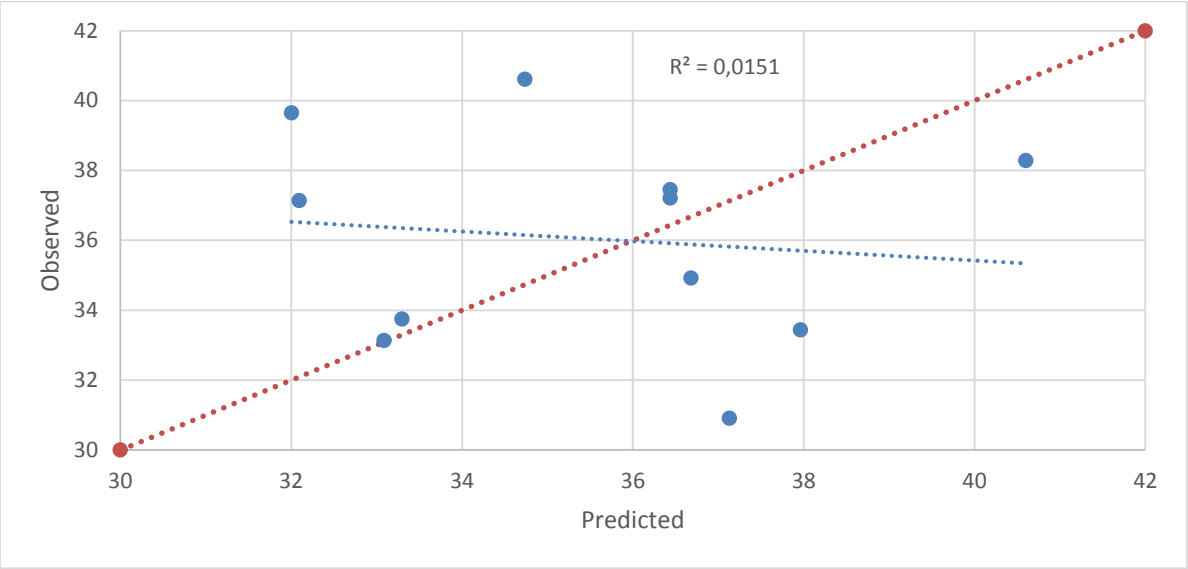

Figure 5.16 Observed versus predicted validation values for the linear model with interaction terms particle porosity regression model ●observed versus predicted ●identity line

In Figure 5.16 the lack of relationship between the observed and predicted porosity values is again seen as with the second order model. The model equally under and overestimates the values. The R^2 value of 0.015 confirms the extreme lack of fit of the porosity values. A comparison of the R^2 and MSr values of these two models for the validation data can be seen in in the following table.

Table 5.9 Comparison of validation models for particle porosity

Model	**MS_r**	**R^2**
Linear model with interactions	13.428	0.015
Second order model	17.534	0.038

From Table 5.9 it is visible that both of these models produce extremely high error values and extremely low R^2 values, indicating that both of these models are incapable of predicting the validation values. In the following figure a visual comparison between the predicted and the observed values over the various validation runs is seen.

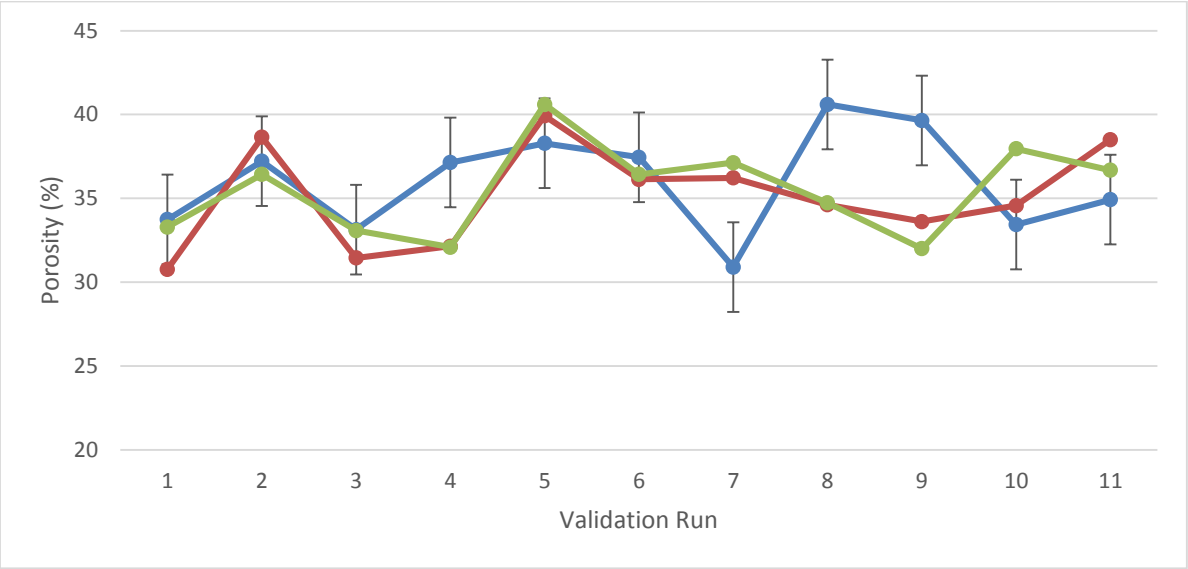

Figure 5.17 Comparison of the predicted and observed values for the validation of the particle porosity models ●observed ● linear with interactions ● second order model

Figure 5.17 shows that, while some of the porosity values are described within the experimental error for porosity, just as many are predicted outside of the experimental error range. Both of the models are concluded inadequate in describing particle porosity, which can be attributed to the inaccuracy of the oil absorption method in determining particle porosity, or maybe the influence of other factors, like other types of non-linearity in the relationships, not included in this study.

5.3.5 Flowability

The following figure presents the observed versus predicted results for the second order regression model obtained for flowability.

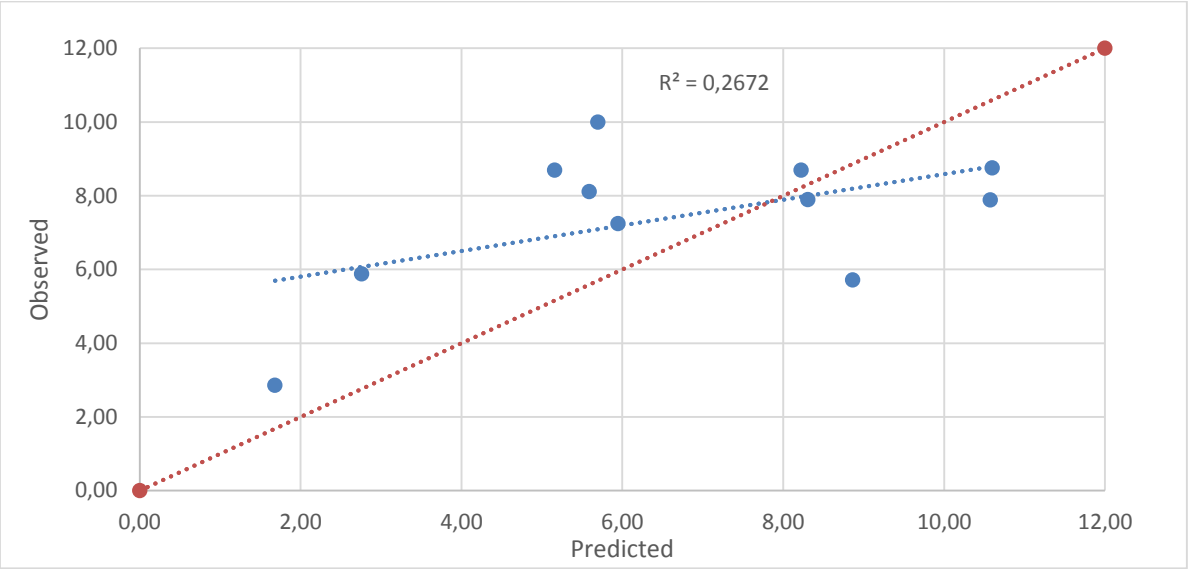

Figure 5.18 Observed versus predicted validation values for the second order flowability regression model ●observed versus predicted ●identity line

In Figure 5.18 the data points are distributed randomly around the identity line, indicating a visible difference between the predicted and observed results. The model underestimates the flowability from the point 1.8 to 6.0 and then goes on to overestimate the values from point 8.5 to 11.0. The relationship between the model and the data is random and is confirmed by an R^2 value of 0.267. The observed versus predicted result for the linear model with interactions is presented in Figure 5.19.

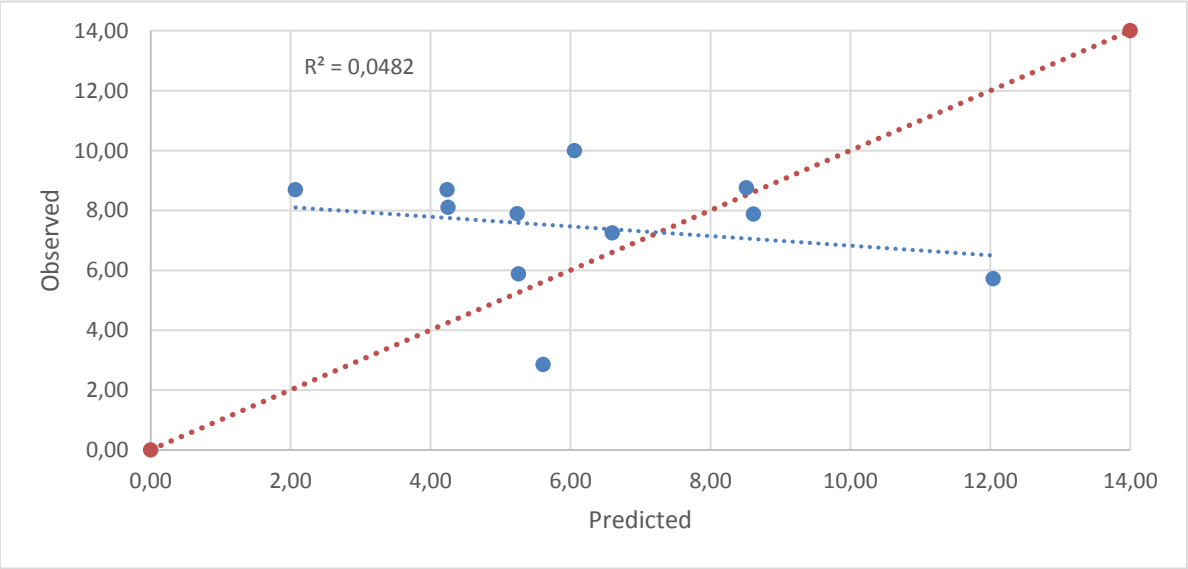

Figure 5.19 Observed versus predicted validation values for the overall linear model with interaction terms flowability regression model ●observed versus predicted ●identity line

In the Figure 5.19 it can be seen that the predicted flowability values fall significantly away from the identity line, suggesting a completely random relationship between the model and the data. The R^2 value of 0.048 also indicates this extreme lack of fit associated with this model. A comparison of the R^2 and MSr values of these two models for the validation data

can be seen in Table 5.10. Additionally a negative correlation is observed between the actual and predicted values, as indicated by the negative slope of the regression line, which shows that the model predicts the opposite direction than what would be expected.

Table 5.10 Comparison of validation models for particle flowability

Model	**MS_r**	**R^2**
Linear model with interactions	10.738	0.267
Second order model	7.909	0.048

In the table above high error values and low R^2 values are observed for both models indicating inadequate prediction capability by both of them. Figure 5.20 presents a comparison of the predicted values from both models along with the observed values.

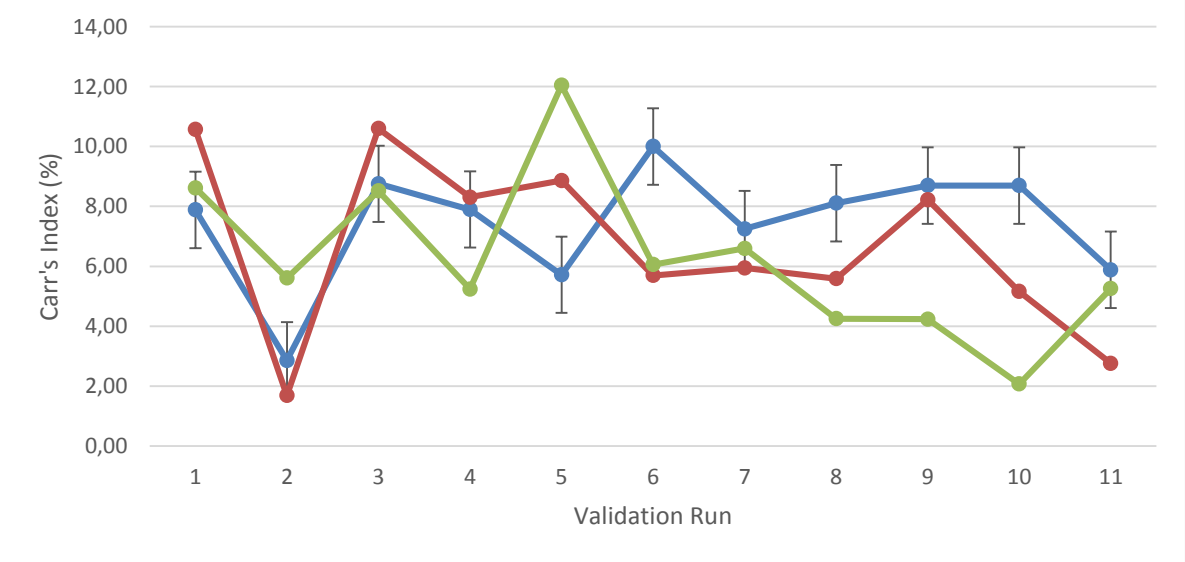

Figure 5.20 Comparison of the predicted and observed values for the validation of the product flowability
●observed ● linear with interactions ● second order model

From the figure above it is visible that not one of these two models predicts the particle flowability, not even within the experimental error. Both of these models are inadequate in explaining particle flowability. This observations correlates with the lack of statistical reliability obtained for all the flowability models in section 5.2.5.

In this chapter successful models were obtained for the abrasion resistance and particle shape and thus these two quality parameters can be predicted when the physicochemical material feed properties of AN are varied and the rest of the process variables are

maintained at standard operating conditions. No adequate models were obtained for the particle size, porosity and flowability. The physicochemical material feed properties of AN successfully describes the abrasion resistance but is adequate in describing particle size, porosity and flowability. All conclusion drawn from this chapter will be presented in the following section.

---

6. Conclusions and Recommendations

6.1 Introduction

In this chapter the conclusions drawn from this study are presented and recommendations are given for subsequent work on the fluidised bed granulator.

6.2 Conclusions

The abrasion resistance and particle shape were successfully described by multiple linear regression models with interactions. The second order models obtained for both these quality parameters performed well during model development, but poorly during validation indicating the second order models over-fit the data during model development. These two models are able to predict the abrasion resistance and particle shape respectively when all other process variable are held constant at their standard operating values. The capability of these models also indicates that the physicochemical material feed properties of AN does indeed have a significant effect on abrasion resistance and particle shape.

The second order and multiple regression model with two-way interactions for particle size were found adequate during model development but inadequate during validation and thus neither of these two models can be used to predict particle size. This is a result of either a shortage in variable and level combinations or the omission of factors that have a distinct influence on particle size, e.g. fluidising air flow rate, nozzle spray conditions or fluctuations in any of the variables which were kept constant during this study. The physicochemical material feed properties of AN alone was not able to describe the particle size and thus further investigation of particle size is needed.

No adequate models were obtained for the particle porosity or flowability and is attributed to the high measurement error and difficulties associated with the oil absorption technique to determine porosity, and the tapped density technique to determine the Carr's index. The possibility of other production related factors influencing these two quality parameters can also not be excluded. The physicochemical material feed properties of AN were concluded incapable of describing the particle porosity and flowability. Further investigation into particle porosity and flowability with relations to other production related variables is needed.

6.3 Recommendations

Exploring other porosity measurement methods would assist in reducing the large experimental errors associated with this measurement, and will assist in an improved modelling efficiency of particle porosity. The use of an automatic tapper instead of hand

tapping the sample in a measuring cylinder to determine tapped density can assist in improving accuracy of the measurement of Carr's index. Once the measurement techniques are improved the study could be repeated to determine the effect of the physicochemical material feed properties of AN on these two quality parameters. Attention could also be given to the high error associated with the determination of the particle abrasion resistance.

Using the central composite design proved to be more than adequate. Expanding the level and variable combinations could help to improve the particle size regression models. Exploring other nonlinear modelling methods, such as artificial neural networks, could also prove to be useful.

Obtaining the stipulated variable levels in the central composite design more accurately during the experimental trails, such as the spray liquid flowrate which is dependent on opening or closing nozzles, would assist in achieving more accurate and usable models.

Repeating this experimental design including different sets of fluidising air flow values can be useful to determine the effects of the fluidising air flow, which, according to literature, has a significant effect on granule quality.

References

Abberger, T., Seo, A., & Schæfer, T. 2002. The effect of droplet size and powder particle size on the mechanisms of nucleation and growth in fluid bed melt agglomeration. *Int. J. Pharm.* 249(1–2):185–197.

Albuquerque, T., Dias, V.H., Poellinger, N., & Pinto, J.F. 2010. Construction of a quality index for granules produced by fluidized bed technology and application of the correspondence analysis as a discriminant procedure. *Eur. J. Pharm. Biopharm. Elsevier B.V.* 75(3):418–424.

Aleksić, I., Crossed D Signuriš, J., Ibrić, S., & Parojčić, J. 2015. An investigation into the usefulness of different empirical modeling techniques for better control of spray-on fluidized bed melt granulation. *Int. J. Pharm.* 496(2):627–635.

Becher, R. & Schlünder, E.-U. 1998. Fluidized bed granulation — the importance of a drying zone for the particle growth mechanism 1. *Chem. Eng. Process.* 37:1–6.

Behzadi, S.S., Klocker, J., Hüttlin, H., Wolschann, P., & Viernstein, H. 2005. Validation of fluid bed granulation utilizing artificial neural network. *Int. J. Pharm.* 291(1–2):139–148.

Bodhmage, A. 2006. Correlation between physical properties and flowability indicators for fine powders.

Braumann, A., Kraft, M., & Mort, P.R. 2010. Parameter estimation in a multidimensional granulation model. *Powder Technol. Elsevier B.V.* 197(3):196–210.

Cameron, I.T., Wang, F.Y., Immanuel, C.D., & Stepanek, F. 2005. Process systems modelling and applications in granulation: A review. *Chem. Eng. Sci.* 60(14):3723–3750.

Dadkhah, M. & Tsotsas, E. 2014. Influence of process variables on internal particle structure in spray fluidized bed agglomeration. *Powder Technol. Elsevier B.V.* 258:165–173.

Ennis, B. & Litster, J.D. 1997. Perry's Chemical Engineers' Handbook. 7th ed. McGraw-Hill: New York.

Faure, A, York, P., & Rowe, R.C. 2001. Process control and scale-up of pharmaceutical wet granulation processes: A review. *Eur. J. Pharm. Biopharm.* 52(3):269–277.

Ferreira, S.L.C., Bruns, R.E., da Silva, E.G.P., dos Santos, W.N.L., Quintella, C.M., David, J.M., de Andrade, J.B., Breitkreitz, M.C., Jardim, I.C.S.F., & Neto, B.B. 2007. Statistical

designs and response surface techniques for the optimization of chromatographic systems. *J. Chromatogr. A*. 1158(1–2):2–14.

Goldschmidt, M.J. V, Weijers, G.G.C., Boerefijn, R., & Kuipers, J. a M. 2003. Discrete element modelling of fluidised bed spray granulation. *Powder Technol.* 138(1):39–45.

Hemati, M., Cherif, R., Saleh, K., & Pont, V. 2003. Fluidized bed coating and granulation: Influence of process-related variables and physicochemical properties on the growth kinetics. , in: Powder Technology. . pp. 18–34.

Hussain, M., Kumar, J., & Tsotsas, E. 2015. Modeling aggregation kinetics of fluidized bed spray agglomeration for porous particles. *Powder Technol. Elsevier B.V.* 270(PB):584–591.

International Plant Nutrition Institute. 2015. Ammonium nitrate. *Nutr. Source Specifics No. 22*. (22):11083.

Iveson, S.M., Litster, J.D., Hapgood, K.P., & Ennis, B.J. 2001. Nucleation, growth and breakage phenomena in agitated wet granulation processes: a review. *Powder Technol.* 117:3–39.

Jansens, P.J. 2000. Melt Crystallization. , Industrial Crystallization of Melts. Marcel Dekker: New York.

Kukec, S., Vrečer, F., & Dreu, R. 2012. A study of in situ fluid bed melt granulation using response surface methodology. *Acta Pharm.* 62(4):497–513.

Lazic, Z.I.R. 2004. Design of Experiments in Chemical Engineering: A Practical Guide. 1st ed. Wiley-VCH: Weinheim.

Lee, T.Z.E., Krongchai, C., Mohd Irwn Lu, N.A.L., Kittiwachana, S., & Sim, S.F. 2015. Application of central composite design for optimization of the removal of humic substances using coconut copra. *Int. J. Ind. Chem. Springer Berlin Heidelberg*. 6(3):185–191.

Liu, H., Wang, K., Schlindwein, W., & Li, M. 2013. Using the Box-Behnken experimental design to optimise operating parameters in pulsed spray fluidised bed granulation. *Int. J. Pharm. Elsevier B.V.* 448(2):329–338.

Mehta, K.A., Rekhi, G.S., & Parikh, D.M. 2005. Extrusion/Spheronization as a Granulation Technique. *Handb. Pharm. Granulation Technol.* :333–363.

Mort, P. & Tardos, G. 1999. Scale-up of agglomeration processes using transformations.

Kona. 17(17):64–75.

Nagaiah, C., Warnecke, G., Heinrich, S., & Peglow, M. 2008. Three-dimensional numerical study of heat and mass transfer in fluidized beds with spray nozzle. *Comput. Chem. Eng.* 32:2877–2890.

Närvänen, T., Antikainen, O., & Yliruusi, J. 2009. Predicting particle size during fluid bed granulation using process measurement data. *AAPS PharmSciTech*. 10(4):1268–1275.

Närvänen, T., Lipsanen, T., Antikainen, O., Räikkönen, H., & Yliruusi, J. 2008. Controlling granule size by granulation liquid feed pulsing. *Int. J. Pharm.* 357(1–2):132–138.

Parikh, D.M. 2009. Handbook of Pharmaceutical Granulation Technology. 3rd ed. Cambridge University Press: New York.

Park, S.H., Kim, H.J., & Cho, J.-I. 2003. Optimal central composite designs for fitting second order response surface regression models. *Korea Sci. Eng. Found.* (Ccd):1–23.

Patel, T.B., Patel, L.D., Patel, T.B., Makwana, S.H., & Patel, T.R. 2010. Influence of process variables on physicochemical properties of the granulation mechanismo of diclofenac sodium in fluid bed granulation. *Int. J. Pharm. Rev. Res.* 3(1):61–65.

Patnaik, P. 2003. Handbook of Inorganic Chemicals. 1st ed. , Ebook. McGraw-Hill: New York.

Petrovic, J., Chansanroj, K., Meier, B., Ibric, S., & Betz, G. 2011. Analysis of fluidized bed granulation process using conventional and novel modeling techniques. *Eur. J. Pharm. Sci.* 44(3):227–234.

Phan-Tan-Luu, R. & Sergent, M. 2009. 1.14 - Nonclassical Experimental Designs. *Compr. Chemom.* :453–499.

Poncelet, D. & Vétérinaire, É.N. 2002. Batch and Continuous Fluid Bed Coating — Review and State of the Art. *J. Food Eng.* 53:325–340.

Pont, V., Saleh, K., Steinmetz, D., & Hémati, M. 2001. Influence of the physicochemical properties on the growth of solid particles by granulation in fluidized bed. *Powder Technol.* 120(1–2):97–104.

Prion, S. & Haerling, K.A. 2014. Making sense of methods and measurement: Pearson product-moment correlation coefficient. *Clin. Simul. Nurs. International Nursing Association for Clinical Simulation and Learning*. 10(11):587–588.

Puth, M.T., Neuhäuser, M., & Ruxton, G.D. 2015. Effective use of Spearman's and Kendall's correlation coefficients forassociation between two measured traits. *Anim. Behav.* 102:77–84.

Rajniak, P., Mancinelli, C., Chern, R.T., Stepanek, F., Farber, L., & Hill, B.T. 2007. Experimental study of wet granulation in fluidized bed: Impact of the binder properties on the granule morphology. *Int. J. Pharm.* 334(1–2):92–102.

Ramachandran, R., Poon, J.M.H., Sanders, C.F.W., Glaser, T., Immanuel, C.D., Doyle, F.J., Litster, J.D., Stepanek, F., Wang, F.Y., & Cameron, I.T. 2008. Experimental studies on distributions of granule size, binder content and porosity in batch drum granulation: Inferences on process modelling requirements and process sensitivities. *Powder Technol. Elsevier B.V.* 188(2):89–101.

Rieck, C., Hoffmann, T., Beck, a., Peglow, M., & Tsotsas, E. 2015. Influence of drying conditions on layer porosity in fluidized bed spray granulation. *Powder Technol. Elsevier B.V.* 272:120–131.

Rutland, D.W. 1986. Manual for Determining Physical Properties of Fertilizer.

Saleh, K., Steinmetz, D., & Hemati, M. 2003. Experimental study and modeling of fluidized bed coating and agglomeration. , in: Powder Technology. . pp. 116–123.

Schæfer, T. 2001. Growth mechanisms in melt agglomeration in high shear mixers. *Powder Technol.* 117(1–2):68–82.

Schubert, H., Herrmann, W., & Rumpf, H. 1975. Deformation behaviour of agglomerates under tensile stress. *Powder Technol.* 11(2):121–131.

Smith, P.G. & Nienow, A. W. 1983. Particle growth mechanisms in fluidised bed granulation-I. The effect of process variables. *Chem. Eng. Sci.* 38(8):1223–1231.

Srinivasakannan, C. & Balasubramaniam, N. 2003. Particle Growth in Fluidised Bed Granulation. *Chem. Biochem. Eng.* 17(3):201–205.

Talu, I., Tardos, G.I., & Khan, M.I. 2000. Computer simulation of wet granulation. *Powder Technol.* 110(1–2):59–75.

Tan, H.S., Salman, A. D., & Hounslow, M.J. 2005. Kinetics of fluidised bed melt granulation III: Tracer studies. *Chem. Eng. Sci.* 60(14):3835–3845.

Tan, H.S., Salman, A. D., & Hounslow, M.J. 2006. Kinetics of fluidised bed melt granulation

I: The effect of process variables. *Chem. Eng. Sci.* 61(5):1585–1601.

Vargeese, A. a., Joshi, S.S., & Krishnamurthy, V.N. 2009. Effect of method of crystallization on the IV-III and IV-II polymorphic transitions of ammonium nitrate. *J. Hazard. Mater.* 161(1):373–379.

Veliz Moraga, S., Villa, M.P., Bertan, D.E., Cotabarren, I.M., Pia, J., Pedernera, M., & Bucal, V. 2015. Fluidized-bed melt granulation: The effect of operating variables on process performance and granule properties. *Powder Technol. Elsevier B.V.* 286:654–667.

Walker, G.M., Holland, C.R., Ahmad, M.M.N., & Craig, D.Q.M. 2005. Influence of process parameters on fluidised hot-melt granulation and tablet pressing of pharmaceutical powders. *Chem. Eng. Sci.* 60(14):3867–3877.

Wong, P.M., Chan, L.W., & Heng, P.W.S. 2013. Investigation on Side-Spray Fluidized Bed Granulation with Swirling Airflow. *AAPS PharmSciTech*. 14(1):211–221.

Zhai, H., Li, S., Andrews, G., Jones, D., Bell, S., & Walker, G. 2009. Nucleation and growth in fluidised hot melt granulation. *Powder Technol. Elsevier B.V.* 189(2):230–237.

Zhang, W.Y., Wei, Z.W., Wang, B.H., & Han, X.P. 2016. Measuring mixing patterns in complex networks by Spearman rank correlation coefficient. *Phys. A Stat. Mech. its Appl. Elsevier B.V.* 451:440–450.

Appendix A – Experimental procedure

Table A.0.1 Complete experimental design phase two

Run Name	Atomizing Air Pressure (kPa)	Flowrate (tons/hr)	Spray Liquid Concentration			Spray Liquid Temperature (Degrees C)	Seed Particle Size (mm)
			Concentration (wt%)	Falling film evaporator (Degrees C)	Vacuum Pressure (kpa)		
1	-10	5	91	39,1	60	125	1,3
2	-10	5	91	44,7	71	135	1,1
3	-10	5	93	49,1	60	135	1,1
4	-10	5	93	49,1	60	135	1,3
5	-10	8	91	39,1	60	125	1,1
6	-10	8	91	44,7	71	135	1,3
7	-10	8	93	52,1	65	140	1,3
8	-10	5	93	49,1	60	135	1,1
9	15	5	91	39,1	60	125	1,1
10	15	5	91	44,7	71	135	1,3
11	15	5	93	52,1	65	140	1,3
12	15	5	93	49,1	60	135	1,1
13	15	8	91	39,1	60	125	1,3
14	15	8	91	44,7	71	135	1,1
15	15	8	93	52,1	65	140	1,1
16	15	8	93	49,1	60	135	1,3
17	-15	6,5	92	44,1	60	130	1,2
18	30	6,5	92	44,1	60	130	1,2
19	0	3,5	92	44,1	60	130	1,2
20	0	9,5	92	44,1	60	130	1,2
21	0	6,5	90	41,9	68	130	1,2
22	0	6,5	93,5	44,1	60	130	1,2
23	0	6,5	92	47,5	64	135	1,2
24	0	6,5	92	47,5	64	135	1,2
25	0	6,5	92	44,7	60	130	1
26	0	6,5	92	48,3	75	140	1,4
27	0	6,5	92	48,3	75	140	1,2
27R	0	6,5	92	48,3	75	140	1,2
27R	0	6,5	92	48,3	75	140	1,2
27R	0	6,5	92	48,3	75	140	1,2

Appendix B – Experimental Error

In order to determine the experimental error for the measure methods, one analysis of each of the measurement methods was repeated five times. The experimental error was then determined by firstly calculating the average value of the three repeats using equation B.1.

$$\bar{x} = \frac{1}{N}\sum_{i=1}^{N} x_i$$

[B.1]

The standard deviation was calculated using equation B.2.

$$\sigma = \sqrt{\frac{\sum_{i=1}^{N}(x_i - \bar{x})^2}{N-1}}$$

[B.2]

Using the standard deviation, the standard error is calculated using the following equation:

$$SE = \frac{\sigma}{\sqrt{N}}$$

[B.3]

The margin of error was then calculated using t-distribution values of 2.78, for a confidence level of 95% and degree of freedom = 4, and then used to determine a confidence interval (Lazic, 2004):

$$CI = \bar{x} \pm (SE \times t)$$

[B.4]

Thereafter, the experimental error was calculated using equation B.5.

$$Error\ (\%) = \frac{CI}{\bar{x}} \times 100$$

[B.5]

Appendix C – Raw Data

Table C.0.1 Experimental phase two raw data

Run	Difference Atomizing Air Pressure (kPa)	Spray Liquid flowrate (tons/hr)	Spray Liquid Concentration (wt%)	Spray Liquid Temperature (degree C)	Seed Particle Size (mm)	Oil Absorption (%)	Abrasion (%)	Product Size (mm)	Circularity	Carr Index (%)
1	-12,223	5,217	89,421	124,939	1,709	33,994	0,257	2,100	0,905	8,571
2	-11,182	5,406	90,842	138,300	1,789	33,494	1,028	2,125	0,905	5,882
3	-11,289	5,816	92,225	134,546	1,662	36,325	0,775	2,004	0,892	7,353
4	-10,559	5,092	92,221	135,156	1,635	35,810	0,519	2,053	0,891	5,970
5	-8,236	7,839	89,287	124,587	1,903	35,725	0,643	2,433	0,897	2,857
6	-17,014	5,959	90,945	135,234	1,832	38,988	1,031	2,282	0,888	5,405
7	-14,380	4,579	91,774	141,623	1,576	37,580	1,673	1,812	0,896	8,333
8	13,586	5,620	93,020	140,354	1,808	33,433	1,034	2,126	0,897	4,762
9	16,155	3,028	89,565	124,872	1,622	39,354	1,038	2,057	0,902	9,459
10	11,553	6,021	90,915	135,608	1,695	35,015	0,907	2,009	0,907	5,714
11	11,470	5,310	92,913	140,088	1,823	34,325	0,257	2,080	0,895	7,576
12	14,521	4,950	92,389	134,169	1,739	36,765	1,167	2,040	0,892	10,145
13	14,863	8,141	89,410	125,090	1,961	36,838	0,389	2,148	0,910	5,882
14	13,811	7,547	90,955	133,945	1,728	36,265	0,644	2,234	0,893	7,813
15	13,540	5,675	93,009	144,054	1,692	37,665	2,059	1,925	0,896	5,714
16	-7,374	6,125	92,475	134,926	1,664	35,827	0,515	2,085	0,891	3,292
17	-11,271	6,016	91,165	128,377	1,697	42,223	0,777	1,947	0,897	8,333
18	1,746	6,768	92,465	134,977	1,574	36,013	0,516	2,056	0,892	7,407
19	1,787	6,133	91,530	131,306	1,746	40,207	0,388	2,143	0,901	5,556
20	5,359	6,455	91,230	130,090	1,761	39,616	0,515	2,062	0,894	5,714
21	0,604	7,022	89,995	129,812	1,781	35,189	0,775	2,275	0,896	8,824
22	-0,201	6,260	91,675	129,764	1,641	34,875	0,779	2,094	0,891	7,353
23	-2,773	6,153	91,885	136,196	1,731	36,654	1,030	1,979	0,895	5,556
24	-3,368	6,309	91,932	135,216	1,725	40,400	1,031	2,057	0,898	6,516
25	2,865	6,389	91,358	129,455	1,601	37,284	0,649	2,013	0,899	7,246
26	1,049	8,640	91,597	142,659	1,542	38,436	1,032	1,849	0,903	10,145
27	2,750	8,446	91,838	140,362	1,605	36,081	0,773	1,862	0,897	4,025
27	0,222	7,032	91,170	129,171	1,604	35,714	0,259	1,919	0,896	4,478
27	-10,429	5,934	92,992	142,188	1,730	37,432	0,646	1,935	0,897	8,696
27	-12,596	6,982	92,592	140,614	1,579	37,626	0,514	1,908	0,896	8,451

Appendix D – Results phase one

The purpose of phase one was to determine which process variables had the largest effect on product quality and to establish how the effects of the physicochemical feed properties of ammonium nitrate compares with the rest of the process variables. Both Spearman's correlation as well as multiple linear regression was used.

D.1 Spearman Correlation

Spearman's correlation was used to determine if there were any statistical correlations between the process variables and the product quality. The results are presented in a Spearman's correlations matrix. The correlations between the process variables and the product quality is presented in the following table.

Table D.0.1 Spearman's correlation between the process variables and product quality for phase one

	POA	HEP	PD_{50}	C
FAF	0,213	**0,371**	-0,315	0,298
FAT	**-0,332**	0,001	0,125	0,178
SLF	0,281	**0,384**	0,037	-0,037
SLT	-0,256	0,094	0,098	**-0,335**
SLC	-0,166	**-0,575**	**0,334**	**-0,488**
Fd50	-0,051	0,123	0,199	0,246
DP	-0,267	-0,191	-0,190	0,275
AAT	0,168	-0,044	-0,096	-0,292

All correlations with a significance level of P <.05 are underlined (indicating a confidence interval of ≥ 95 %) which suggests a high probability of seeing the given correlation or stronger. The table is color-coded, with dark red indicating a strong negative effect and dark green indicating a strong positive effect. From Table D.0.1 it can be seen that there is a weak negative correlation between the particle porosity and fluidising air temperature, indicating that as the fluidising air temperature increases lower particle porosity is observed. No process variable seems to have a significant correlation with the particle porosity, which is also found during the modelling of this attribute.

The true density of the particles had a weak positive correlation with the fluidising air flow and spray liquid flowrate suggesting an increase of these two variables correlates with increase in the particle's true density while the spray liquid concentration shows a moderate negative correlation with the true density. The spray liquid concentration has a weak positive correlation with the product d_{50} while the particle circularity has a weak negative correlation with spray liquid temperature and a moderate weak correlation with spray liquid concentration.

From the spearman's correlation matrix it is noticeable that of all the variables, the physicochemical material feed properties had the highest correlations with the product quality parameters, especially the spray liquid concentration, having correlations with three of the four quality parameter. Spray liquid temperature and spray liquid flowrate also showed good correlations with some of the quality parameters, while the feed particle d_{50} and the atomising air pressure difference had no significant correlations with any of the product quality parameters.

D.2 Regression Analysis

Multiple linear regression was done on the data obtained during experimental phase one. Due to the nature of and the purpose of this experimental phase only a quick overview of the regression result will be given in this section. Al regression results were obtained using STATISTICA® software.

The regression coefficients for each of the quality parameters and their corresponding significance values are given in Table D.0.2.

Table D.0.2 Multiple linear regression coefficients and significance values for phase one

	Porosity		**True Density**		**Pd_{50}**		**Circularity**	
	β	**P Value**	**β**	**P Value**	**β**	**P Value**	**β**	**P Value**
Mean	34.620	0.646	2.082*	0.000	-0.037	0,980	1.019*	0.000
FAF	0.001	0.528	0.00001	0.131	-0.0001*	0,019	0.000003*	0.020
FAT	0.052	0.569	0.0004	0.155	0.001	0,553	0.0001	0.435
SLF	-0.022	0.986	0.003	0.469	0.001	0,972	-0.0001	0.911

SLT	-0.062	0.733	0.001*	0.039	-0.002	0,673	-0.0002	0.205
SLC	-0.056	0.950	-0.007*	0.026	0.026	0,153	-0.002	0.076
Fd50	-7.084	0.468	-0.025	0.435	0.303	0,120	0.015	0.157
DP	-0.040	0.439	-0.0001	0.747	-0.001	0,356	0.00005	0.366
AAT	0.006	0.934	0.00004	0.873	-0.002	0,244	-0.00003	0.737
R^2	0.134		0.358		0.488		0.498	
F	0.579		2.092		3.571*		3.714*	

The confidence interval for this study was chosen as 95% and thus a coefficient can only be statistically significant if P<.05. All regression coefficients that are statistically significant are indicated with an asterisk. The R^2 and F-test values given are of the overall model, which is the model containing all coefficients and not only the statistically significant ones.

D.2.1. Porosity

The linear regression model obtained for particle porosity can be seen in equation D.1.

$$P = 34.620 + 0.001\mathrm{FAF} + 0.052\mathrm{FAT} - 0.022\mathrm{SLF} - 0.062\mathrm{SLT} - 0.056\mathrm{SLC} - 7.084\mathrm{Fd50} - 0.040\mathrm{DP} + 0.006\mathrm{AAT} \quad [D.1]$$

As seen in Table D.0.2 no statistically significant regression coefficients were obtained for the particle porosity model, and, consequently, no indication is given of which process variables exhibits a statistically significantly effect on particle porosity. In Figure D.1 a comparison of the values predicted by the regression coefficients and the observed porosity values over the data points can be seen.

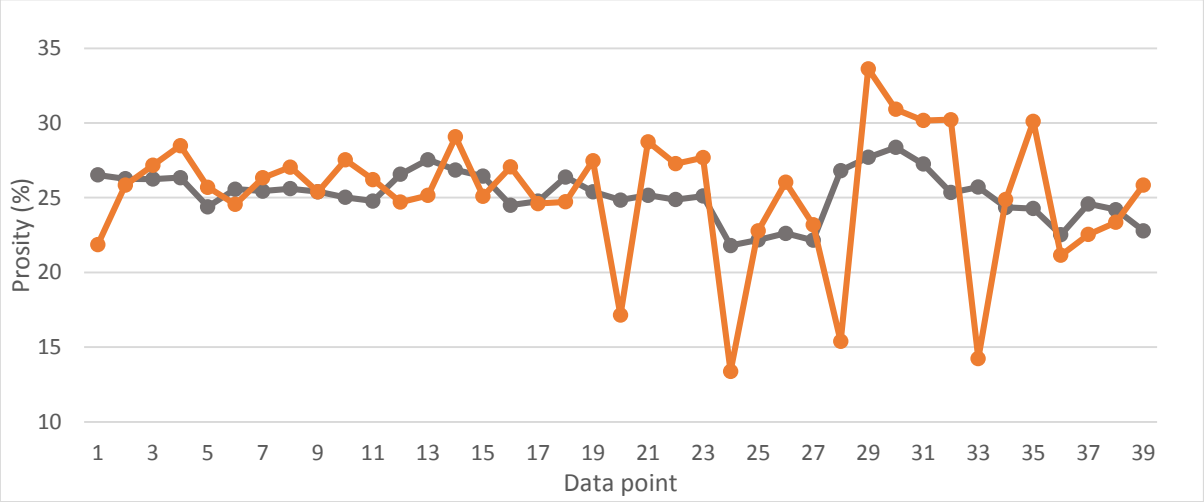

Figure D.1 Comparison of observed and predicted porosity values ●observed ●Insignificant predicted

In the figure, the predicted and observed values do not correlate that well, especially at very high or low porosity values. This model was expected to be inadequate with a low R^2 value of 0.134, only explaining 13.4% of the variance in the system, and an insignificant F-test value indicating a lack of fit and the inability of the variables to describe porosity.

D.2.2 True density

The model obtained can be seen in the following equation.

$$True\ density = 2.082 + 0.00001\mathrm{FAF} + 0.0004\mathrm{FAT} + 0.003\mathrm{SLF} + 0.001SLT - 0.007SLC - 0.025\mathrm{Fd50} - 0.0001\mathrm{DP} + 0.00004\mathrm{AAT} \quad [D.2]$$

For the true density, the mean or intercept value along with the spray liquid temperature and concentration were seen to be statistically significant. This equation shows that an increase in spray liquid temperature will result in an increase in density while an increase in spray liquid concentration will result in a decrease. Figure D.2 shows a comparison of the predicted values as well as the observed density values of the various data points.

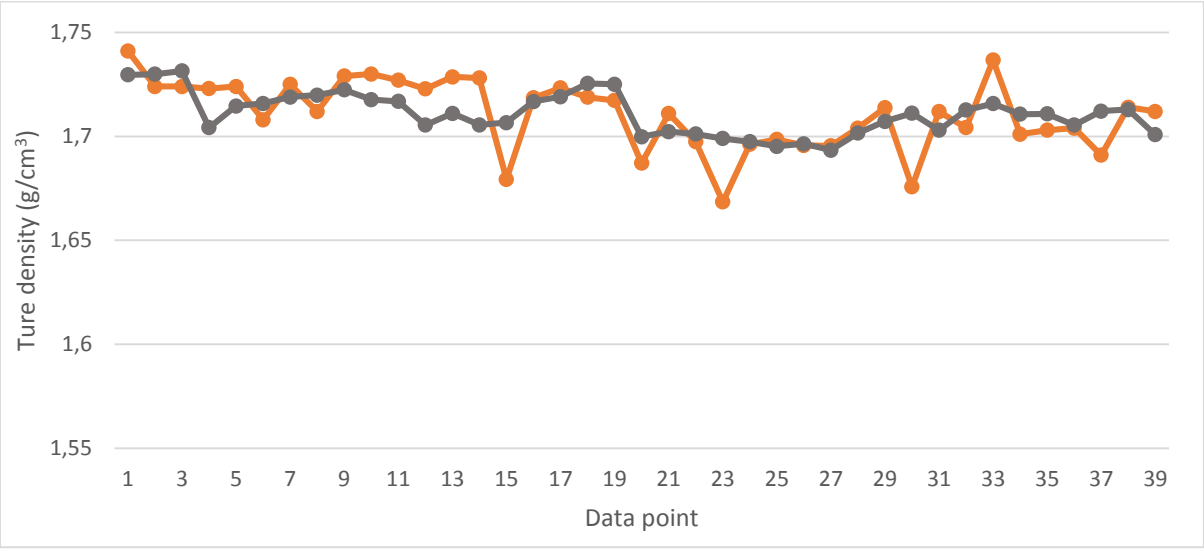

Figure D.2 Comparison of observed and predicted density values ●observed ●Insignificant predicted

From the figure it is visible that values predicted by the regression coefficients fall within the range of the observed values, but is not completely predictive, with a R^2 value of 0.358 and an insignificant F-test value. This model is concluded inadequate in predicting the observed values.

D.2.3 Particle mean diameter Pd_{50}

The regression model obtained for the product size can be seen in equation D.3.

$$Pd_{50} = -0.037 - 0.0001\mathrm{FAF} + 0.001\mathrm{FAT} + 0.001\mathrm{SLF} - 0.002SLT + 0.026SLC + 0.303\mathrm{Fd50} + 0.00005\mathrm{DP} - 0.00003\mathrm{AAT} \quad [D.3]$$

The fluidising air flowrate is the only variable found statistically significant for influencing particle mean diameter. This indicates that an increase in fluidising air flow will lead to a decrease in mean particle size. The results of the significant model and all the regression coefficients are presented in Figure D.4.

The values obtained from the regression model and the observed values fell into the same range and seems to almost follow the trend of the observed values. With a R^2 of 0.488, this model accounts for almost 50% of the variance in the system. The F-test value is significant which indicates that at least one of the independent variables influences mean particle size.

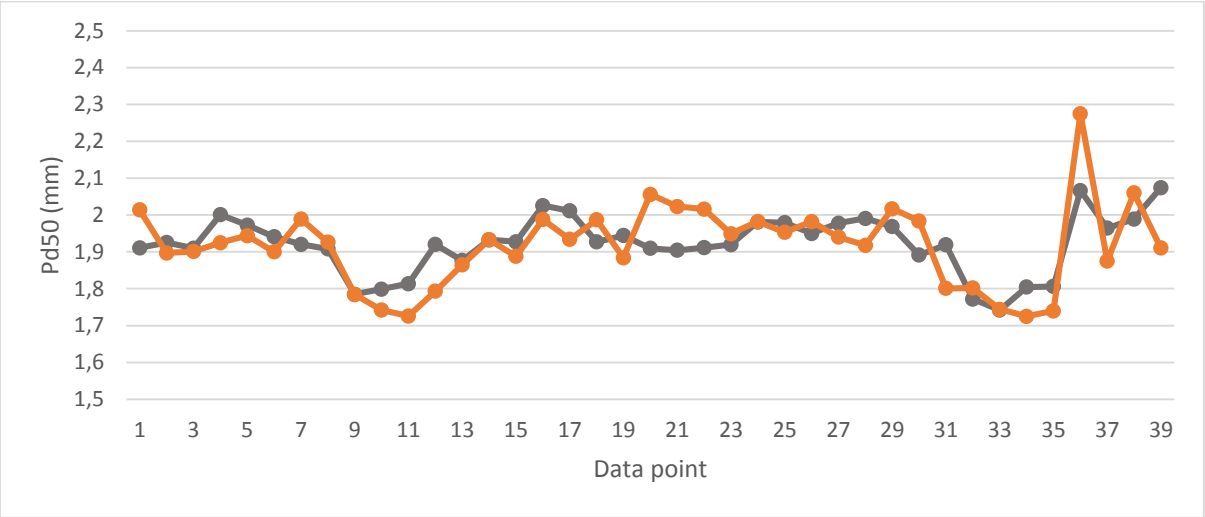

Figure D.3 Comparison of observed and predicted Pd_{50} values ●observed ● predicted

D.2.4 Circularity

Equation D.4 presents the regression model obtained for circularity.

$$C = 1.019 + 0.000003\mathrm{FAF} + 0.0001\mathrm{FAT} - 0.0001\mathrm{SLF} - 0.0002SLT - 0.002SLC + 0.015\mathrm{Fd50} - 0.001\mathrm{DP} - 0.002\mathrm{AAT} \quad [D.4]$$

From the regression results in Table D.0.2 the intercept and the fluidising air flow are the process variable seen to influence particle circularity. In Figure D.6 the observed and the predicted values can be seen for the various data points.

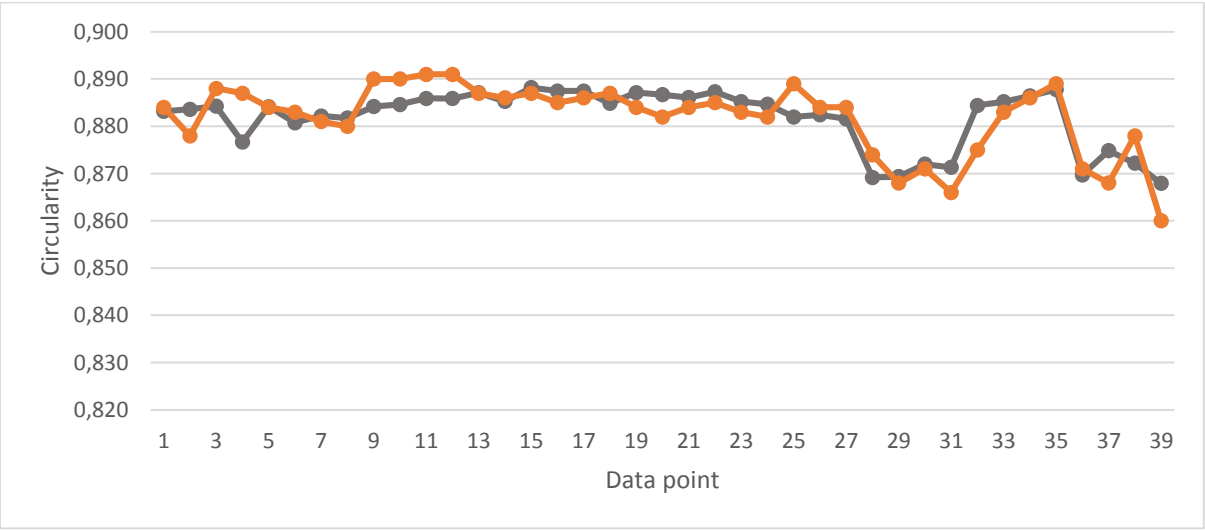

Figure D.4 Comparison of observed and predicted circularity values ●observed ● predicted

The values predicted by the model and the observed values fall within the same range. As seen in Figure D.4 the modelled values correlates very well with the observed values and follows the same trend. This model has a significant F-test value and a R^2 value of 0.684.

D.3 Conclusion

From the Spearman's correlation study, spray liquid concentration was found to have a fairly good correlation with all of the quality parameters, except particle porosity. The spray liquid temperature and flow rate was seen to have correlations with the particle spray rate and the true particle density respectively. Other physicochemical material feed properties such as the feed particle mean diameter and the atomising air pressure difference had no correlations with any of the quality parameters.

From the regression results, low R^2 values were observed. By the addition of interaction terms or second order terms as well as reducing the number of variables, the predictive capability of the models should increase.

Appendix E – Basic experimental phase two results

E.1 Particle Abrasion Resistance

The percentage degradation for the various experimental runs can be seen in Figure E.1.

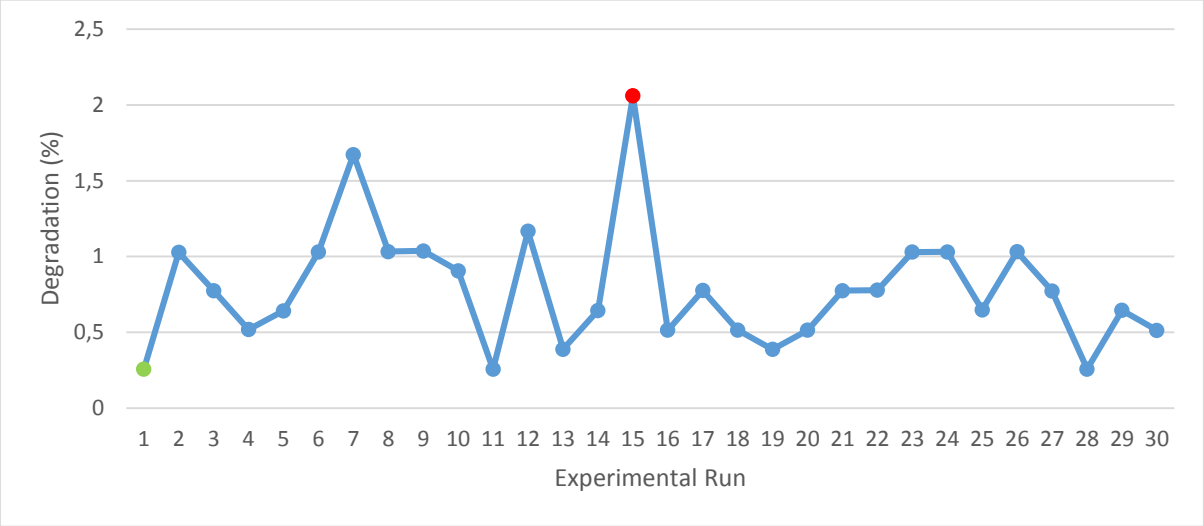

Figure E.1 Particle degradation for the various experimental runs

●lowest value and ●highest value

The values obtained during this study falls between 0.25 and 2.06 %, indicating a high particle resistance to abrasion and falling well below the expected 7.8 % degradation for prilled ammonium nitrate as seen in section 2.4.2.5. This agrees with literature indicating that granulation produces stronger particles than prilling. Regression plots were drawn up of the particle abrasion resistance versus the process variables. In Figure E.2 the percentage degradation versus spray liquid temperature can be seen.

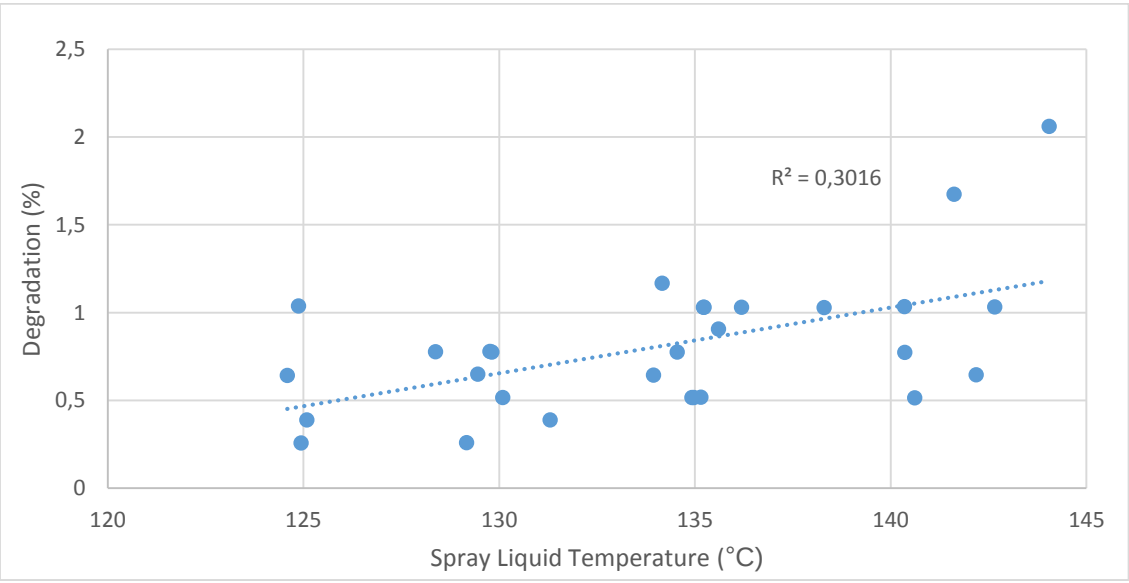

Figure E.2 Percentage degradation versus spray liquid temperature

In the chart above a visible increase in degradation percentage is visible with an increase in spray liquid temperature with a coefficient of determination value of 0.302. Although the R^2 value isn't high it is still worthwhile to make note of this correlation. No other regression plots provide observable correlations.

E.2 Product d_{50}

The mean granule diameter over the course of the experimental runs can be seen in the following figure.

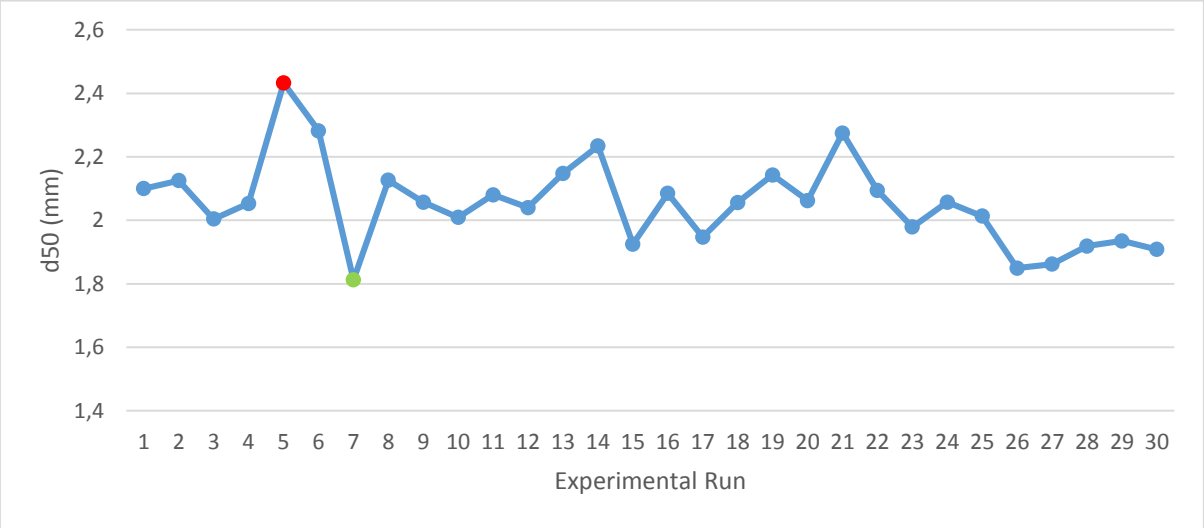

Figure E.3 Mean granule diameter for the various experimental runs

●lowest value and ●highest value

These sizes varied between 1.812 and 2.433 mm, the smallest and largest size respectively. In the following chart a regression plot of product particle d_{50} versus feed particle d_{50} is presented.

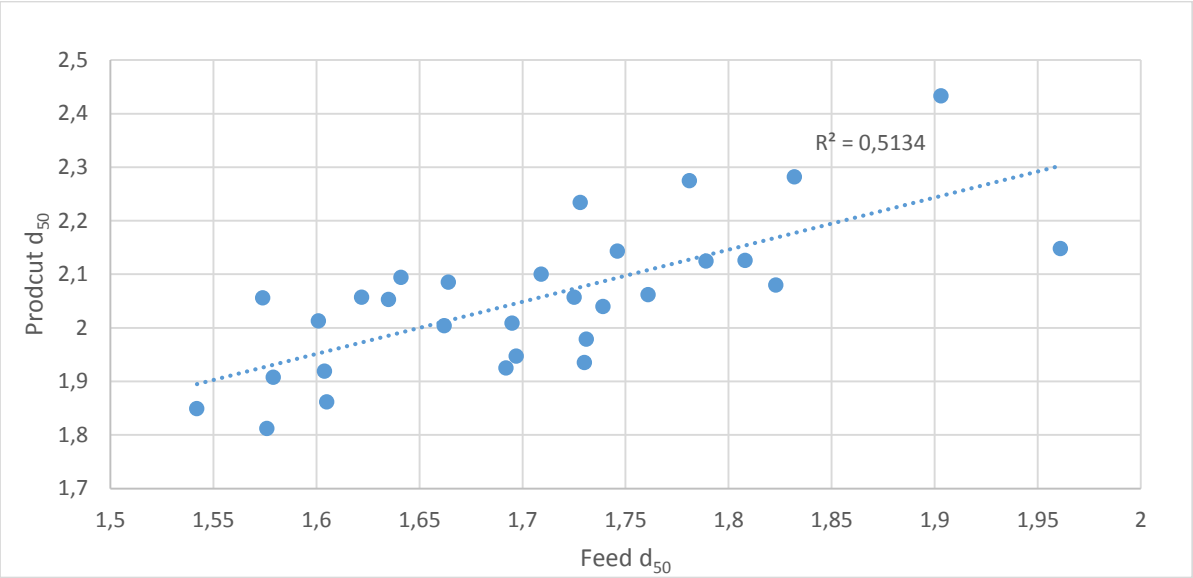

Figure E.4 Product d50 versus feed d50

An increase in feed particle size shows an increase in product particle size with a R^2 of 0.513 indicating a moderate correlation. This agrees with literature (section 2.4.1.4) which states that an increase in feed size will result in an increase in product size. The following figures give the relationship between product d_{50} and spray liquid concentration as well as spray liquid temperature.

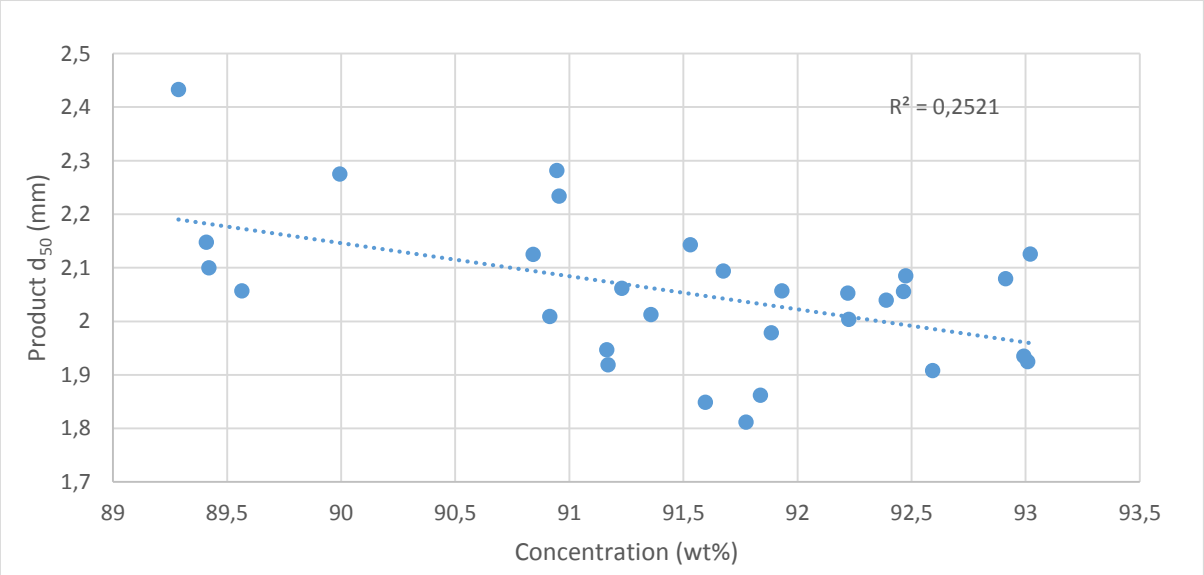

Figure E.5 Product d50 versus concentration

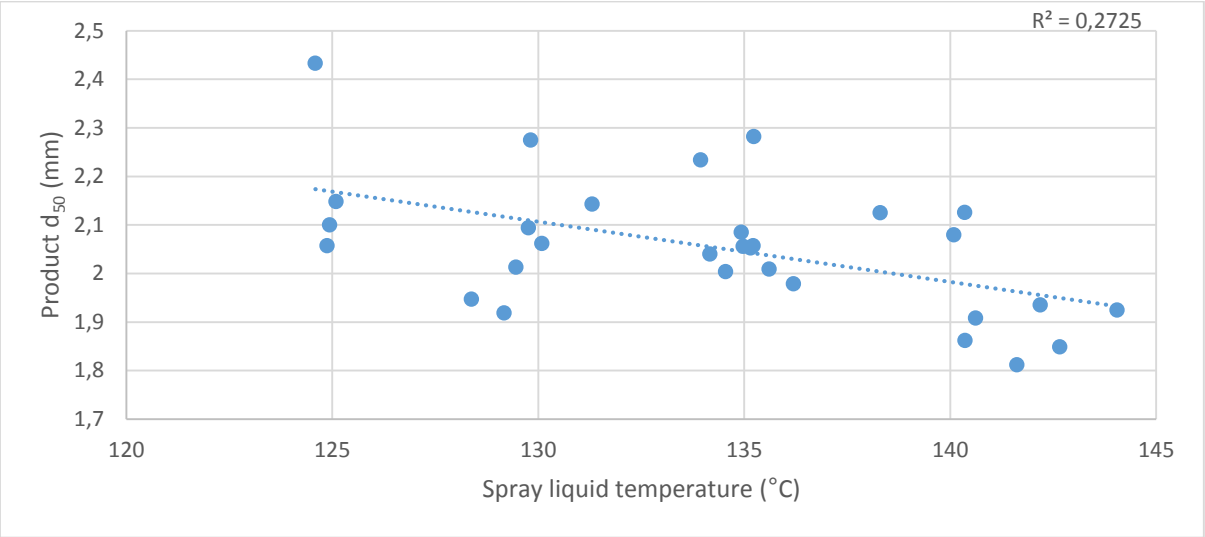

Figure E.6 Product d50 versus spray liquid temperature

Figure E.5 and E.6 shows a visible decrease in particle size with an increase in spray liquid concentration and spray liquid temperature respectively.

E.3 Particle Shape

Figure E.7 presents the circularity for each of the experimental runs.

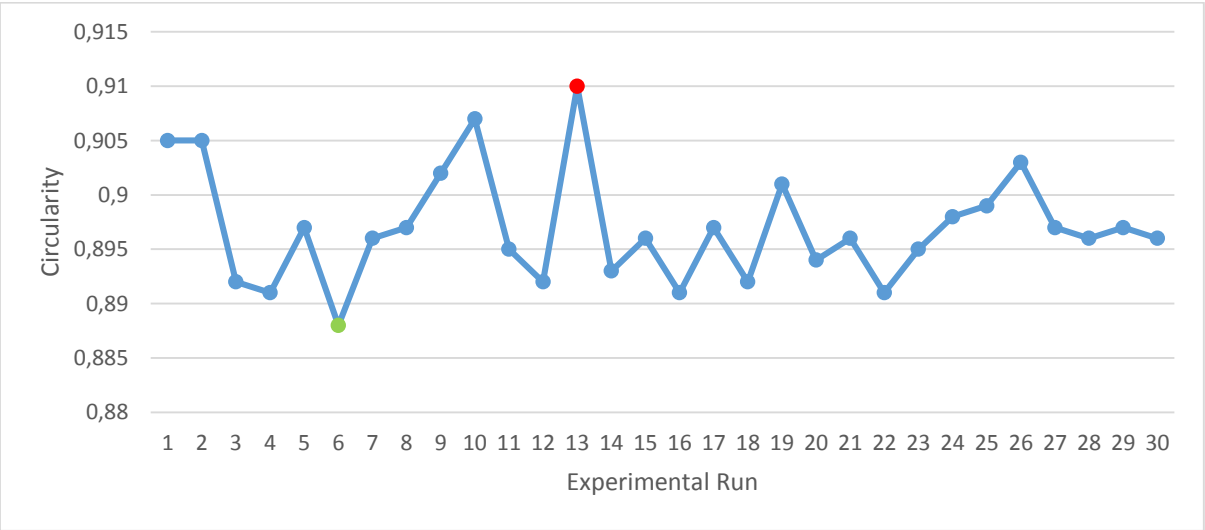

Figure E.7 Particle shape for various experimental runs

The obtained circularity values for this study falls between 0.888 and 0.910. These values are leaning towards a value of 1 which indicated very circular particles. A plot of circularity against binder concentration can be seen in Figure E.8.

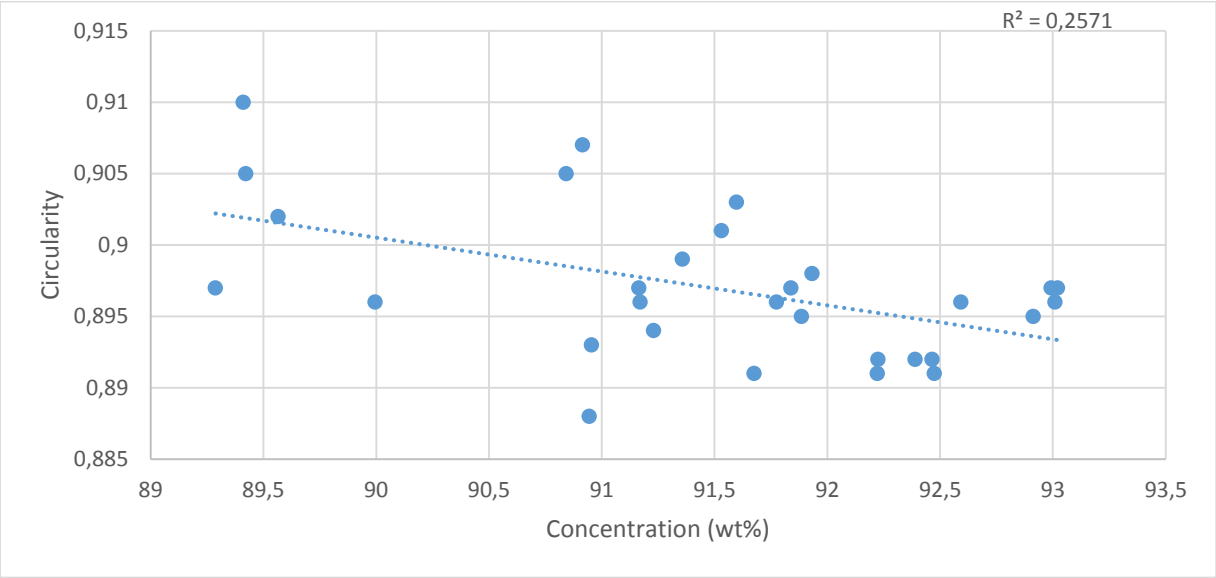

Figure E.8 Circularity versus concentration

A decrease in circularity is observed with an increase in binder concentration. This coincides with literature which indicates that a higher binder concentration would increase binder viscosity, thus lessening particle wettability and result in a less spherical particle, as discussed in section 2.4.1.1.

E.4 Porosity

In Figure E.9 the porosity for the various runs can be seen,

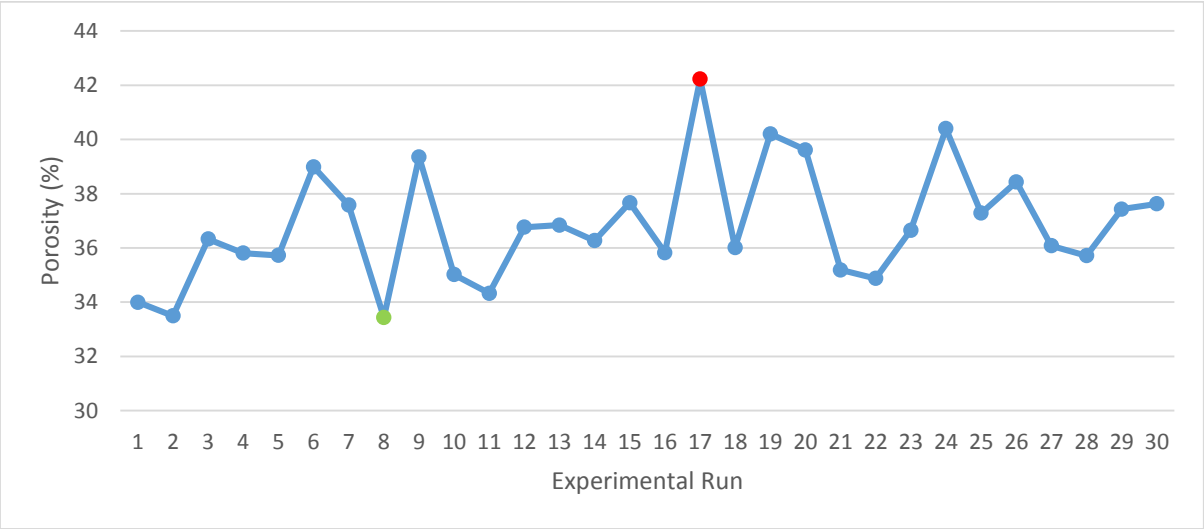

Figure E.9 Porosity for the various experimental runs

The porosity values varied between 33.43 and 42.22%. No visible correlations with any of the process variables were obtained through regression plots.

E.5 Flowability

The flowability of particles, indicated by Carr's index, is presented in Figure E.10.

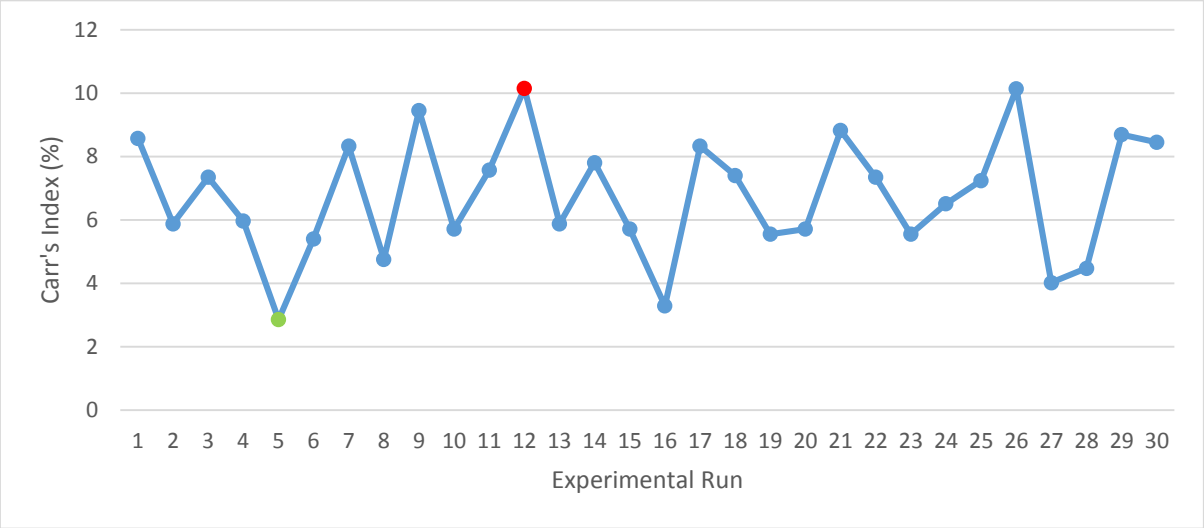

Figure E.10 Carr's index for the various experimental runs

The calculated values fall within the range of 2.85 and 10 % and, according to literature (section 2.4.2.3) this indicates on excellent flowability with values equal or less than 10. No visible correlations were obtained through regression plots.

E.6 Spearman Correlation

The Spearman's correlations between the process variables and product quality can be seen in Table E.0.1.

Table E.0.1 Spearman's correlation between the process variables and product quality for phase two

	P	A	Pd50	C	CI
DAAP	-0,028	0,086	0,140	0,204	0,004
SLF	0,081	-0,327	0,039	0,108	-0,238
SLC	0,028	0,121	**-0,440**	**-0,437**	0,006
SLT	0,042	**0,369**	**-0,498**	-0,090	-0,008
Fd50	-0,159	-0,095	**0,729**	0,073	-0,258

All correlations with a significance level of $P \leq 0.05$ are underlined, indicating that the value falls within a confidence interval of 95%. The table is also colour-coded, with dark red indicating a strong negative effect and dark green indicating a strong positive effect. From

the table above it can be seen that there is no correlation between any of the process variables and porosity as well as with particle flowability. This agrees with the fact that no visible correlations were obtained for both particle porosity and flowability through the use of regression plots in the previous section.

The particle abrasion resistance had a positive weak correlation with spray liquid temperature and agrees with the regression plot obtained in section E.1.1. The product d_{50} had a moderate negative correlation with the spray liquid temperature and concentration and a strong positive correlation with the feed particle $d_{50.}$ Particle circularity only had a moderate negative correlation with the spray liquid concentration. All these correlations are confirmed by the regression plots in section E.1.1. Comparing this Spearman's matrix to the one obtained during phase one shows that the spray liquid concentration still has an effect on both particle size and circularity.

The fact that all of the significant correlations between the process variables and the product quality parameters match the regression plot analyses performed in the previous section confirms the importance of these variables in the modelling of this system.

Appendix F – Validation data

Table F.0.1 Validation data

	Difference in Atomizing Air Pressure (kPa)	Spray Liquid flowrate (tons/hr)	Spray Liquid Concentration (wt%)	Spray Liquid Temperature (Degrees C)	Seed Particle Size (mm)	Oil Absorption (%)	Abrasion (%)	Product Size (mm)	Circularity	Carr Index (%)
1	-11,517	5,421	89,140	124,495	1,685	33,747	0,517	2,294	0,906	5,882
2	-9,811	5,840	90,745	134,867	1,932	37,214	0,386	2,215	0,897	2,857
3	-10,511	6,078	89,307	124,995	1,696	33,138	0,515	2,157	0,897	7,246
4	-10,340	6,227	90,720	137,876	1,779	39,143	0,516	2,107	0,895	7,895
5	16,832	3,210	89,545	125,435	1,689	38,285	0,258	2,059	0,904	5,714
6	14,227	5,646	90,963	137,247	1,722	37,451	0,642	2,011	0,910	10,000
7	14,808	8,544	89,550	124,776	1,902	27,906	0,385	1,990	0,907	7,246
8	18,004	8,208	90,975	135,108	1,745	40,609	0,642	1,871	0,893	8,108
9	-9,163	8,251	91,310	138,769	1,686	39,653	0,773	1,817	0,894	8,696
10	15,880	7,013	92,924	138,359	1,740	33,435	1,546	2,015	0,895	8,696
11	3,561	6,770	90,040	129,474	1,954	34,923	0,902	2,250	0,893	5,882